NASA CONTRACTOR REPORT

NASA CR-1282

ANALYSIS OF TWO ALTERNATE DAMPING SYSTEMS FOR THE GEOS GRAVITY GRADIENT STABILIZED SATELLITE

Prepared by
COMMUNICATIONS & SYSTEMS, INC.
Falls Church, Va.
for

NATIONAL AERONAUTICS AND SPACE ADMINISTRATION • WASHINGTON, D. C. • FEBRUARY 1969

ANALYSIS OF TWO ALTERNATE DAMPING SYSTEMS FOR THE GEOS GRAVITY GRADIENT STABILIZED SATELLITE

Issued by Originator as Report No. R-4035-30-1

Prepared under Contract No. NASw-1503 by
COMMUNICATIONS & SYSTEMS, INC.
Falls Church, Va.

for

NATIONAL AERONAUTICS AND SPACE ADMINISTRATION

For sale by the Clearinghouse for Federal Scientific and Technical Information
Springfield, Virginia 22151 – CFSTI price $3.00

TABLE OF CONTENTS

TABLE OF CONTENTS (Continued)

LIST OF ILLUSTRATIONS

LIST OF ILLUSTRATIONS (Continued)

1. INTRODUCTION

1.1 OBJECT

The object of this report is to present the results of an analysis of two types of gravity-gradient damping systems which were considered for use on the NASA GEOS geodetic satellites. The purpose of the analysis was to derive the theoretical performance characteristics of each system and to determine which type of system is more suitable for application to the GEOS satellites.

1.2 SCOPE

The first technique considered was a magnetically anchored eddy current damper similar to the one used successfully on the GEOS-A satellite. This damper features a frictionless suspended permanent magnet which is aligned by the earth's magnetic field. Attitude motions of the satellite cause relative motion between the magnet and a conducting shell. The induced eddy currents in the shell dissipate kinetic energy in the form of heat.

The second technique is a new concept which uses a number of long, ferromagnetic rods rigidly mounted in the satellite. The rods are sheathed with copper to provide eddy current damping of satellite attitude motions in the earth's magnetic field.

The analysis in this report proceeds from fundamental principles to derive the torque generated by each type of damper. Within certain limitations which must be imposed to facilitate analysis, enough information can be derived to make possible a

comparison of the two damping techniques in relation to the GEOS satellites. For a more precise evaluation of the absolute performance, a computer simulation of the damper and satellite equations of motion would be required. However, this is deemed to be unnecessary for the purpose of the present study.

The analysis consists of three parts as follows:

Section 3: Analysis of Magnetically Anchored Damper

Section 4: Analysis of Eddy Current Rod Damping Concept

Section 5: Comparison of Damping Techniques

Equations and figures are numbered from (1) in each section, and cross-references are indicated by the appropriate section number preceding the equation or figure number; e.g., (3.1-1) is the first equation of section 3.1.

2. CONCLUSIONS

Beginning from fundamental principles, the magnetically anchored eddy current damper and the eddy current rod damper have been studied individually to determine their major operating characteristics. The characteristics of the two dampers have been compared under conditions appropriate to GEOS satellites such as operating altitude and size limitations.

Based on the results of the analyses and the comparison, the following conclusions can be reached concerning the feasibility of each damper for application to GEOS satellites:

1. Damping by eddy current rods is more than an order of magnitude less than the amount obtained with the magnetically anchored damper for a polar orbit of 600 n. mi. altitude. The time required to damp transient librations would be correspondingly longer.

2. For non-polar orbits or at higher altitudes, the performance of the eddy current rod damper deteriorates more rapidly than the magnetically anchored damper performance.

3. Although damping performance could be improved by providing more rods than considered, a significant improvement would require more rods than could be carried on the satellite.

As a possible technique for use on other satellites, the rods should be kept in mind. Significant improvement in transient damping could be obtained, if the satellite could accommodate rods of twice the length which can be accommodated in GEOS satellites.

It appears that the magnetically anchored damper is well-suited for application to the GEOS satellites; however, there are two effects which have not been adequately explained. First, it is shown that the axis of relative rotation between the two major components of the damper is, in general, not stationary with respect to either part. Apparently, this behavior has not been simulated in laboratory tests of the damper. It would be useful to simulate the rotation more realistically to see if there is any peculiarity associated with the more complex motion. Second, it is shown that only a certain component of the damper generated torque is effective in damping satellite librations. There is another component of the generated torque that is directed normal to the satellite rotation axis. The effect of this component should be shown to be negligible or, otherwise, included in computer simulations of the satellite attitude dynamics.

3. ANALYSIS OF THE MAGNETICALLY ANCHORED EDDY CURRENT DAMPER

3.1 DAMPER DESCRIPTION

A brief description of the magnetically anchored damper will be given in order to justify the nature of the theoretical model that will be obtained. The damper consists basically of an assembly of six cylindrical permanent magnets, arranged in the shape of a three dimensional + sign or a cruciform, with opposite poles at opposite ends of the cruciform. The magnet assembly is contained within a spherical copper shell for eddy current damping purposes. Another outer shell made of pyrolytic graphite, which is a diamagnetic substance, exerts a centering force on the magnet assembly and provides a frictionless suspension mechanism in an orbital environment. Finally a third outer shell, made of aluminum, provides a protective housing for the damper and a means for attaching the damper to the satellite.

The operation of the damper is as follows: When the satellite is in orbit, the magnet assembly is suspended by the diamagnetic force and is free to rotate. The net magnetic dipole of the cruciform magnet assembly tends to align itself in the direction of the local magnetic field of the earth. As the satellite undergoes librations, there is relative motion between the conducting shell and the magnet assembly. This induces an electric field within the conductor which causes eddy currents to flow. The magnetic field of the eddy currents interacts with that of the cruciform to produce a retarding torque. An initial energy of libration is gradually dissipated in heating the copper shell.

3.2 THEORETICAL MODEL OF THE MAGNETICALLY ANCHORED DAMPER

For the purpose of deriving the damping torque, a theoretical model of the magnetically anchored damper will be studied. The theoretical model consists of an idealized cruciform magnet suspended at the center of a single conducting spherical shell. The center of the magnet is assumed to remain fixed at the center of the shell, but otherwise the magnet is free to rotate about an arbitrary axis through the center. The magnetic field of the cruciform magnet assembly is assumed to be equivalent to superposing the three fields produced by a single cylindrical bar magnet which occupies, in turn, the position of each arm of the cruciform. The bar magnet is assumed to be uniformly magnetized along its longitudinal axis.

With this model, the essential nature of the practical damper is retained, but extraneous details of construction of a practical damper are omitted. The analysis will be considerably simplified and, therefore, will be easier to interpret, but the results should nevertheless adequately indicate the performance of the practical damper. There is experimental evidence to support these assumptions. It is known that the pyrolytic graphite shell between the two conducting shells does not contribute appreciably to the torque. The torque due to eddy currents induced in the outer aluminum shell, according to laboratory tests, is about 12% of the total torque; hence, a correction factor can be applied to the results of the analysis to account for the presence of the aluminum shell.

Concerning the magnet assembly, the idealized magnet may not give an accurate representation of the field in the region near the center; where the six magnets are mounted in a steel fitting, however, the field in that region does not interact very strongly with the magnetic field of the induced eddy currents in the shell. The error, therefore, should not be significant.

Two further assumptions are made in the model. The resistivity of the magnet alloy is assumed to be very much greater than that of the shell, so that the flow of eddy currents in the magnet induced by the magnetic field of the shell can be neglected. Finally, the conducting shell is assumed to have the permeability of free space.

3.3 ANALYTICAL APPROACH

The torque on the spherical conducting shell generated by relative motion of the magnet is obtained from the distributed forces due to the interaction of induced currents and the magnetic field. Specifically, the force $\overline{f}$ on an elemental volume in which the current density in $\overline{J}$ (amp/m^2) and the magnetic induction is $\overline{B}$ (wb/m^2) given by [1]

$$\overline{f} = \overline{J} \times \overline{B} \qquad (\text{nt-m}^{-3}) \tag{1}$$

In order to obtain the net torque about a particular axis of the damper, it is necessary, therefore, to first obtain the eddy current density and the magnetic field induction at all points within the shell. Basically, this is a problem in magnetostatics, since it can be assumed that all field effects are propagated instantaneously, and, therefore, Maxwell's displacement current can be neglected.

The required field relationships are given by Maxwell's field equations, omitting the displacement current. A unified formulation is obtained in terms of the magnetic vector potential $\overline{A}$ which is defined in the following manner:

$$\overline{B} = \nabla \times \overline{A}, \quad \nabla \cdot \overline{A} = 0 \tag{2}$$

Note that the above definition satisfies the requirement that $\nabla \cdot \overline{B} = 0$, since the divergence of the curl of any vector is zero. The additional specification that the divergence of $\overline{A}$ is zero, corresponds to the assumption that there is no free charge in the region of interest.

It will be shown that $\overline{A}$ satisfies certain partial differential equations which depend on the nature of the medium. The analysis of the damper, therefore, requires the simultaneous solution of the appropriate equations for each region having distinct electrical or magnetic properties in such a way that certain boundary conditions are satisfied. The basic theory will be outlined in the next section.

3.4 VECTOR POTENTIAL THEORY

As stated previously the fact that $\nabla \cdot \overline{B} = 0$ permits $\overline{B}$ to be obtained as the curl of a vector potential $\overline{A}$.

$$\overline{B} = \nabla \times \overline{A} \tag{1}$$

In the absence of free charge

$$\nabla \cdot \overline{A} = 0 \tag{2}$$

Thus the vector potential $\overline{A}$ can be derived in turn from a higher potential $\overline{W}$; i.e.,

$$\overline{A} = \nabla \times \overline{W} \tag{3}$$

with the auxiliary condition that

$$\nabla \cdot \overline{W} = 0 \tag{4}$$

This fact will be of considerable importance in the solution of the boundary value problem for the vector potential $\overline{A}$. Note that the vector potential from which $\overline{B}$ is obtained is not unique, because $\overline{A}^* = \overline{A} + \nabla\varphi$, where φ is a scalar field also satisfies (2).

The equations that $\overline{A}$ must satisfy are obtained from Maxwell's equations. According to Faraday's law, a time varying magnetic induction $\overline{B}$ will produce an electric field $\overline{E}$ such that

$$\nabla \times \overline{E} = - \frac{\partial \overline{B}}{\partial t} \tag{5}$$

From the definition of $\overline{A}$

$$\overline{E} = - \frac{\partial \overline{A}}{\partial t} \tag{6}$$

If the field is produced in a conductor of volume resistivity ρ, then a current density, $\bar{J} = \bar{E}/\rho$, will flow. Thus,

$$\rho\bar{J} = \frac{-\partial\bar{A}}{\partial t} \tag{7}$$

The current in turn will produce a magnetic field, according to Ampere's law

$$\nabla \times \bar{B} = \mu\bar{J} \tag{8}$$

where μ is the permeability of the medium.

$$\therefore \quad \nabla^2\bar{A} = -\mu\bar{J} \tag{9}$$

In rectangular coordinates, each component of $\bar{A}$ satisfies Poisson's equation in which the inhomogeneous term is proportional to a component of the current density. When the current density is known, the above equation can be solved for $\bar{A}$. In the case where $\bar{J}$ is an unknown current distribution arising from a time-varying magnetic field, (7) and (9) can be combined to yield

$$\nabla^2\bar{A} = \frac{\mu}{\rho}\frac{\partial\bar{A}}{\partial t} \tag{10}$$

Now the components of $\bar{A}$ in rectangular coordinates satisfy diffusion or "heat" equations.

When the medium is an insulator ($\rho = \infty$), then $\bar{J} = 0$, and the vector potential satisfies a vector form of Laplace's equation; i.e.,

$$\nabla^2\bar{A} = 0 \tag{11}$$

The nature of the boundary conditions which the vector potential must satisfy are discussed by Panofsky and Phillips [2]. From the conservation of magnetic flux across the boundary, the line integral of $\bar{A}$ along any arbitrary closed path in the boundary surface must be zero; hence, on the interface between regions 1 and 2,

$$(\bar{A}_1)_t = (\bar{A}_2)_t \tag{12}$$

where the subscript $_t$ denotes the tangential component. In the absence of true surface currents, the tangential component of magnetic field intensity $\bar{H}$ is conserved; thus,

$$\frac{1}{\mu_1} (\nabla \times \bar{A}_1)_t = \frac{1}{\mu_2} (\nabla \times \bar{A}_2)_t \tag{13}$$

Each of these boundary conditions has two components, so that altogether four boundary conditions are obtained at each boundary.

3.5 MATHEMATICAL FORMULATION OF THE BOUNDARY VALUE PROBLEM FOR THE VECTOR POTENTIAL

It is now possible to formulate the damper analysis as a boundary value problem for the vector potential. Denote the vector potential of the cruciform magnet by $\bar{A}'$. This is the potential of the field that would exist when the magnet is in free space. Under the assumption that the field is equivalent to superposing the fields of a single uniformly magnetized bar magnet occupying, in turn, the position of each arm of the cruciform, then $\bar{A}'$ is the sum of the individual vector potentials of each arm. Now a uniformly magnetized bar magnet is equivalent to a current sheet around the surface of the cylinder, and the interior may be regarded as a region of free space.* Thus, the vector potential of the magnet can be derived from an equation of the form (3.4-9).

The space surrounding the magnet when it is in the damper shell is divided into three distinct regions as follows:

Region I: free space inside the spherical shell

Region II: the shell

Region III: free space outside the shell

In Region I, a perturbing potential $\bar{A}_1$ must be added to $\bar{A}'$ in order to satisfy the boundary conditions at the inside surface of the shell. Since the magnet is equivalent to free space, insofar as external fields are concerned, the boundary of the magnet can be ignored, and the potential $\bar{A}_1$ can be extended through the magnet.

* See [3] pp. 427-429.

The net potentials in Regions II and III will be denoted by $\bar{A}_2$ and $\bar{A}_3$, respectively.

The appropriate equations for the vector potential in each region are the following:

Region I: $$\nabla^2(\bar{A}_1+\bar{A}') = 0 \qquad (1)$$

Region II: $$\nabla^2\bar{A}_2 = \frac{\mu_2}{\rho}\frac{\partial\bar{A}_2}{\partial t}\ , \quad \mu_2 = \mu_o \qquad (2)$$

Region III: $$\nabla^2\bar{A}_3 = 0 \qquad (3)$$

In addition the boundary conditions at the surfaces of the shell are the following:

Inside surface:

$$(\bar{A}_1+\bar{A}')_t = (\bar{A}_2)_t \qquad (4)$$

$$\frac{1}{\mu_1}[\nabla x(\bar{A}_1+\bar{A}')]_t = \frac{1}{\mu_2}(\nabla x\bar{A}_2)_t, \quad \mu_1=\mu_2=\mu_o \qquad (5)$$

Outside surface:

$$(\bar{A}_2)_t = (\bar{A}_3)_t \qquad (6)$$

$$\frac{1}{\mu_2}(\nabla x\bar{A}_2)_t = \frac{1}{\mu_3}(\nabla x\bar{A}_3)_t \qquad \mu_2=\mu_3=\mu_o \qquad (7)$$

Equation (2) is written with respect to a coordinate system fixed in the shell. In this coordinate system $\bar{A}'$ is a function of time at a given point as the magnet rotates, so that $\bar{A}_2$ is subject to a time-varying boundary condition in (4).

Although the solution of the boundary value problem for the vector potential can be carried out in principle, formidable problems are encountered in deriving a suitable expression for $\bar{A}'$ with respect to a coordinate system fixed in the shell, and

also, from the fact that the Laplacian operator operates on the unit vectors in all coordinate systems except rectangular systems. Since the geometry is spherical, a spherical coordinate system would simplify the task of obtaining separable solutions which satisfy the boundary conditions.

These difficulties may be avoided by reformulating the problem in terms of two scalar potentials, W_1 and W_2, from which the vector potential $\bar{A}$ can be derived. The scalar potentials are not nearly so troublesome to work with as will be seen.

3.6 GENERAL REMARKS ON THE SOLUTION OF VECTOR POTENTIAL PROBLEMS

At each point in space, a vector is specified by its components along three orthogonal axes. Thus, a vector potential is derivable from three scalar potentials. With the auxiliary condition that $\nabla\cdot\bar{A} = 0$, one of the scalar potentials can be expressed in terms of the other two, so that only two independent potentials are needed. Earlier it was mentioned that since $\nabla\cdot\bar{A} = 0$, $\bar{A} = \nabla x\bar{W}$, where $\bar{W}$ is a vector potential. For spherical geometry it is convenient to express $\bar{W}$ as the sum of a radial component and a tangential component in the form

$$\bar{W} = \bar{r}W_1 + \nabla x\bar{r}W_2 \qquad (1)$$

where W_1 and W_2 are the two scalar potentials, and $\bar{r}$ is the radius vector from the origin at the center to the field point. The particular form of (1) is chosen on the following basis: Since

$$\nabla^2\bar{A} = \nabla^2(\nabla x\bar{W}) = \nabla x(\nabla^2\bar{W}) \qquad (2)$$

and
$$\nabla^2\bar{W} = \nabla^2(\bar{r}W_1 + \bar{r}x\nabla W_2) = \bar{r}\nabla^2 W_1 + 2\nabla W_1 + \bar{r}x\nabla(\nabla^2 W_2) \qquad (3)$$

then (I) $\nabla^2 W_i = 0,\ i=1,2 \Rightarrow \nabla^2\bar{A} = 0 \qquad (4)$

(II) $\nabla^2 W_i = k\frac{\partial W_i}{\partial t},\ i=1,2 \Rightarrow \nabla^2\bar{A} = k\frac{\partial\bar{A}}{\partial t} \qquad (5)$

The significance of results (I) and (II) is that certain boundary value problems for vector potentials may be formulated as analogous boundary value problems for scalar potentials. The boundary conditions for W_1 and W_2 are chosen so that the boundary conditions on $\bar{A}$ (or $\bar{B}$ and $\bar{H}$) are identically satisfied. The

manner in which W_1 and W_2 contribute to the boundary conditions can be made clear by obtaining explicit formulas for $\bar{A}$ and $\bar{B}$.

Let $\bar{W}_r = \bar{r}W_1$ and $\bar{W}_t = \bar{r}\times\nabla W_2$. Also, let $\bar{M} = \nabla\times\bar{W}_r$ and $\bar{N} = \nabla\times\bar{W}_t$. Then $\bar{A} = \bar{M}+\bar{N}$. Let the radial and tangential components of $\bar{A}$ be $\bar{A}_r$ and $\bar{A}_t$, respectively. Next, let $\bar{U} = \nabla\times\bar{M}$ and $\bar{V} = \nabla\times\bar{N}$. Then $\bar{B} = \bar{U}+\bar{V}$. Finally, denote the radial and tangential components of $\bar{B}$ by $\bar{B}_r$ and $\bar{B}_t$, respectively.

Using spherical polar coordinates with unit vectors $\bar{e}_r$, $\bar{e}_\theta$, and $\bar{e}_\varphi$ in the directions of increasing r, θ, and φ at the field point the following results are obtained:

$$\bar{M} = \nabla\times(\bar{r}W_1) = -\bar{r}\times\nabla W_1 \tag{6}$$

$$= \frac{\bar{e}_\theta}{\sin\theta}\frac{\partial W_1}{\partial\varphi} - \bar{e}_\varphi\frac{\partial W_1}{\partial\theta} \tag{7}$$

$$\bar{N} = \nabla\times(\bar{r}\times\nabla W_2) = \bar{r}\nabla^2 W_2 - \nabla(\bar{r}\cdot\nabla W_2) - \nabla W_2 \tag{8}$$

$$= \bar{r}\nabla^2 W_2 - \nabla\left[\frac{\partial}{\partial r}(rW_2)\right] \tag{9}$$

$$= \bar{r}\nabla^2 W_2 - \left(\bar{e}_r\frac{\partial u_2}{\partial r} + \frac{\bar{e}_\theta}{r}\frac{\partial u_2}{\partial\theta} + \frac{\bar{e}_\theta}{r\sin\theta}\frac{\partial u_2}{\partial\varphi}\right) \tag{10}$$

where $u_2 = \dfrac{\partial(rW_2)}{\partial r}$. Combining terms in $\bar{e}_r$

$$\bar{A}_r = r\bar{e}_r\left(\nabla^2 W_2 - \frac{1}{r}\frac{\partial u_2}{\partial r}\right) = \bar{r}\left(\nabla^2 W_2 - \frac{1}{r}\frac{\partial^2(rW_2)}{\partial r^2}\right) \tag{11}$$

But $$\nabla^2 W_2 = \frac{1}{r}\frac{\partial^2(rW_2)}{\partial r^2} + \frac{1}{r^2}L_\omega[W_2] \tag{12}$$

where

$$L_\omega[W_2] = \frac{\partial^2 W_2}{\partial\theta^2} + \cot\theta\frac{\partial W_2}{\partial\theta} + \csc^2\theta\frac{\partial^2 W_2}{\partial\varphi^2} \tag{13}$$

$$\therefore \quad \bar{A}_r = \frac{\bar{e}_r}{r}L_\omega[W_2] \tag{14}$$

Note that only W_2 contributes anything to $\bar{A}_r$. Combining $\bar{e}_\theta$ and $\bar{e}_\varphi$ terms from (7) and (10) yields

$$\bar{A}_t = \bar{e}_\theta \left(\frac{1}{\sin\theta} \frac{\partial W_1}{\partial \varphi} - \frac{1}{r} \frac{\partial u_2}{\partial \theta} \right) - \bar{e}_\varphi \left(\frac{\partial W_1}{\partial \theta} + \frac{1}{r\sin\theta} \frac{\partial u_2}{\partial \varphi} \right) \tag{15}$$

Both W_1 and W_2 contribute terms to $\bar{A}_t$. Next

$$\bar{U} = \nabla x(\nabla x \bar{r} W_1) = -\nabla x(\bar{r} x \nabla W_1) \tag{16}$$

$$= -\bar{r}\nabla^2 W_1 + \nabla\left[\frac{\partial}{\partial r}(rW_1)\right] \tag{17}$$

Note the similarity between (9) and (17).

Next from (9)

$$\bar{V} = \nabla x[\nabla x(rx\nabla W_2)] = \nabla x \bar{r} \nabla^2 W_2 \tag{18}$$

The second term in (9) is the gradient of a scalar and the result of taking the curl is identically zero. In insulators, where W_2 is a solution of $\nabla^2 W_2 = 0$, $V \equiv 0$, and W_2 makes no contribution to $\bar{B}$; however, W_2 may be needed to satisfy boundary conditions. In conductors, where W_2 is a solution of the diffusion equation,

$$\bar{V} = \nabla x \bar{r}\, k \frac{\partial W_2}{\partial t} = k \frac{\partial}{\partial t}(\nabla x \bar{r} W_2) = -k \frac{\partial}{\partial t}(\bar{r} x \nabla W_2) \tag{19}$$

$$= k \frac{\partial}{\partial t} \left(\frac{\bar{e}_\theta}{\sin\theta} \frac{\partial W_2}{\partial \varphi} - \bar{e}_\varphi \frac{\partial W_2}{\partial \theta} \right) \tag{20}$$

Combining terms in $\bar{e}_r$ from (17) yields

$$\bar{B}_r = -\bar{r}\left(\nabla^2 W_1 - \frac{1}{r}\frac{\partial u_1}{\partial r}\right) = \frac{-e_r}{r} L_\omega[W_1] \qquad (21)$$

where $u_1 = \partial(rW_1)/\partial r$. Note the similarity between (11) and (21). Also note that W_2 makes no contribution to $\bar{B}_r$. Finally, combining terms in $\bar{e}_\theta$ and $\bar{e}_\varphi$ from (17) and (20) yields

$$B_t = \bar{e}_\theta\left(\frac{1}{r}\frac{\partial u_1}{\partial\theta} + \frac{k}{\sin\theta}\frac{\partial^2 W_2}{\partial t\partial\theta}\right) + \bar{e}_\varphi\left(\frac{1}{r\sin\theta}\frac{\partial u_1}{\partial\varphi} - k\frac{\partial^2 W_2}{\partial t\partial\varphi}\right) \qquad (22)$$

Sufficient conditions on W_1 and W_2 for the boundary conditions on $\bar{A}_t$ and $\bar{H}_t$ to be satisfied can be determined from inspection of (12) and (22). The results are as follows:

(A) $(W_i)_1 = (W_i)_2$ at r=a. i=1,2 (23)

(B) $\frac{1}{\mu_1}\left[\frac{\partial}{\partial r}(rW_i)\right]_1 = \frac{1}{\mu_2}\left[\frac{\partial}{\partial r}(rW_i)\right]_2$ (24)

at r=a. i=1,2. Outside subscripts denote that the quantity is evaluated on opposite sides of the boundary at r=a.

3.7 SYMMETRY CONSIDERATIONS

Under the assumption that the cruciform magnet remains centered in the spherical shell while rotating, certain simplifications in the analysis can be made on account of symmetry. The essential point that will be made is that $\bar{A}'$ has no radial component, and therefore, one of the two scalar potentials, W_2, will not be required.

As discussed in Stratton [1], the vector potential of a permanent magnet can be derived from the equivalent surface and volume currents within the magnet. Since the field of the cruciform can be resolved into three component fields generated by bar magnets, the nature of the vector potential of a cylindrical bar magnet which is uniformly magnetized in the axial direction will be examined. For a magnetic moment per unit volume $\bar{M}$, the equivalent surface current density is

$$\bar{K} = \bar{M} \times \bar{n} \tag{1}$$

where $\bar{n}$ is a unit vector normal to the surface.* The equivalent volume current is

$$\bar{J} = \nabla \times \bar{M} \tag{2}$$

and since $\bar{M}$ is constant, $\bar{J} = 0$. The formula for $\bar{A}'$ is, therefore,

$$\bar{A}' = \frac{\mu_o}{4\pi} \int_S \frac{\bar{M} \times \bar{n}}{r} \, dS \tag{3}$$

where r is the distance from the elemental surface area dS to the field point. At present only the symmetry properties of $\bar{A}'$ are of interest, and the evaluation of the integral will be postponed until later when the results are needed.

* $\bar{M}$ is also the loop magnetization (amp/m) of circulating currents or spinning electric charges within the magnet.

Let ρ, φ, and z denote a set of cylindrical coordinates with origin at the center of the bar magnet. Denote the unit vectors in the directions of increasing ρ, φ, and z by $\bar{e}_\rho$, $\bar{e}_\varphi$, and $\bar{k}$, respectively. Clearly, the end surfaces contribute nothing to the integral, because $\bar{M} = \bar{k}M$ and $\bar{n}$ are collinear. For an element of area on the curved surface, $\bar{n} = \bar{e}_\rho$, and $\bar{k} \times \bar{e}_\rho = \bar{e}_\varphi$.

$$\therefore \quad \bar{A}' = \bar{e}_\varphi A'_\varphi \tag{4}$$

Because of axial symmetry A'_φ is independent of φ and $A'_\varphi = f(\rho, z)$. Changing to spherical polar coordinates r, θ, φ

$$\rho = r \sin\theta \tag{5}$$

$$z = r \cos\theta \tag{6}$$

obtain $$\bar{A}' = \bar{e}_\varphi A'_\varphi (r, \theta) \tag{7}$$

since $\bar{e}_\varphi$ is invariant under the transformation. Obviously $\bar{A}'$ for a single bar magnet has no radial component, and, therefore, the net vector potential obtained by superposing vector potentials of each arm of the cruciform also has no radial component. With respect to a set of spherical polar coordinates referenced to rectangular axes coinciding with the axes of the cruciform, it should be apparent that the net vector potential can be described in the following manner:

$$\bar{A}' = \bar{e}_\varphi A'_\varphi (r, \theta, \varphi) + \bar{e}_\theta A'_\theta (r, \theta, \varphi) \tag{8}$$

The $\bar{e}_\theta$ term is contributed by the x and y arms of the cruciform, and A'_φ is now a function of φ to account for the contribution of the x and y arms.

In section (3.6) it was pointed out that the vector potential is, in general, derivable from two scalar potential functions, W_1 and W_2, and furthermore, that only W_2 contributes a radial component of $\bar{A}$. Thus, a sufficient condition for $\bar{A}'$ to have zero radial component is that $W_2' \equiv 0$. This might be expected, since a vector which has zero radial part and zero divergence can be specified by a single scalar quantity. Although $W_2' = 0$ is not a necessary condition for $\bar{A}_r' = 0$, the only other possibility is that W_2' must have a form that contributes nothing to either $\bar{A}'$ or $\bar{B}'$.

From (3.6-14)

$$\bar{A}_r' = \frac{\bar{e}_r}{r} L_{(\omega)}[W_2'] \tag{9}$$

Hence, a necessary and sufficient condition that $\bar{A}_r' = 0$ is for

$$L_{(\omega)}[W_2'] = 0 \tag{10}$$

Since $\nabla^2 \bar{A}' = 0$ at all points outside of the magnet, W_2' must satisfy $\nabla^2 W_2' = 0$. Thus, W_2' must be a spherical harmonic of zero degree which has the form

$$W_2' = (A+Br^{-1})\left(C\cot^m \frac{\theta}{2} + D\tan^m \frac{\theta}{2}\right)\cos(m\varphi + \delta_m) \tag{11}$$

where A,B,C,D and δ_m are arbitrary constants and m is an integer. But this solution is singular for either $\theta=0$ or π radians, unless $m=0$. Although $m=0$ gives

$$W_2' = A + Br^{-1} \tag{12}$$

as a possible form of W_2' which makes $\bar{A}_r'$ zero, nothing is contributed to $\bar{A}_t$ either, since $\bar{A}_t$ involves the partial derivatives of W_2' with respect to θ and φ as seen in (7-15).

It follows that when $\bar{A}_r' = 0$, W_2' can be set equal to zero without loss of generality. Then $\bar{A}'$ is derivable from a single scalar potential W' in the following manner:

$$\bar{A}' = \nabla x \bar{W}' = \nabla x \bar{r} W' \tag{13}$$

The relation between $\bar{A}'$ and W' for a single bar magnet along the z-axis will be of interest for later analysis. Since $\bar{A}' = \bar{e}_\varphi A_\varphi'(r,\theta)$ and A_φ is independent of φ, W' is also independent of φ. Thus,

$$\bar{A}' = \nabla x \bar{r} W'(r,\theta) = -\bar{e}_\varphi \frac{\partial W'}{\partial \theta} \tag{14}$$

so that $A_\varphi' = -\frac{\partial W'}{\partial \theta}$. (15)

3.8 FORMULATION OF THE BOUNDARY VALUE PROBLEM FOR THE SCALAR POTENTIAL

The required scalar potential, from which the magnetic vector potential is derived, is obtained as the solution of a boundary value problem which will be posed in this section. The resulting solution for the scalar potential at all points of interest will be obtained in terms of the scalar potential of the magnet. Although the scalar potential of the magnet is unknown a priori, the unknown parameters can be identified by taking the curl of the scalar potential and comparing the result with the known vector potential.

The scalar potential problem may be stated as follows: Let W' denote the scalar potential of the magnet in free space. The perturbing potential which must be added to W' in region I to satisfy boundary conditions at the inner surface of the shell is denoted by W_1. The net scalar potentials in regions II and III are denoted by W_2 and W_3, respectively. The equations appropriate to each region are the following:

Region I: $$\nabla^2 (W_1 + W') = 0 \qquad (1)$$

Region II: $$\nabla^2 W_2 = \frac{\mu_2}{\rho} \frac{\partial W_2}{\partial t} \qquad (2)$$

Region III: $$\nabla^2 W_3 = 0 \qquad (3)$$

The boundary conditions at the surfaces of the shell are as follows:

Inside surface:

$$W'+W_1 = W_2 \tag{4}$$

$$\frac{1}{\mu_2}\frac{\partial}{\partial r}[r(W'+W_1)] = \frac{1}{\mu_3}\frac{\partial}{\partial r}(rW_2) \tag{5}$$

Outside surface:

$$W_2 = W_3 \tag{6}$$

$$\frac{1}{\mu_2}\frac{\partial}{\partial r}(rW_2) = \frac{1}{\mu_3}\frac{\partial(rW_3)}{\partial r} \tag{7}$$

Before solving this problem, it is necessary to see how the scalar potential of the cruciform magnet can be obtained and how the potential can be referenced to a set of axes fixed in the shell.

3.9 EXPANSION OF THE SCALAR POTENTIAL IN A SERIES OF SPHERICAL HARMONICS

Since W' is a solution of Laplace's equation in the region outside of the magnet, it is possible to expand W' in a series of spherical harmonics with respect to a set of reference coordinate axes. The coefficients of this expansion must be obtainable from the known vector potential of the magnet. Also, the expansion should be in a form which simplifies the transformation from coordinates fixed in the magnet to coordinates fixed in the shell.

Let x', y', z' denote a set of rectangular coordinate axes coinciding with the axes of the cruciform, and let the positive axes correspond with the north magnetic poles. Consider first the potential W_z' of the equivalent bar magnet along the z' axis. Let r, θ', φ' denote the spherical polar coordinates of an arbitrary point P with respect to the x', y', z' axes. Since W_z' is independent of φ' as discussed earlier, W_z' can be expanded in a series of zonal harmonics $P_n(\cos\theta')$ on the surface, $r = r_1$, coinciding with the inside surface of the shell. Thus, for $W_z' = W_z'(r,\theta')$ and $r = r_1$,

$$W_z' = W_z'(r_1,\theta') = \sum_{n=1}^{\infty} a_n P_n(\cos\theta') = \sum_{n=1}^{\infty} a_n P_n(u') \qquad (1)$$

where $u' = \cos\theta'$. According to (3.7-14) and (3.7-15) W_z' is related to the vector potential $\bar{A}_z'$ by

$$\bar{A}_z' = \bar{e}_\varphi' A_{z\varphi}' = -\bar{e}_\varphi' \frac{\partial W_z'}{\partial \theta'} \qquad (2)$$

so that

$$A'_{z_\varphi} = - \frac{\partial W'_z}{\partial \theta'} \tag{3}$$

On the surface $r = r_1$,

$$\begin{aligned} A'_{z_\varphi}(r_1, \theta') &= - \frac{\partial W'_z}{\partial \theta'} (r_1, \theta') \\ &= - \sum_{n=1}^{\infty} a_n \frac{dP_n(u')}{du'} \frac{du'}{d\theta'} \\ &= (1-u'^2)^{\frac{1}{2}} \sum_{n=1}^{\infty} a_n \frac{dP_n(u')}{du'} \\ &= \sum_{n=1}^{\infty} a_n P_n^1(u') \end{aligned} \tag{4}$$

where $P_n^1(u')$ is an associated Legendre function of the first kind. The coefficients of the expansion can be obtained from the known function, $A'_{z_\varphi}(r,\theta)$ by means of the formula,

$$a_n = \left(\frac{2n+1}{2}\right) \frac{(n-1)!}{(n+1)!} \int_{-1}^{+1} A'_{z_\varphi}(u') P_n^1(u') du' \tag{5}$$

where $A'_{z_\varphi}(u') \triangleq A'_{z_\varphi}(r_1, \theta')$.

The above formula follows from the orthogonality properties of associated Legendre functions; viz.

$$\int_{-1}^{+1} P_n^m(u) P_{n'}^m(u) du = 0, \quad n \neq n' \tag{6}$$

$$\int_{-1}^{+1} [P_n^m(u)]^2 \, du = \frac{2}{2n+1} \frac{(n+m)!}{(n-m)!} \tag{7}$$

Once the coefficients a_n of the zonal harmonic expansion of W_Z' on the surface $r = r_1$ have been determined, the spherical harmonic expansion of W_Z' at all points in the space, $b<r<r_1$, where b is the length of each arm of the cruciform, must have the form,

$$W_Z' = W_Z'(r,\theta') = \sum_{n=1}^{\infty} a_n \left(\frac{r}{r_1}\right)^{-n-1} P_n(u') \qquad (8)$$

Note that the singularity is placed at the origin, because the source of potential is enclosed by the shell.

Formula (5) provides the necessary link between the vector boundary value problem and the corresponding scalar problem; i.e. the results can be obtained in terms of known quantities. The actual calculation of these coefficients appears in Appendix A.

Similar expressions for the scalar potentials W_X' and W_Y' of the x′ and y′ bar magnets can be derived using new sets of polar coordinates. By means of the biaxial expansion theorem for zonal harmonics, which is stated in the next section, each potential can be expressed in a common reference coordinate system to obtain the net potential, $W' = W_X' + W_Y' + W_Z'$.

3.10 EXPANSION OF THE SCALAR POTENTIAL WITH RESPECT TO THE AXIS OF ROTATION OF THE MAGNET

In the previous section the scalar potential of a cylindrical bar magnet was expanded in a series of zonal harmonics on the surface $r=r_1$. These harmonics are referenced to the axis of the cylinder. By means of the biaxial expansion theorem*, it is possible to obtain the expansion of the potential in general surface harmonics referenced to an arbitrary axis passing through the origin. The particular axis of interest is the axis of rotation of the cruciform magnet relative to the shell. For the purpose of this analysis, the location of the axis of rotation can be specified by its direction cosines or by the corresponding angles between the rotation axis and each of the axes of the cruciform. The individual expansions for each equivalent bar magnet in the cruciform are readily combined to give the surface harmonic expansion of the net potential W′ with respect to the axis of rotation.

According to the biaxial expansion theorem, a zonal harmonic referred to a θ' axis can be expanded in a series of surface harmonics $S_n^m(\theta,\varphi)$ referred to another θ axis which passes through the origin and makes an angle Θ with the θ' axis; i.e.

$$P_n(\cos\theta') = \sum_{m=0}^{n} (2-\delta_m^0)\frac{(n-m)!}{(n+m)!} P_n^m(\cos\Theta)P_n^m(\cos\theta)\cos m(\varphi-\Phi) \qquad (1)$$

where Φ is the azimuth angle of the θ' axis relative to the θ axis. In the above formula $\delta_0^0 = 1$ and $\delta_m^0 = 0$ if $m\neq 0$.

---

*Reference [3], pp. 154-155.

To apply the biaxial expansion theorem, let ξ, η, ζ denote a set of rectangular coordinate axes fixed with respect to the axes of the cruciform magnet, and let the ζ axis be the axis of relative motion between the magnet and the spherical shell. Denote the angles between the ζ axis and the x′, y′, z′ axes by Θ_x, Θ_y, Θ_z, respectively. Also denote the azimuth angles of the x′, y′, z′ axes in the ξ, η, ζ coordinate system by Φ_x, Φ_y, Φ_z, respectively*. Then the biaxial expansion theorem gives for the scalar potential W_z' on the surface $r=r_1$,

$$W_z' = \sum_{n=1}^{\infty} \sum_{m=0}^{n} a_n (2-\delta_m^0) \frac{(n-m)!}{(n+m)!} P_n^m(\cos\Theta_z) P_n^m(\cos\theta) \cos m(\varphi-\Phi_z) \qquad (2)$$

Similar formulas hold for W_x' and W_y' with Θ_z and Φ_z replaced by the appropriate angles with respect to the x′ and y′ axes.

Then the spherical harmonic expansion of W′ in region I referred to the ξ, η, ζ axes is

$$W' = \sum_{n=1}^{\infty} \sum_{m=0}^{n} a_n \left(\frac{r}{r_1}\right)^{-n-1} (2-\delta_m^0) \frac{(n-m)!}{(n+m)!} P_n^m(\cos\theta)$$

$$\times \left[P_n^m(\cos\Theta_x)\cos m(\varphi-\Phi_x) + P_n^m(\cos\Theta_y)\cos m(\varphi-\Phi_y) \right.$$

$$\left. + P_n^m(\cos\Theta_z)\cos m(\varphi-\Phi_z) \right] \qquad (3)$$

The terms within the bracket may be combined as follows: Let $\alpha_{nm} = P_n^m(\cos\Theta_x)$, $\beta_{nm} = P_n^m(\cos\Theta_y)$, and $\gamma_{nm} = P_n^m(\cos\Theta_z)$. Then

$$\alpha_{nm}\cos m(\varphi-\Phi_x) + \beta_{nm}\cos m(\varphi-\Phi_y) + \gamma_{nm}\cos m(\varphi-\Phi_x)$$

$$= (\alpha_{nm}\cos m\Phi_x + \beta_{nm}\cos m\Phi_y + \gamma_{nm}\cos m\Phi_z)\cos m\varphi$$

$$+ (\alpha_{nm}\sin m\Phi_x + \beta_{nm}\sin m\Phi_y + \gamma_{nm}\sin m\Phi_z)\sin m\varphi \qquad (4)$$

*The degenerate cases corresponding to $\Theta_x=0$, etc., are excluded from the present discussion.

Let

$$\sigma_{nm} = \alpha_{nm}\cos m\Phi_x + \beta_{nm}\cos m\Phi_y + \gamma_{nm}\cos m\Phi_z \tag{5}$$

$$\tau_{nm} = \alpha_{nm}\sin m\Phi_x + \beta_{nm}\sin m\Phi_y + \gamma_{nm}\sin m\Phi_z \tag{6}$$

$$\epsilon_{nm} = \tan^{-1}(\tau_{nm}/\sigma_{nm}) \tag{7}$$

Then

$$\alpha_{nm}\cos m(\varphi-\Phi_x) + \beta_{nm}\cos m(\varphi-\Phi_y) + \gamma_{nm}\cos m(\varphi-\Phi_z)$$

$$= \sqrt{\sigma_{nm}^2 + \tau_{nm}^2}\,\cos(m\varphi-\epsilon_{nm}) \tag{8}$$

so that

$$W' = \sum_{n=1}^{\infty}\sum_{m=0}^{n} a_n\left(\frac{r}{r_1}\right)^{-n-1}(2-\delta_m^0)\frac{(n-m)!}{(n+m)!}P_n^m(\cos\theta)\sqrt{\sigma_{nm}^2+\tau_{nm}^2}\,\cos(m\varphi-\epsilon_{nm}) \tag{9}$$

Finally, it is a simple matter to express W′ in a coordinate system fixed in the shell. Let x, y, z be a set of rectangular coordinate axes fixed in the shell, such that z = ζ. If the rotation of the magnet is measured by the angle ψ that the ξ axis makes with the x axis, then the expression for W′ relative to the x, y, z axes is obtained from (9) with $\varphi \rightarrow \varphi+\psi$.

$$W' = \sum_{n=1}^{\infty}\sum_{m=0}^{n} a_n\left(\frac{r}{r_1}\right)^{-n-1}(2-\delta_m^0)\frac{(n-m)!}{(n+m)!}\sqrt{\sigma_{nm}^2 + \tau_{nm}^2}\,P_n^m(\cos\theta)$$

$$\times\,\cos[m(\varphi+\psi)-\epsilon_{nm}] \tag{10}$$

In (10) φ is measured from the x axis. For steady rotation, $\psi=\Omega t$.

It is apparent that the above result is in a form that is particularly convenient for further analysis. A set of coefficients, a_n, which characterize the magnet is computed from (3.9-5). These coefficients depend only on the parameters of the magnet and are

shell and are independent of the rotation. The quantities σ_{nm}, τ_{nm}, and ϵ_{nm} are expressed in terms of the angles Θ_X, Θ_Y, Θ_Z, Φ_X, Φ_Y, and Φ_Z, which relate the axis of rotation to the axes of the cruciform. The θ coordinate is invariant under rotation about the ζ axis, and the angle ψ which describes the rotation is contained in only one factor of each term in the summation. Thus, when ψ is dependent upon t, it is a simple matter to compute the time derivative. Further analysis to eliminate the azimuth angles Φ_X, Φ_Y, and Φ_Z from the quantity, $\sigma_{nm}^2 + \tau_{nm}^2$ is presented in Appendix B.

3.11 STEADY-STATE SOLUTION OF THE BOUNDARY VALUE PROBLEM FOR THE SCALAR POTENTIAL

Enough theory has now been developed to enable the boundary value problem for the scalar potential to be solved for a specified rotation of the cruciform magnet. This section will be devoted to obtaining the steady-state solution for the case, $\psi=\Omega t$ in the expression (3.10-10) for W'.

It will be convenient to use phasor quantities in the subsequent analysis. A phasor will be denoted by an inverted circumflex $\check{\ }$ and the complex conjugate phasor will be denoted by the circumflex $\hat{\ }$.

The solution for a general term in the expansion of (3.10-11) will be derived, and the solution for the complete expansion of W' can then be obtained by superposition.

Denote the general term in the expansion for W' by

$$\check{W}'_{nm} = \check{A}_{nm}\left(\frac{r}{r_1}\right)^{-n-1} P_n^m(\cos\theta)e^{im(\varphi+\Omega t)} \qquad (1)$$

where the phase angle ε_{nm} of (3.10-11) has been absorbed by the complex coefficient $\check{A}_{nm}$. The above expression may be written in the equivalent forms

$$\check{W}'_{nm} = \check{A}_{nm}\left(\frac{r}{r_1}\right)^{-n-1}\check{S}_n^m(\theta,\varphi)e^{im\Omega t} = \check{V}'_{nm}e^{im\Omega t} \qquad (2)$$

where

$$\check{S}_n^m(\theta,\varphi) = P_n^m(\cos\theta)e^{im\varphi} \qquad (3)$$

and

$$\check{V}'_{nm} = \check{A}_{nm}\left(\frac{r}{r_1}\right)^{-n-1}\check{S}_n^m(\theta,\varphi) \qquad (4)$$

The problem is to solve

$$\nabla^2 \overset{v}{W}_2 = \frac{\mu_2}{\rho} \frac{\partial \overset{v}{W}_2}{\partial t} \tag{5}$$

in region II ($r_1 \le r \le r_2$) subject to the inhomogeneous, time-varying boundary conditions at $r=r_1$,

$$\overset{v}{W}'_{nm} + \overset{v}{W}_1 = \overset{v}{W}_2 \tag{6}$$

$$\frac{1}{\mu_1} \frac{\partial}{\partial r}\left[r(\overset{v}{W}'_{nm} + \overset{v}{W}_1)\right] = \frac{1}{\mu_2} \frac{\partial}{\partial r}(r\overset{v}{W}_2) \tag{7}$$

and the homogeneous boundary conditions at $r=r_2$,

$$\overset{v}{W}_2 = \overset{v}{W}_3 \tag{8}$$

$$\frac{1}{\mu_2} \frac{\partial}{\partial r}(r\overset{v}{W}_2) = \frac{1}{\mu_3} \frac{\partial}{\partial r}(r\overset{v}{W}_3) \tag{9}$$

The perturbing potentials $\overset{v}{W}_1$ and $\overset{v}{W}_3$ must satisfy Laplace's equation in regions I and III, respectively; i.e.,

$$\nabla^2 \overset{v}{W}_1 = 0 \qquad 0<r\le r_1 \tag{10}$$

$$\nabla^2 \overset{v}{W}_3 = 0 \qquad r\ge r_2 \tag{11}$$

For the steady-state solution assume that $\overset{v}{W}_j = \overset{v}{V}_j e^{im\Omega t}$ for $j=1,2,3$. The above equations reduce as follows:

$$\nabla^2 \overset{v}{V}_2 - \lambda_m^2 \overset{v}{V}_2 = 0 \quad , \quad r_1 \le r \le r_2 \tag{12}$$

where $$\lambda_m = \sqrt{i\mu_2 m\Omega/\rho} = \sqrt{\mu_2 m\Omega/\rho}\, e^{i\pi/4} \tag{13}$$

At $r=r_1$

$$\overset{v}{V}_{nm} + \overset{v}{V}_1 = \overset{v}{V}_2 \tag{14}$$

$$\frac{1}{\mu_2} \frac{\partial}{\partial r}\left[r(\overset{v}{V}_{nm} + \overset{v}{V}'_1)\right] = \frac{1}{\mu_1} \frac{\partial}{\partial r}(r\overset{v}{V}_2) \tag{15}$$

At $r=r_2$,

$$\overset{v}{V}_2 = \overset{v}{V}_3 \tag{16}$$

$$\frac{1}{\mu_2}\frac{\partial}{\partial r}(r\overset{v}{V}_2) = \frac{1}{\mu_3}\frac{\partial}{\partial r}(r\overset{v}{V}_3) \tag{17}$$

Also,

$$\nabla^2 \overset{v}{V}_1 = 0 \qquad 0 \le r \le r_1 \tag{18}$$

$$\nabla^2 \overset{v}{V}_3 = 0 \qquad r \ge r_2 \tag{19}$$

Consider first the equation (12) for $\overset{v}{V}_2$. Assume that $\overset{v}{V}_2 = \overset{v}{R}_2(r)\overset{v}{Q}_2(\theta,\varphi)$. In spherical polar coordinates,

$$\nabla^2 = \frac{\partial^2}{\partial r^2} + \frac{2}{r}\frac{\partial}{\partial r} + \frac{1}{r^2}L_\omega \tag{20}$$

where

$$L_\omega = \frac{\partial^2}{\partial\theta^2} + \cot\theta\,\frac{\partial}{\partial\theta} + \csc^2\theta\,\frac{\partial^2}{\partial\varphi^2} \tag{21}$$

Substitution for $\overset{v}{V}_2$ in (12) yields the following two separated equations for the radial and angular factors:

$$\frac{d^2\overset{v}{R}_2}{dr^2} + \frac{2}{r}\frac{d\overset{v}{R}_2}{dr} - \left(\lambda^2 + \frac{K_1}{r^2}\right)\overset{v}{R}_2 = 0 \tag{22}$$

and

$$\frac{\partial^2\overset{v}{Q}_2}{\partial\theta^2} + \cot\frac{\partial\overset{v}{Q}_2}{\partial\theta} + \csc^2\theta\,\frac{\partial^2\overset{v}{Q}_2}{\partial\varphi^2} + K_1\overset{v}{Q}_2 = 0 \tag{23}$$

where K_1 is the separation constant. For $K_1 = N(N+1)$, where N is a positive integer, equation (15) defines $\overset{v}{Q}_2$ to be a surface harmonic of degree N and order M; i.e.,

$$\overset{v}{Q}_2 = \overset{v}{B}_{NM}\,\overset{v}{S}_N^M(\theta,\varphi) = \overset{v}{B}_{NM}\,P_N^M(\cos\theta)e^{iM\varphi} \tag{24}$$

where M is an integer less than or equal to N. For each pair of integers N, M, the arbitrary constant $\overset{v}{B}_{N\,M}$ is evaluated from the boundary conditions. Since the only inhomogeneous term in the boundary conditions contains a surface harmonic, $S_n^m(\theta,\varphi)$, as seen from (14) and (4), the appropriate values of N and M are N=n and M=m. Thus,

$$\overset{v}{Q}_2 = \overset{v}{B}_{n\,m}\overset{v}{S}_n^m(\theta,\varphi) = \overset{v}{B}_{n\,m}P_n^m(\cos\theta)e^{im\varphi} \tag{25}$$

The equation for $\overset{v}{R}_2$ is now

$$\frac{d^2\overset{v}{R}_2}{dr^2} + \frac{2}{r}\frac{d\overset{v}{R}_2}{dr} - \left[\lambda_m^2 + \frac{n(n+1)}{r^2}\right]\overset{v}{R}_2 = 0 \tag{26}$$

Let $z=\lambda_m r$. Then (26) becomes

$$\frac{d^2\overset{v}{R}_2}{dz^2} + \frac{2}{z}\frac{d\overset{v}{R}_2}{dz} - \left[1 + \frac{n(n+1)}{z^2}\right]\overset{v}{R}_2 = 0 \tag{27}$$

This is a modified spherical Bessel equation in the complex domain ($z=|\lambda_m|re^{i\pi/4}$). Two linearly independent solutions are the modified spherical Bessel functions of the first kind

$$\xi_n(z) = \sqrt{\frac{\pi}{2z}}\,I_{n+1/2}(z) \tag{28}$$

and the second kind,

$$\eta_n(z) = \sqrt{\frac{\pi}{2z}}\,I_{-n-1/2}(z) \tag{29}$$

The singularities of $\xi_n(z)$ and $\eta_n(z)$ occur at z=0 and $z=\infty$. A general solution of (27) which is regular in the interval $r_1 \le r \le r_2$ is, therefore,

$$\overset{v}{R}_2 = \overset{v}{C}_n \xi_n(z) + \overset{v}{D}_n \eta_n(z) \tag{30}$$

From (25) and (30) the solution of (12) has the form

$$\overset{v}{V}_2 = [\overset{v}{C}_{nm} \xi_n(z) + \overset{v}{D}_{nm} \eta_n(z)] P_n^m(\cos\theta) e^{im\varphi} \tag{31}$$

where $\overset{v}{C}_{nm} = \overset{v}{C}_n \overset{v}{B}_{nm}$ and $\overset{v}{D}_{nm} = \overset{v}{D}_n \overset{v}{B}_{nm}$.

The solutions of Laplace's equation for $\overset{v}{V}_1$ and $\overset{v}{V}_3$ are spherical harmonics. In the region $0 \le r \le r_1$, the harmonic has the form

$$\overset{v}{V}_1 = \overset{v}{E}_{nm} \left(\frac{r}{r_1}\right)^n P_n^m(\cos\theta) e^{im\varphi} \tag{32}$$

This harmonic is regular at the origin, corresponding with the fact that the source of potential is exterior to the region $0 \le r \le r_1$. In region III, $r \ge r_2$, the harmonic should be regular at $r=\infty$, since the source of potential is within region II, $r_1 \le r \le r_2$.

$$\therefore \overset{v}{V}_3 = \overset{v}{F}_{nm} \left(\frac{r}{r_2}\right)^{-n-1} P_n^m(\cos\theta) e^{im\varphi} \tag{33}$$

Note that the radial part of $\overset{v}{V}_3$ is normalized with respect to r_2.

There are now four arbitrary constants, $\overset{v}{C}_{nm}$, $\overset{v}{D}_{nm}$, $\overset{v}{E}_{nm}$ and $\overset{v}{F}_{nm}$ which must be evaluated. These can be determined from the four boundary conditions.

Substituting (4), (31), and (32) into (14) and canceling $P_n^m(\cos\theta) e^{im\varphi}$ yields for $r=r_1$,

$$\overset{v}{A}_{nm} + \overset{v}{E}_{nm} = \overset{v}{C}_{nm} \xi_n(z_1) + \overset{v}{D}_{nm} \eta_n(z_1) \tag{34}$$

where $z_1=\lambda_m r_1$. Since $\mu_1=\mu_2=\mu_o$, substituting (4), (31), and (32) into (15) yields for $r=r_1$,

$$-\overset{v}{A}_{nm}(n+1) + \overset{v}{E}_{nm}\, n = z_1\left[\overset{v}{C}_{nm}\xi_n'(z_1) + \overset{v}{D}_{nm}\eta_n'(z_1)\right] \qquad (35)$$

where the primes denote the derivative with respect to z. The boundary conditions (16) and (17) give the following two relations between the constants:

$$\overset{v}{C}_{nm}\xi_n(z_2) + \overset{v}{D}_{nm}\eta_n(z_2) = \overset{v}{F}_{nm} \qquad (36)$$

$$z_2\left[\overset{v}{C}_{nm}\xi_n'(z_2) + \overset{v}{D}_{nm}\eta_n'(z_2)\right] = -\overset{v}{F}_{nm}(n+1) \qquad (37)$$

Equations (34), (35), (36), and (37) can now be solved simultaneously for the four unknown constants.

First eliminate $\overset{v}{E}_{nm}$ from (34) and (35) by multiplying each term in (34) by n and then subtracting (35). Thus,

$$(2n+1)\overset{v}{A}_{nm} = \left[n\xi_n(z_1)-z_1\xi_n'(z_1)\right]\overset{v}{C}_{nm} + \left[n\eta_n(z_2)-z_1\eta_n'(z_1)\right]\overset{v}{D}_{nm} \qquad (38)$$

Next eliminate $\overset{v}{F}_{nm}$ from (36) and (37) in a similar manner.

$$0 = \left[(n+1)\xi_n(z_2)+z_2\xi_n'(z_2)\right]\overset{v}{C}_{nm} + \left[(n+1)\eta_n(z_2)+z_2\eta_n'(z_2)\right]\overset{v}{D}_{nm} \qquad (39)$$

Before solving (38) and (41) for $\overset{v}{C}_{nm}$ and $\overset{v}{D}_{nm}$, it is possible to simplify the coefficients considerably by using the following recurrence relations for the modified spherical Bessel functions:

$$\frac{n+1}{z} f_n(z) + \frac{df_n(z)}{dz} = f_{n-1}(z) \qquad (40)$$

$$-\frac{n}{z} f_n(z) + \frac{df_n(z)}{dz} = f_{n+1}(z) \qquad (41)$$

where $f_n(z) = \xi_n(z)$ or $\eta_n(z)$.

Application of (40) and (41) to (38) and (39) yields

$$(2n+1)\overset{\vee}{A}_{nm} = -z_1[\xi_{n+1}(z_1)\overset{\vee}{C}_{nm}+\eta_{n+1}(z_1)\overset{\vee}{D}_{nm}] \tag{42}$$

$$0 = z_2[\xi_{n-1}(z_2)\overset{\vee}{C}_{nm}+\eta_{n-1}(z_2)\overset{\vee}{D}_{nm}] \tag{43}$$

A necessary and sufficient condition for these two equations to have a unique solution for $\overset{\vee}{C}_{nm}$ and $\overset{\vee}{D}_{nm}$ is that

$$\Delta_{n+1,n-1}(z_1,z_2) = \xi_{n+1}(z_1)\eta_{n-1}(z_2)-\eta_{n+1}(z_1)\xi_{n-1}(z_2) \neq 0 \tag{44}$$

Assuming that this condition is satisfied*, the solutions for $\overset{\vee}{C}_{nm}$ and $\overset{\vee}{D}_{nm}$ are as follows:

$$\overset{\vee}{C}_{nm} = -\left(\frac{2n+1}{z_1}\right)\frac{\eta_{n-1}(z_2)}{\Delta_{n+1,n-1}(z_1,z_2)}\overset{\vee}{A}_{nm} \tag{45}$$

$$\overset{\vee}{D}_{nm} = \left(\frac{2n+1}{z_1}\right)\frac{\xi_{n-1}(z_2)}{\Delta_{n+1,n-1}(z_1,z_2)}\overset{\vee}{A}_{nm} \tag{46}$$

The two remaining constants, $\overset{\vee}{E}_{nm}$ and $\overset{\vee}{F}_{nm}$, can now be determined. From (34)

$$\begin{aligned}\overset{\vee}{E}_{nm} &= \left\{\left(\frac{2n+1}{z_1}\right)\frac{1}{\Delta_{n+1,n-1}(z_1,z_2)}[-\eta_{n-1}(z_2)\xi_n(z_1)+\xi_{n-1}(z_2)\eta_n(z_1)]-1\right\}\overset{\vee}{A}_{nm} \\ &= \Big\{-[(2n+1)\xi_n(z_1)+z_1\xi_{n+1}(z_1)]\eta_{n-1}(z_2) \\ &\qquad +[(2n+1)\eta_n(z_1)+z_1\eta_{n+1}(z_1)]\xi_{n-1}(z_2)\Big\}\frac{\overset{\vee}{A}_{nm}}{z_1\Delta_{n+1,n-1}(z_1,z_2)}\end{aligned} \tag{47}$$

This formula can be simplified by means of another recurrence relation for $\xi_n(z)$ or $\eta_n(z)$; viz.

$$(2n+1)f_n(z) = z[f_{n-1}(z) - f_{n+1}(z)] \tag{48}$$

---

*See (3.16-13)

where $f_n(z)$ denotes either of the two functions, $\xi_n(z)$ or $\eta_n(z)$.

$$\therefore \overset{v}{E}_{n\,m} = \frac{[-\xi_{n-1}(z_1)\eta_{n-1}(z_2)+\eta_{n-1}(z_1)\xi_{n-1}(z_2)]}{\Delta_{n+1,n-1}(z_1,z_2)}\overset{v}{A}_{n\,m} \qquad (49)$$

Using the notation of (44)

$$\overset{v}{E}_{n\,m} = -\frac{\Delta_{n-1,n-1}(z_1,z_2)}{\Delta_{n+1,n-1}(z_1,z_2)}\overset{v}{A}_{n\,m} \qquad (50)$$

Finally from (36),

$$\overset{v}{F}_{n\,m} = \left(\frac{2n+1}{z_1}\right)\frac{1}{\Delta_{n+1,n-1}(z_1,z_2)}[-\eta_{n-1}(z_2)\xi_n(z_2)+\xi_{n-1}(z_2)\eta_n(z_2)]\overset{v}{A}_{n\,m} \qquad (51)$$

$$= -\left(\frac{2n+1}{z_1}\right)\frac{\Delta_{n,n-1}(z_2,z_2)}{\Delta_{n+1,n-1}(z_1,z_2)}\overset{v}{A}_{n\,m} \qquad (52)$$

This completes the evaluation of the constants.

The potential of main interest is $\overset{v}{W}_2$, since the eddy currents are derived from it.

$$\overset{v}{W}_2 = [\overset{v}{C}_{n\,m}\xi_n(z)+\overset{v}{D}_{n\,m}\eta_n(z)]P_n^m(\cos\theta)e^{im(\varphi+\Omega t)} \qquad (53)$$

$$= \left(\frac{2n+1}{z_1}\right)\frac{\overset{v}{A}_{n\,m}}{\Delta_{n+1,n-1}(z_1,z_2)}[-\eta_{n-1}(z_2)\xi_n(z)+\xi_{n-1}(z_2)\eta_n(z)]$$

$$\times P_n^m(\cos\theta)e^{im(\varphi+\Omega t)} \qquad (54)$$

$$= -\left(\frac{2n+1}{z_1}\right)\frac{\Delta_{n,n-1}(z,z_2)}{\Delta_{n+1,n-1}(z_1,z_2)}\overset{v}{A}_{n\,m}P_n^m(\cos\theta)e^{im(\varphi+\Omega t)} \qquad (55)$$

$$= -\left(\frac{2n+1}{z_1}\right)\frac{\Delta_{n,n-1}(z,z_2)}{\Delta_{n+1,n-1}(z_1,z_2)}a_n(2-\delta_m^\circ)\frac{(n-m)!}{(n+m)!}\sqrt{\sigma_{n\,m}^2+\tau_{n\,m}^2}$$

$$\times P_n^m(\cos\theta)e^{i[m(\varphi+\Omega t)-\varepsilon_{n\,m}]} \qquad (56)$$

The solution for the complete expansion of $\overset{v}{W}_2$ is finally

$$\overset{v}{W}_2 = -\sum_{n=1}^{\infty}\sum_{m=0}^{n}\left(\frac{2n+1}{z_1}\right)\frac{\Delta_{n,n-1}(z,z_2)}{\Delta_{n+1,n-1}(z_1,z_2)}\; a_n(2-\delta_m^o)\frac{(n-m)!}{(n+m)!}\sqrt{\sigma_{nm}^2+\tau_{nm}^2}$$

$$\times\; P_n^m(\cos\theta)e^{i[m(\varphi+\Omega t)-\varepsilon_{nm}]} \qquad (57)$$

for $r_1 \le r \le r_2$.

3.12 DERIVATION OF THE STEADY-STATE VECTOR POTENTIAL

The vector potential in region II corresponding to steady rotation of the cruciform magnet relative to the shell is obtained from W_2. The coordinate system (x,y,z) is again fixed in the shell such that the z axis is the axis of rotation of the magnet. The required formula for $\bar{A}_2$ is given by (3.6-15) with appropriate changes in notation; i.e.,

$$\bar{A}_2 = \bar{e}_\theta \frac{1}{\sin\theta} \frac{\partial W_2}{\partial \varphi} - \bar{e}_\varphi \frac{\partial W_2}{\partial \theta} \tag{1}$$

It will be convenient to retain the phasor representation of quantities introduced in section 3.11. From (3.11-57) the basic term in $\overset{v}{W}_2$ is

$$\overset{v}{W}_2 = \overset{v}{K}_{nm} \Delta_{n,n-1}(z,z_2) P_n^m(\cos\theta) e^{im(\varphi+\Omega t)} \tag{2}$$

where $$\overset{v}{K}_{nm} = -\left(\frac{2n+1}{z_1}\right) \frac{\overset{v}{A}_{nm}}{\Delta_{n+1,n-1}(z_1,z_2)} \tag{3}$$

$$\therefore \frac{\partial \overset{v}{W}_2}{2\varphi} = im\overset{v}{K}_{nm} \Delta_{n,n-1}(z,z_2) P_n^m(\cos\theta) e^{im(\varphi+\Omega t)} \tag{4}$$

Next, $$\frac{\partial \overset{v}{W}_2}{\partial \theta} = \overset{v}{K}_{nm} \Delta_{n,n-1}(z,z_2) \frac{dP_n^m(\cos\theta)}{d\theta} e^{im(\varphi+\Omega t)} \tag{5}$$

The derivative can be expressed in terms of associated Legendre functions of order m as follows:

$$\frac{dP_n^m(\cos\theta)}{d\theta} = \frac{dP_n^m(u)}{du} \frac{du}{d\theta} = -(1-u^2)^{\frac{1}{2}} \frac{dP_n^m(u)}{du} \tag{6}$$

where $u=\cos\theta$. Using the recurrence formula in m for associated Legendre functions,

$$(1-u^2)\frac{dP_n^m(u)}{du} = -nuP_n^m(u) + (m+n)P_{n-1}^m(u) \tag{7}$$

obtain

$$\frac{dP_n^m(\cos\theta)}{d\theta} = (1-u^2)^{-\frac{1}{2}}[nuP_n^m(u)-(m+n)P_{n-1}^m(u)] \tag{8}$$

so that

$$\frac{\partial \overset{v}{W}_2}{\partial\theta} = \overset{v}{K}_{nm}\Delta_{n,n-1}(z,z_2)(1-u^2)^{-\frac{1}{2}}[nuP_n^m(u)-(m+n)P_{n-1}^m(u)] \times e^{im(\varphi+\Omega t)} \tag{9}$$

Using the notation

$$\overset{v}{A}_2 = \bar{e}_\theta \overset{v}{A}_{2\theta} + \bar{e}_\varphi \overset{v}{A}_{2\varphi} \tag{10}$$

then the general terms for $\overset{v}{A}_{2\theta}$ and $\overset{v}{A}_{2\varphi}$ are as follows:

$$\overset{v}{A}_{2\theta} = im\overset{v}{K}_{nm}\Delta_{n,n-1}(z,z_2)\frac{P_n^m(\cos\theta)}{\sin\theta}e^{im(\varphi+\Omega t)} \tag{11}$$

$$= im\overset{v}{K}_{nm}\Delta_{n,n-1}(z,z_2)(1-u^2)^{-\frac{1}{2}}P_n^m(u)e^{im(\varphi+\Omega t)} \tag{12}$$

$$\overset{v}{A}_{2\varphi} = -\overset{v}{K}_{nm}\Delta_{n,n-1}(z,z_2)(1-u^2)^{-\frac{1}{2}}[nuP_n^m(u)-(m+n)P_{n-1}^m(u)] \times e^{im(\varphi+\Omega t)} \tag{13}$$

$$= -\overset{v}{K}_{nm}\Delta_{n,n-1}(z,z_2)\left[n\cot\theta P_n^m(\cos\theta)-(m+n)\frac{P_{n-1}^m(\cos\theta)}{\sin\theta}\right] \times e^{im(\varphi+\Omega t)} \tag{14}$$

The complete expression for $\overset{v}{A}_2$ is obtained by substituting (12) and (14) into (10) and summing over m and n; however, this step will be deleted for the sake of brevity.

3.13 DERIVATION OF THE STEADY-STATE EDDY CURRENT DENSITY

According to (3.4-7), the eddy current density $\bar{J}$ in the shell is given by

$$\bar{J} = -\frac{1}{\rho}\frac{\partial \bar{A}_2}{\partial t} \tag{1}$$

where $\bar{A}_2$ is the vector potential for $r_1 \leq r \leq_2$, and ρ is the volume resistivity. Continuing with the use of phasor quantities and substituting the general term of the series expansion of $\overset{\vee}{\bar{A}}$ into (1) gives the following results:

$$\overset{\vee}{\bar{J}} = \bar{e}_\theta \overset{\vee}{J}_\theta + \bar{e}_\varphi \overset{\vee}{J}_\varphi \tag{2}$$

$$\overset{\vee}{J}_\theta = \frac{m^2\Omega}{\rho}\overset{\vee}{K}_{nm}\Delta_{n,n-1}(z,z_2)\frac{P_n^m(\cos\theta)}{\sin\theta}e^{im(\varphi+\Omega t)} \tag{3}$$

$$= \frac{m^2\Omega}{\rho}\overset{\vee}{K}_{nm}\Delta_{n,n-1}(z,z_2)(1-u^2)^{-\frac{1}{2}}P_n^m(u)e^{im(\varphi+\Omega t)} \tag{4}$$

$$\overset{\vee}{J}_\varphi = \frac{im\Omega}{\rho}\overset{\vee}{K}_{nm}\Delta_{n,n-1}(z,z_2)$$

$$x\left[n\cot\theta P_n^m(\cos\theta) - (m+n)\frac{P_{n-1}^m(\cos\theta)}{\sin\theta}\right]e^{im(\varphi+\Omega t)} \tag{5}$$

$$= \frac{im\Omega}{\rho}\overset{\vee}{K}_{nm}\Delta_{n,n-1}(z,z_2)$$

$$x\ (1-u^2)^{-\frac{1}{2}}[nuP_n^m(u) - (m+n)P_{n-1}^m(u)]e^{im(\varphi+\Omega t)} \tag{6}$$

The summations over m and n are omitted.

3.14 DERIVATION OF THE MAGNETIC FIELD INDUCTION

The next task is to derive the steady-state magnetic field induction $\bar{B}_2$ in region II, corresponding to steady rotation of the magnet, from the known potential W_2. This is accomplished with the aid of formulas (3.6-21) and (3.6-22) for the radial and tangential components of $\bar{B}_2$, respectively. With appropriate changes in notation, (3.6-21) becomes

$$\bar{B}_{2r} = -\frac{\bar{e}_r}{r} L_\omega [W_2] = -\frac{\bar{e}_r}{r}\left(\frac{\partial^2 W_2}{\partial\theta^2} + \cot\theta \frac{\partial W_2}{\partial\theta} + \csc^2\theta \frac{\partial^2 W_2}{\partial\varphi^2}\right) \quad (1)$$

The general term in the series expansion for the phasor potential $\overset{v}{W}_2$ is, from (3.12-2)

$$\overset{v}{W}_2 = \overset{v}{K}_{nm}\Delta_{n,n-1}(z,z_2)P_n^m(u)e^{im(\varphi+\Omega t)}$$

$$= \overset{v}{K}_{nm}\Delta_{n,n-1}(z,z_2)\overset{v}{S}_n^m(\theta,\varphi)e^{im\Omega t} \quad (2)$$

$$\therefore \quad L_\omega[\overset{v}{W}_2] = \overset{v}{K}_{nm}\Delta_{n,n-1}(z,z_2)L_\omega[\overset{v}{S}_n^m(\theta,\varphi)]e^{im\Omega t} \quad (3)$$

But $$L_\omega[\overset{v}{S}_n^m(\theta,\varphi)] = -n(n+1)\overset{v}{S}_n^m(\theta,\varphi) \quad (4)$$

according to (3.11-23) with $K_1 = n(n+1)$

$$\therefore \quad L_\omega[\overset{v}{W}_2] = -n(n+1)\overset{v}{K}_{nm}\Delta_{n,n-1}(z,z_2)\overset{v}{S}_n^m(\theta,\varphi)e^{im\Omega t} \quad (5)$$

$$= -n(n+1)\overset{v}{W}_2 \quad (6)$$

Substituting into (1)

$$\overset{v}{\bar{B}}_{2r} = \frac{\bar{e}_r}{r} n(n+1)\overset{v}{W}_2 \quad (7)$$

$$= \frac{\bar{e}_r}{r} n(n+1)\overset{v}{K}_{nm}\Delta_{n,n-1}(z,z_2)P_n^m(u)e^{im(\varphi+\Omega t)} \quad (8)$$

Since the second scalar potential discussed in Section 3.6 is zero, (3.6-22) becomes

$$\overset{v}{B}_{2t} = \bar{e}_\theta \frac{1}{r} \frac{\partial^2 (rW_2)}{\partial\theta\partial r} + \bar{e}_\varphi \frac{1}{r\sin\theta} \frac{\partial^2 (rW_2)}{\partial\varphi\partial r} \tag{9}$$

$$= \bar{e}_\theta \frac{\partial}{\partial\theta}\left(\frac{\partial W_2}{\partial r} + \frac{W_2}{r}\right) + \bar{e}_\varphi \frac{1}{\sin\theta} \frac{\partial}{\partial\varphi}\left(\frac{\partial W_2}{\partial r} + \frac{W_2}{r}\right) \tag{10}$$

Using phasor quantities,

$$\frac{\partial W_2}{\partial r} = \lambda_m \overset{v}{K}_{nm} \Delta'_{n,n-1}(z, z_2) P_n^m(u) e^{im(\varphi+\Omega t)} \tag{11}$$

where $z = \lambda_m r$, and the prime denotes the derivative with respect to z. But

$$\Delta_{n,n-1}(z, z_2) = \xi_n(z)\eta_{n-1}(z_2) - \eta_n(z)\xi_{n-1}(z_2) \tag{12}$$

Thus, $\Delta'_{n,n-1}(z, z_2) = \xi'_n(z)\eta_{n-1}(z_2) - \eta'_n(z)\xi_{n-1}(z_2)$ (13)

Using (3.11-42),

$$\Delta'_{n,n-1}(z, z_2) = \left[\xi_{n-1}(z) - \left(\frac{n+1}{z}\right)\xi_n(z)\right] \eta_{n-1}(z_2)$$

$$- \left[\eta_{n-1}(z) - \left(\frac{n+1}{z}\right)\eta_n(z)\right] \xi_{n-1}(z_2)$$

$$= \xi_{n-1}(z)\eta_{n-1}(z_2) - \eta_{n-1}(z)\xi_{n-1}(z_2)$$

$$- \frac{(n+1)}{z}\left[\xi_n(z)\eta_{n-1}(z_2) - \eta_n(z)\right]\xi_{n-1}(z_2)$$

$$= \Delta_{n-1,n-1}(z, z_2) - \left(\frac{n+1}{z}\right)\Delta_{n,n-1}(z, z_2) \tag{14}$$

$$\therefore \quad \frac{\partial W_2}{\partial r} = \lambda_m K_{nm}\left[\Delta_{n-1,n-1}(z, z_2) - \left(\frac{n+1}{z}\right)\Delta_{n,n-1}(z, z_2)\right]$$

$$\times P_n^m(u) e^{im(\varphi+\Omega t)} \tag{15}$$

Combining (2) and (15) yields

$$\frac{\partial \overset{v}{W}_2}{\partial r} + \frac{\overset{v}{W}_2}{r} = \lambda_m \overset{v}{K}_{nm}\left[\Delta_{n-1,n-1}(z,z_2) - \left(\frac{n}{z}\right)\Delta_{n,n-1}(z,z_2)\right]$$

$$\times P_n^m(u)e^{im(\varphi+\Omega t)} \qquad (16)$$

Next,

$$\frac{\partial}{\partial\varphi}\left(\frac{\partial \overset{v}{W}_2}{\partial r} + \frac{\overset{v}{W}_2}{r}\right) = \lambda_m \overset{v}{K}_{nm}\left[\Delta_{n-1,n-1}(z,z_2) - \left(\frac{n}{z}\right)\Delta_{n,n-1}(z,z_2)\right]$$

$$\times (1-u^2)^{-\frac{1}{2}}\left[nuP_n^m(u) - (m+n)P_{n-1}^m(u)\right]e^{im(\varphi+\Omega t)} \qquad (17)$$

Finally,

$$\frac{\partial}{\partial\varphi}\left(\frac{\partial \overset{v}{W}_2}{\partial r} + \frac{\overset{v}{W}_2}{r}\right) = im\lambda_m \overset{v}{K}_{nm}\left[\Delta_{n-1,n-1}(z,z_2) - \left(\frac{n}{z}\right)\Delta_{n,n-1}(z,z_2)\right]$$

$$\times P_n^m(u)e^{im(\varphi+\Omega t)} \qquad (18)$$

Letting $\bar{B}_t = \bar{e}_\theta B_{2\theta} + \bar{e}_\varphi B_{2\varphi}$ (19)

$$B_{2\theta} = \lambda_m \overset{v}{K}_{nm}\left[\Delta_{n-1,n-1}(z,z_2) - \left(\frac{n}{z}\right)\Delta_{n,n-1}(z,z_2)\right]$$

$$\times (1-u^2)^{-\frac{1}{2}}\left[nuP_n^m(u) - (m+n)P_{n-1}^m(u)\right]e^{im(\varphi+\Omega t)} \qquad (20)$$

$$B_{2\varphi} = im\lambda_m \overset{v}{K}_{nm}\left[\Delta_{n-1,n-1}(z,z_2) - \left(\frac{n}{z}\right)\Delta_{n,n-1}(z,z_2)\right]$$

$$\times (1-u^2)^{-\frac{1}{2}}P_n^m(u)e^{im(\varphi+\Omega t)} \qquad (21)$$

The complete expressions for the components of $\bar{B}_2$ are obtained by summing (8), (20) and (21) over m and n.

3.15 DERIVATION OF THE TORQUE FOR A STEADY ROTATION OF THE MAGNET

In section 3.3, it was stated that the force $\bar{f}$ exerted on an elemental volume of a conductor in which the current density is $\bar{J}$ and the magnetic induction is $\bar{B}$ is

$$\bar{f} = \bar{J} \times \bar{B} \qquad (nt - m^{-3}) \tag{1}$$

Expressing J and B_2 in terms of their components in the r, θ, and φ directions

$$\bar{J} = \bar{e}_\varphi J_\varphi + \bar{e}_\theta J_\theta \tag{2}$$

$$\bar{B}_2 = \bar{e}_r B_{2r} + \bar{e}_\theta B_{2\theta} + \bar{e}_\varphi B_{2\varphi} \tag{3}$$

obtain

$$f_r = J_\theta B_{2\varphi} - J_\varphi B_{2\theta} \tag{4}$$

$$f_\theta = J_\varphi B_{2r} \tag{5}$$

$$f_\varphi = -J_\theta B_{2r} \tag{6}$$

These forces on the elemental volume produce torques about the x, y, and z axes fixed in the shell.

The torque about the z axis, due to the force $\bar{f}_\varphi$ acting on the elemental volume dV is

$$n_z = r \sin \theta \; f_\varphi = -r \sin \theta \; J_\theta B_{2r} \qquad (nt - m^{-2}) \tag{7}$$

Neither $\bar{f}_\theta$ nor $\bar{f}_r$ contribute any torque about the z axis. Now in terms of the phasor quantities, $\overset{v}{J}_\theta$ and $\overset{v}{B}_{2r}$, corresponding to steady rotation of the magnet,

$$J_\theta = \mathrm{Re}\{\overset{v}{J}_\theta\}$$

$$= \sum_{n=1}^{\infty}\sum_{m=1}^{n} \frac{m^2\Omega}{\rho}\left|\overset{v}{K}_{nm}\Delta_{n,n-1}(z,z_2)\right| \times \frac{P_n^m(\cos\theta)}{\sin\theta}\cos[m(\varphi+\Omega t)+\chi_{nm}] \qquad (8)$$

where $\chi_{nm} = \arg[\overset{v}{K}_{nm}\Delta_{n,n-1}(z,z_2)]$ (9)

Also,

$$B_{2r} = \mathrm{Re}\{\overset{v}{B}_{2r}\}$$

$$= \sum_{n=1}^{\infty}\sum_{m=0}^{n} \frac{n(n+1)}{r}\left|\overset{v}{K}_{nm}\Delta_{n,n-1}(z,z_2)\right| \times P_n^m(\cos\theta)\cos[m(\varphi+\Omega t)+\chi_{nm}] \qquad (10)$$

Thus,

$$n_z = \sum_{n=1}^{\infty}\sum_{m=1}^{n}\sum_{k=1}^{\infty}\sum_{\ell=0}^{k} -\frac{m^2\Omega}{2\rho}\, k(k+1)\left|\overset{v}{K}_{nm}\Delta_{n,n-1}(z,z_2)\right| \times \left|\overset{v}{K}_{k\ell}\Delta_{k,k-1}(z,z_2)\right| \times P_n^m(\cos\theta)P_k^\ell(\cos\theta)$$

$$\times\{\cos[(m-\ell)(\varphi+\Omega t)+\chi_{nm}-\chi_{k\ell}] + \cos[(m+\ell)(\varphi+\Omega t)+\chi_{nm}+\chi_{k\ell}]\} \qquad (11)$$

The net torque about the z axis due to the forces on all elemental volumes is obtained by integrating (11) over the volume of the shell:

$$N_z = \int_V n_z\, dV = \int_{r_1}^{r_2}\int_0^{\pi}\int_0^{2\pi} n_z r^2 \sin\theta\, d\varphi\, d\theta\, dr \quad (nt - m) \qquad (12)$$

Consider first the integral over φ.

$$I_{\varphi} = \int_0^{2\pi} \{\cos[(m-\ell)(\varphi+\Omega t)+\chi_{nm}-\chi_{k\ell}]$$

$$+ \cos[(m+\ell)(\varphi+\Omega t)+\chi_{nm}+\chi_{k\ell}]\}d\varphi \qquad (13)$$

For m and ℓ positive integers, the value of I_{φ} is zero unless $m=\ell$. Then

$$I_{\varphi} = 2\pi\cos(\chi_{nm}-\chi_{km}) \qquad (14)$$

Thus, terms in (11) for $\ell \neq m$ are zero. Next consider the integral over θ.

$$I_{\theta} = \int_0^{\pi} P_n^m(\cos\theta)P_k^m(\cos\theta)\sin\theta d\theta$$

$$= \int_{-1}^{+1} P_n^m(u)P_k^m(u)du \qquad (15)$$

For $k\neq n$, $I_{\theta} = 0$. For $k=n$

$$I_{\theta} = \int_{-1}^{+1} [P_n^m(u)]^2 du = \frac{2}{2n+1}\frac{(n+m)!}{(n-m)!} \qquad (16)$$

Hence, only terms for which $\ell=m$ and $k=n$ remain in (11), and (14) gives $I_{\varphi} = 2\pi$.

The last integral to be evaluated is

$$I_r = \int_{r_1}^{r_2} |\Delta_{n,n-1}(z,z_2)|^2 \, r^2 dr$$

$$= \int_{r_1}^{r_2} \Delta_{n,n-1}(z,z_2)\Delta^*_{n,n-1}(z,z_2)r^2 dr \qquad (17)$$

where $z=\lambda_m r$, and where the asterisk denotes the complex conjugate. This integral can be evaluated by means of formula (21)

derived in Appendix C, since $\Delta_{n,n-1}(z,z_2)$ satisfies the conditions on $u_n(\lambda r,r)$ and since $v_n(\lambda_m r,\lambda) = u_n(\lambda r,\lambda)$. The required formula is repeated below for convenient reference.

$$\int_{r_1}^{r_2} r^2 u_n u_n^* dr = \frac{1}{|\lambda_m|^3}\left[|z|\,\mathrm{Im}(z u_n^* u_{n-1})\right]_{z_1}^{z_2} \qquad (18)$$

Thus,

$$I_r = \frac{1}{|\lambda_m|^3}\left\{|z_2|\,\mathrm{Im}\left[z_2\Delta^*_{n,n-1}(z_2,z_2)\Delta_{n-1,n-1}(z_2,z_2)\right]\right.$$

$$\left. - |z_1|\,\mathrm{Im}\left[z_1\Delta^*_{n,n-1}(z_1,z_2)\Delta_{n-1,n-1}(z_1,z_2)\right]\right\}$$

$$= \frac{-|z_1|}{|\lambda_m|^3}\,\mathrm{Im}\left[z_1\Delta^*_{n,n-1}(z_1,z_2)\Delta_{n-1,n-1}(z_1,z_2)\right] \qquad (19)$$

since $\Delta_{n-1,n-1}(z_2,z_2) = 0$. Now substitute (14), (16), and (19) into (11) and (12). The result is

$$N_z = \sum_{n=1}^{\infty}\sum_{m=1}^{n} 2\pi\left(\frac{m^2\Omega}{\rho}\right)n(n+1)\left(\frac{2}{2n+1}\right)\frac{(n+m)!}{(n-m)!}\,\overset{v}{K}_{nm}\,\hat{K}_{nm}$$

$$\times \frac{|z_1|}{|\lambda_m|^3}\,\mathrm{Im}\left[z_1\,\Delta^*_{n,n-1}(z_1,z_2)\Delta_{n-1,n-1}(z_1,z_2)\right] \qquad (20)$$

Using (3.12-3)

$$N_z = \sum_{n=1}^{\infty}\sum_{m=1}^{n} 2\pi\left(\frac{m^2\Omega}{\rho}\right)n(n+1)\frac{(n+m)!}{(n-m)!}\frac{(2n+1)}{|z_1|}\,|A_{nm}|^2$$

$$\times \frac{1}{|\lambda_m|^3}\,\frac{\mathrm{Im}\left[z_1\Delta^*_{n,n-1}(z_1,z_2)\Delta_{n-1,n-1}(z_1,z_2)\right]}{|\Delta_{n+1,n-1}(z_1,z_2|^2} \qquad (21)$$

Since $\overset{\vee}{A}_{nm} = 2a_n \frac{(n-m)!}{(n+m)!} \sqrt{\sigma_{nm}^2+\tau_{nm}^2}\ e^{-i\epsilon_{nm}}$, $(m \geq 1)$ (22)

$$|A_{nm}|^2 = \overset{\vee}{A}_{nm}\ \hat{A}_{nm}$$

$$= 4a_n^2 \left[\frac{(n-m)!}{(n+m)!}\right]^2 (\sigma_{nm}^2+\tau_{nm}^2) \qquad (23)$$

$$\therefore \quad N_z = \sum_{n=1}^{\infty} \sum_{m=1}^{n} 8\pi \left(\frac{m^2\Omega}{\rho}\right) a_n^2 n(n+1)(2n+1)\ \frac{(n-m)!}{(n+m)!}\ (\sigma_{nm}^2 + \tau_{nm}^2)$$

$$\times \frac{1}{|z_1||\lambda_m|^3}\ \mathrm{Im}\ \frac{[z_1 \Delta^*_{n,n-1}(z_1,z_2)\Delta_{n-1,n-1}(z_1,z_2)]}{|\Delta_{n+1,n-1}(z_1,z_2)|^2} \qquad (24)$$

This formula expresses the torque in terms of the quantities, a_n which characterize the cruciform magnet; $\sigma_{nm}^2+\tau_{nm}^2$, which depends on the location of the axis of rotation; and the complex functions, $\Delta_{n,n-1}(z_1,z_2)$, $\Delta_{n-1,n-1}(z_1,z_2)$ and $\Delta_{n+1,n-1}(z_1,z_2)$ of the dimensionless complex numbers z_1 and z_2, which are proportional to the inner and outer radii of the copper shell respectively.

3.16 APPROXIMATE RESULTS FOR THE CASES OF SLOW DAMPER ROTATION AND THIN CONDUCTING SHELLS

Within the limitations of the theoretical model assumed for the damper, the derivation of the formula for the damping torque was performed without approximations. For the purpose of evaluating the damping torque produced under normal operating conditions and practical damper configurations, it will now be convenient to introduce certain approximations in the exact formula (3.15-24). In particular, certain approximations are valid when the rate of relative rotation is sufficiently slow, corresponding to satellite libration periods of several hours, and for thin conducting shells that are actually used in the fabrication of practical dampers.

Consider first the case of slow rotation rates ($\Omega \ll 1$)*. For a fixed value of the summation index m, $|\lambda_m| \to 0$ as $\Omega \to 0$; hence, $z \to 0$. Thus, the asymptotic forms of the spherical Bessel functions for small argument can be used, if Ω is sufficiently small. To obtain an idea of the numbers involved, it is instructive to calculate $|\lambda_m|$ for a rotation period of one hour, for example. From formula (3.11-13)

$$|\lambda_m| = \sqrt{m\mu\Omega/\rho} \tag{1}$$

where m is a positive integer. Assuming rapid convergence of the series in m, all terms for $m>10$, say, will be negligible. If the conducting shell is pure copper,

*For convenience assume $\Omega \geq 0$.

$$\mu \approx \mu_o = 1.26 \times 10^{-6} \text{ (hy/m)} \tag{2}$$

$$\rho = 1.724 \times 10^{-8} \text{ (ohm·m)} \tag{3}$$

and for a period of relative rotation between damper parts of one hour

$$\Omega = 1.74 \times 10^{-3} \text{ (rad/sec)} \tag{4}$$

Thus, for $m \leq 10$, $|\lambda_m| \leq 1.13$ (m^{-1}). For a practical sized damper $r_2 \approx .1(m)$, so that $|z| \leq 0.113$, and $|z| \ll 1$. Increasing the shell resistivity or the period of damper rotation has the effect of reducing $|\lambda_m|$ and $|z|$ still further.

Consider the expansions of $\xi_n(z)$ and $\eta_n(z)$ in ascending powers of z [4]; viz.

$$\xi_n(z) = \frac{z^n}{(2n+1)!!}\left[1 + \frac{z^2/2}{1!(2n+3)} + \frac{(z^2/2)^2}{2!(2n+3)(2n+5)} + \text{---}\right] \tag{5}$$

$$\eta_n(z) = (-1)^n \frac{(2n-1)!!}{z^{n+1}}\left[1 + \frac{z^2/2}{1!(1-2n)} + \frac{(z^2/2)^2}{2!(1-2n)(3-2n)} + \text{---}\right] \tag{6}$$

For $|z| \ll 1$:

$$\xi_n(z) \sim \frac{z^n}{(2n+1)!!}, \qquad \eta_n(z) \sim \frac{(-1)^n(2n-1)!!}{z^{n+1}} \tag{7}$$

These asymptotic formulas yield values of $\xi_n(z)$ and $\eta_n(z)$ accurate to about 1% for $|z| \leq 0.1$, and the nature of the formulas is such that a greatly simplified torque formula can be derived.

For $z = \tilde{x}e^{i\pi/4}$ and $\tilde{x} \ll 1$:

$$\Delta_{n,n-1}(z_1,z_2) = \xi_n(z_1)\eta_{n-1}(z_2) - \eta_n(z_1)\xi_{n-1}(z_2)$$

$$\sim(-1)^{n-1}\frac{(2n-3)!!}{(2n+1)!!}\left(\frac{z_1^n}{z_2^n}\right) - (-1)^n\left(\frac{z_2^{n-2}}{z_1^{n+1}}\right)$$

$$\sim(-1)^{n-1}\left(\frac{\tilde{x}_2}{\tilde{x}_1}\right)^n\left[\frac{(2n-3)!!}{(2n+1)!!}\left(\frac{\tilde{x}_1}{\tilde{x}_2}\right)^{2n} + \frac{i}{\tilde{x}_1\tilde{x}_2}\right] \qquad (8)$$

$$\Delta_{n-1,n-1}(z_1,z_2) = \xi_{n-1}(z_1)\eta_{n-1}(z_2) - \eta_{n-1}(z_1)\xi_{n-1}(z_2)$$

$$\sim(-1)^{n-1}\frac{(2n-3)!!}{(2n-1)!!}\left(\frac{z_1^{n-1}}{z_2^n} - \frac{z_2^{n-1}}{z_1^n}\right)$$

$$\sim(-1)^{n-1}\frac{1}{(2n-1)}\left(\frac{1}{z_1}\right)\left(\frac{z_1}{z_2}\right)^n\left[1 - \left(\frac{z_2}{z_1}\right)^{2n-1}\right]$$

$$\sim(-1)^{n-1}\frac{1}{(2n-1)}\left(\frac{1}{z_1}\right)\left(\frac{\tilde{x}_1}{\tilde{x}_2}\right)^n\left[1 - \left(\frac{\tilde{x}_2}{\tilde{x}_1}\right)^{2n-1}\right] \qquad (9)$$

$$\therefore z_1\Delta_n^*{}_{,n-1}\Delta_{n-1,\,n-1} \sim \frac{1}{(2n-1)}\left[\frac{(2n-3)!!}{(2n+1)!!}\left(\frac{\tilde{x}_1}{\tilde{x}_2}\right)^{2n} - \frac{i}{\tilde{x}_1\tilde{x}_2}\right]$$

$$x\left[1 - \left(\frac{\tilde{x}_2}{\tilde{x}_1}\right)^{2n-1}\right] \qquad (10)$$

$$\therefore \mathrm{Im}(z_1\Delta_n^*{}_{,n-1}\Delta_{n-1,n-1}) \sim \frac{1}{(2n-1)}\left(\frac{1}{\tilde{x}_1\tilde{x}_2}\right)\left[\left(\frac{\tilde{x}_2}{\tilde{x}_2}\right)^{2n-1} - 1\right] \qquad (11)$$

Next the asymptotic form of $|\Delta_{n+1,n-1}|^2$ will be determined for $z = \tilde{x}e^{i\pi/4}$ and $\tilde{x}<<1$.

$$\Delta_{n+1,n-1}(z_1,z_2) = \xi_{n+1}(z_1)\eta_{n-1}(z_2) - \eta_{n+1}(z_1)\xi_{n-1}(z_2)$$

$$\sim (-1)^{n-1}\frac{(2n-3)!!}{(2n+3)!!}\left(\frac{z_1^{n+1}}{z_2^{n}}\right) - (-1)^{n+1}\frac{(2n+1)!!}{(2n-1)!!}\left(\frac{z_2^{n-1}}{z_1^{n+2}}\right)$$

$$\sim (-1)^{n-1}\left[\frac{(2n-3)!!}{(2n+3)!!}\left(\frac{\tilde{x}_1}{\tilde{x}_2}\right)^n \tilde{x}_1 e^{i\pi/4} - (2n+1)\left(\frac{\tilde{x}_2}{\tilde{x}_1}\right)^n \frac{e^{-i3\pi/4}}{\tilde{x}_1^2\,\tilde{x}_2}\right]$$

$$\Delta_{n+1,n-1}(z_1,z_2) \sim (-1)^{n-1} e^{i\pi/4}\left[\frac{(2n-3)!!}{(2n+3)!!}\left(\frac{\tilde{x}_1}{\tilde{x}_2}\right)^n \tilde{x}_1 + (2n+1)\left(\frac{\tilde{x}_2}{\tilde{x}_1}\right)^n \frac{1}{\tilde{x}_1^2\tilde{x}_2}\right]$$

$$\sim (-1)^{n-1} e^{i\pi/4}(2n+1)\left(\frac{\tilde{x}_2}{\tilde{x}_1}\right)^n \frac{1}{\tilde{x}_1^2\tilde{x}_2} \qquad (12)$$

$$\therefore |\Delta_{n+1,n-1}(z_1,z_2)|^2 \sim (2n+1)^2\left(\frac{\tilde{x}_2}{\tilde{x}_1}\right)^{2n}\frac{1}{\tilde{x}_1^4\tilde{x}_2^2} \qquad (13)$$

Note that $|\Delta_{n+1,n-1}(z_1,z_2)|^2>0$ and the existence condition (3.11-44) is satisfied when $\tilde{x}<<1$.

$$\therefore \frac{\mathrm{Im}(z_1\Delta^*_{n,n-1}\Delta_{n-1,n-1})}{|\Delta_{n+1,n-1}|^2} \sim \frac{1}{(2n+1)^2(2n-1)}\left(\frac{\tilde{x}_1}{\tilde{x}_2}\right)\tilde{x}_1^3\,\tilde{x}_2\left[\left(\frac{\tilde{x}_2}{\tilde{x}_1}\right)^{2n-1} - 1\right] \qquad (14)$$

$$\frac{1}{|z_1||\lambda|^3}\frac{\mathrm{Im}(z_1\Lambda^*_{n,n-1}\Delta_{n-1,n-1})}{|\Delta_{n+1,n-1}|^2} \sim \frac{1}{(2n+1)^2(2n-1)}\left(\frac{r_1}{r_2}\right)^{2n-1} r_1^3$$

$$x\left[\left(\frac{r_2}{r_1}\right)^{2n-1} - 1\right] \qquad (15)$$

since $x = |\lambda_m|r$. Now substitute this result in formula (3.15-24) for the torque and also substitute the results of Appendices A, B, and E in order to obtain the parametric relationships explicitly. The result is the following:

$$N_z \approx 8\pi\left(\frac{\Omega}{\rho}\right)(\mu_0 M)^2\left(\frac{a^4c^2}{r_1}\right)\sum_{\substack{n=1\\(n\ \mathrm{odd})}}^{N}{}' \tilde{a}_n^2\,\frac{n(n+1)}{(4n^2-1)}\left[1 - \left(\frac{r_1}{r_2}\right)^{2n-1}\right]$$

$$x\sum_{m=1}^{M} m^2\,\frac{(n-m)!}{(n+m)!}\,F_n^m\,(u_x,u_y,u_z);\quad (a_2+c_2<r_1^2) \qquad (16)$$

where

$$\tilde{a}_n = \frac{1}{2^n}\left(\frac{c}{r_1}\right)^{n-1} \frac{1}{n(n+1)}$$

$$\times \sum_{s=0}^{(n-1)/2} \frac{(-1)^s(2n-2s)!}{s!(n-s)!(n-2s-1)!} \sum_{k=0}^{s} \binom{s}{k} \frac{i}{(n-2s+2k)} \left(\frac{a}{c}\right)^{2} \quad (s-k) \tag{17}$$

$$F_n^m(u_x, u_y, u_z) = [P_n^m(u_x)]^2 + [P_n^m(u_y)]^2 + [P_n^m(u_z)]^2$$
$$+ 2P_n^m(u_x)P_n^m(u_y)\cos m\Phi_1 + 2P_n^m(u_x)P_n^m(u_z)\cos m\Phi_2$$
$$+ 2P_n^m(u_y)P_n^m(u_z)\cos m\Phi_3 \tag{18}$$

$$\Phi_1 = \tan^{-1}\left(\frac{+u_z}{-u_x u_y}\right) \tag{19a}$$

$$\Phi_2 = \tan^{-1}\left(\frac{-u_y}{-u_x u_z}\right) \tag{19b}$$

$$\Phi_3 = \tan^{-1}\left(\frac{+u_x}{-u_y u_z}\right) \tag{19c}$$

$$u_x = \cos\Theta_x, \quad u_y = \cos\Theta_y, \quad u_z = \cos\Theta_z \tag{20}$$

The indeterminate cases corresponding to two zero direction cosines are excluded. Note that the sums over n and m are terminated at finite numbers which indicate the limits of the approximation. In formulas (19a), (19b), and (19c), the appropriate quadrant is determined by the signs of the numerator and the denominator of the fraction.

Finally, for the case of a thin conducting shell a slight additional simplification is obtained. For $\Delta r = r_2 - r_1 \ll r_1$,

$$1 - \left(\frac{r_1}{r_2}\right)^{2n-1} = 1 - \left(1 - \frac{\Delta r}{r_2}\right)^{2n-1} \approx (2n-1)\left(\frac{\Delta r}{r_2}\right) \tag{21}$$

and

$$N_z \approx 8\pi\left(\frac{\Omega}{\rho}\right)(\mu_o M)^2\left(\frac{a^4 c^2}{r_1}\right)\left(\frac{\Delta r}{r_2}\right)\sum_{\substack{n=1 \\ (n\ \text{odd})}}^{N}{}' \tilde{a}_n^2 \frac{n(n+1)}{(2n+1)}$$

$$\times \sum_{m=1}^{M} m^2 \frac{(n-m)!}{(n+m)!} F_n^m(u_X, u_Y, u_Z) \tag{22}$$

Formulas (16) and (22) have the form, $N_z \approx K_\Omega \Omega$, where K_Ω is the damping coefficient.

$$\therefore \quad K_\Omega = 8\pi \frac{(\mu_o M)^2}{\rho} r_2^5 \, S(a/c, c/r_1, r_1/r_2; u_X, u_Y, u_Z) \text{ (nt-m-sec)} \tag{23}$$

where

$$S(a/c, c/r_1, r_1/r_2; u_X, u_Y, u_Z) = \left(\frac{a}{c}\right)^4 \left(\frac{c}{r_1}\right)^6 \left(\frac{r_1}{r_2}\right)^5 \sum_{n=1}^{N}{}' \tilde{a}_n^2 \frac{n(n+1)}{(4n^2-1)}$$

$$\times \left[1 - \left(\frac{r_1}{r_2}\right)^{2n-1}\right] \sum_{m=1}^{M} m^2 \frac{(n-m)!}{(n+m)!} F_n^m(u_X, u_Y, u_Z) \tag{24}$$

is a dimensionless function of certain geometrical ratios and the direction cosines of the axis of relative rotation. Note that K_Ω is proportional to the square of the magnetization M and is inversely proportional to the resistivity ρ. Also K_Ω is proportional to the fifth power of the damper radius, r_2, for fixed geometrical ratios. Sample calculations have shown that, in general, the value of S varies considerably when u_X, u_Y, u_Z are varied; however, in the next section it will be shown that, for

orbital operation, the axis of relative rotation is confined to a certain plane which is fixed relative to the axes of the magnet assembly. In that particular plane, the value of S is apparently constant.

3.17 KINEMATICS OF MAGNETICALLY ANCHORED EDDY CURRENT DAMPER

The previous analysis obtained the torque corresponding to a specified relative rotation between the magnet assembly and the conducting shell. When the damper is functioning on an orbiting satellite, the orientation of the magnet assembly depends on the direction of the earth's magnetic field and the rotation of the shell. The axis and rate of relative rotation are unknown a priori. The purpose of this section is to investigate the kinematics of the magnet assembly and the torque corresponding to a specified rotation of the shell in inertial space and a specified earth's magnetic field vector.

The following assumptions are made in the analysis of this section:

1. A viscous damping torque is obtained

2. Deflection of the net magnetic dipole from the direction of the earth's magnetic field is less than 90°.

3. The magnet inertial torque is negligible compared with the magnetic restoring torque and the damping torque.

Under the last assumption the magnet is always in a position such that the applied torques are in equilibrium.

Denote the torque exerted on the magnet due to the relative rotation of the shell by $\bar{N}_s$.

$$\bar{N}_s = K_\Omega(\bar{\omega}_s - \bar{\omega}_m) \quad \text{(nt-m-sec)} \tag{1}$$

where K_Ω is the damping coefficient, $\bar{\omega}_s$ is the absolute rotation vector of the shell, and $\bar{\omega}_m$ is the absolute rotation vector of the magnet. The restoring torque $\bar{N}_m$, due to the magnetic field of the earth is given by

$$\bar{N}_m = \bar{m} \times \bar{H} \tag{2}$$

where $\bar{m}$ is the net dipole moment of the magnet assembly, and $\bar{H}$ is the intensity of the earth's field at the location of the satellite. The dipole moment $\bar{m}$ is directed along a line which has equal direction cosines with the three N poles of the magnet assembly. For equilibrium,

$$K_\Omega(\bar{\omega}_s - \bar{\omega}_m) = K_\Omega \Delta\bar{\omega} = -\bar{m} \times \bar{H} \tag{3}$$

Clearly the relative rotation vector, $\Delta\bar{\omega}$, is normal to the plane of the magnet dipole vector and the earth's magnetic field vector. It will be assumed that $\bar{\omega}_s$ and $\bar{H}$ are known stationary vectors for the purpose of the present analysis. From (3) it follows that

$$\bar{\omega}_s \cdot \bar{H} = \bar{\omega}_m \cdot \bar{H} \tag{4}$$

and

$$\bar{\omega}_s \cdot \bar{m} = \bar{\omega}_m \cdot \bar{m} \tag{5}$$

Now take the time derivative of both sides of (3) with respect to a rotating reference coordinate frame fixed in the shell*

$$K_\Omega \left(\frac{d\bar{\omega}_s}{dt}\right)_s - K_\Omega \left(\frac{d\bar{\omega}_m}{dt}\right)_s = -\left(\frac{d\bar{m}}{dt}\right)_s \times \bar{H} - \bar{m} \times \left(\frac{d\bar{H}}{dt}\right)_s \tag{6}$$

*Reference [5], pp. 132-133.

For $\bar{\omega}_s$ stationary in the shell and a fixed rate of rotation, $(d\bar{\omega}_s/dt)_s = 0$. Also,

$$\left(\frac{d\bar{\omega}_m}{dt}\right)_s = \left(\frac{d\bar{\omega}_m}{dt}\right)_m - \Delta\bar{\omega} \times \bar{\omega}_m = \left(\frac{d\bar{\omega}_m}{dt}\right)_m + \left(\frac{\bar{m}\times\bar{H}}{K_\Omega}\right) \times \bar{\omega}_m$$

$$= \left(\frac{d\bar{\omega}_m}{dt}\right)_m + \frac{1}{K_\Omega}\left[(\bar{\omega}_m\cdot\bar{m})\bar{H} - (\bar{\omega}_m\cdot\bar{H})\bar{m}\right] \tag{7}$$

where the subscript m denotes that the derivative is taken in a coordinate frame fixed in the magnet assembly. Next,

$$\left(\frac{d\bar{m}}{dt}\right)_s = \left(\frac{d\bar{m}}{dt}\right)_m - \Delta\bar{\omega} \times \bar{m} = -\Delta\bar{\omega} \times \bar{m}$$

$$= +\left(\frac{\bar{m}\times\bar{H}}{K_\Omega}\right) \times \bar{m} = + \frac{1}{K_\Omega}\left[(\bar{m}\cdot\bar{m})\bar{H} - (\bar{m}\cdot\bar{H})\bar{m}\right]$$

$$= + \frac{1}{K_\Omega}\left[m^2\bar{H} - (\bar{m}\cdot\bar{H})\bar{m}\right] \tag{8}$$

since $\bar{m}$ is fixed with respect to the magnet axes. Finally,

$$\left(\frac{d\bar{H}}{dt}\right)_s = \left(\frac{d\bar{H}}{dt}\right)_i - \bar{\omega}_s \times \bar{H} = -\dot{\bar{\omega}}_s \times \bar{H} \tag{9}$$

Substitution of (7), (8), and (9) into (6) gives

$$-K_\Omega\left(\frac{d\bar{\omega}_m}{dt}\right)_m - (\bar{\omega}_m\cdot\bar{m})\bar{H} + (\bar{\omega}_m\cdot\bar{H})\bar{m} = -\frac{1}{K_\Omega}\left[m^2\bar{H} - (\bar{m}\cdot\bar{H})\bar{m}\right] \times \bar{H}$$

$$+ \bar{m}\times(\bar{\omega}_s\times\bar{H}) \tag{10}$$

$$\therefore -K_\Omega\left(\frac{d\bar{\omega}_m}{dt}\right)_m = -(\bar{\omega}_m\cdot\bar{H})\bar{m} + (\bar{\omega}_m\cdot\bar{m})\bar{H} + \frac{(\bar{m}\cdot\bar{H})}{K_\Omega}(\bar{m}x\bar{H})$$

$$- (\bar{m}\cdot\bar{\omega}_s)\bar{H} + (\bar{m}\cdot\bar{H})\bar{\omega}_s$$

$$= -(\bar{\omega}_m\cdot\bar{H})\bar{m} + (\bar{m}\cdot\bar{H})\left(\frac{\bar{m}x\bar{H}}{K_\Omega} + \bar{\omega}_s\right)$$

$$= -(\bar{\omega}_m\cdot\bar{H})\bar{m} + (\bar{m}\cdot\bar{H})\bar{\omega}_m$$

$$= -\bar{H} \times (\bar{m}x\bar{\omega}_m) \qquad (11)$$

Formulas (5) and (1) were used in the derivation of (11). Now take the inner product of $(d\bar{\omega}_m/dt)_m$ with $\bar{H}$.

$$-K_\Omega\left(\frac{d\bar{\omega}_m}{dt}\right)_m\cdot\bar{H} = -(\bar{\omega}_m\cdot\bar{H})(\bar{m}\cdot\bar{H}) + (\bar{m}\cdot\bar{H})(\bar{\omega}_m\cdot\bar{H}) = 0 \qquad (12)$$

Thus, either $(d\bar{\omega}_m/dt)_m = 0$ or $(d\bar{\omega}_m/dt)_m$ is orthogonal to $\bar{H}$. Suppose $(d\bar{\omega}_m/dt)_m = 0$. According to (11) and (4),

$$\bar{\omega}_m = \frac{(\bar{\omega}_s\cdot\bar{H})}{(\bar{m}\cdot\bar{H})}\bar{m} \qquad (13)$$

i.e., $\bar{\omega}_m$ and $\bar{m}$ are collinear vectors.

Enough information is now available to permit a geometrical interpretation of the analysis. The following points are noted.

1. The relative rotation vector $\Delta\bar{\omega}$ is perpendicular to the plane of $\bar{H}$ and $\bar{m}$.

2. The projections of $\bar{\omega}_s$ and $\bar{\omega}_m$ on $\bar{m}$ or $\bar{H}$ are equal.

3. $\bar{\omega}_m$ is collinear with $\bar{m}$

Figure 1 shows the above relationships for $\bar{\omega}_s \cdot \bar{H} > 0$ and $\bar{\omega}_s \cdot \bar{H} < 0$. Although $\Delta\omega$ and α are yet unknown, elementary geometry indicates that the tip of $\bar{\omega}_s$ must lie on a semi-circle which intersects the tips of $\bar{\omega}_s$ and the projection of $\bar{\omega}_s$ on $\bar{H}$. The component of $\bar{\omega}_s$ normal to $\bar{H}$ coincides with the diameter of the semi-circle.

The location of $\bar{m}$ on the semi-circle is determined from formula (1). With reference to Figure 1,

$$a = (\bar{\omega}_s \cdot \bar{e}_H), \quad b = |\bar{\omega}_s - a\bar{e}_H|, \quad c = a \tan \alpha \tag{14}$$

and
$$(\Delta\omega)^2 = b^2 - c^2 \tag{15}$$

From (3)
$$\Delta\omega = \frac{mH}{K_\Omega} \sin \alpha = \tau \sin \alpha \tag{16}$$

where $\bar{e}_H$ is a unit vector along $\bar{H}$ and $\tau = mH/K_\Omega$.

But

$$b^2 = |\bar{\omega}_s - a\bar{e}_H|^2 = \omega_s^2 + a^2 - 2a\bar{\omega}_s \cdot \bar{e}_H = \omega_s^2 - a^2 \tag{17}$$

$$\therefore \quad (\Delta\omega)^2 = \omega_s^2 - a^2 - a^2 \tan^2 \alpha = \omega_s^2 - a^2 \sec^2 \alpha \tag{18}$$

Squaring $\Delta\omega$ in (16) and equating the result with (18) gives

$$\tau^2 (1 - \cos^2 \alpha) = \omega_s^2 - a^2 \sec^2 \alpha \tag{19}$$

or
$$\cos^4 \alpha + (\tilde{\omega}_s^2 - 1)\cos^2 \alpha - \tilde{a}^2 = 0 \tag{20}$$

where
$$\tilde{\omega}_s = \omega_s / \tau \text{ and } \tilde{a} = a/\tau = \tilde{\omega}_s \cos\beta. \tag{21}$$

$$\therefore \quad \cos^2 \alpha = \frac{1}{2} \left\{ 1 - \tilde{\omega}_s^2 + [(1 - \tilde{\omega}_s^2)^2 + 4\tilde{\omega}_s^2 \cos^2 \beta]^{\frac{1}{2}} \right\} \tag{22}$$

The positive square root is taken so that $\omega_s = 0 \Rightarrow \alpha = 0$. After further manipulation,

$$\alpha = \cos^{-1}\left\{ \frac{1}{\sqrt{2}} \left[1 - \tilde{\omega}_s^2 + (1 + 2\tilde{\omega}_s^2 \cos 2\beta + \tilde{\omega}_s^4)^{\frac{1}{2}}\right]^{\frac{1}{2}}\right\} \qquad (23)$$

This formula gives α in terms of known quantities. The normalized relative angular velocity is from (3)

$$\Delta\tilde{\omega} = \frac{\Delta\omega}{\tau} = (1-\cos^2\alpha)^{\frac{1}{2}} = \sin\alpha \qquad (24)$$

Figure 2 is a graph of α vs. $\tilde{\omega}_s$ with β as a parameter. It is seen that the magnetic dipole remains captured ($\alpha<90^\circ$) by the earth's magnetic field for all angles β except $\beta=90^\circ$, regardless of the absolute rate of rotation of the shell. For $\beta=90^\circ$, the dipole deflection angle α is less than 90° for $\tilde{\omega}_s<1$. The case, $\tilde{\omega}_s>1$ and $\beta=90^\circ$, will not be considered in the present analysis. In this case $(d\bar{\omega}_m/dt)_m \neq 0$, but $(d\bar{\omega}_m/dt)_m \cdot \bar{H} = 0$.

Figure 3 shows the value of $\Delta\tilde{\omega}$ as a function of $\tilde{\omega}_s$ with β as a parameter. For $\beta = 90^\circ$, $\Delta\tilde{\omega} = \tilde{\omega}_s$, if $\tilde{\omega}_s < 1$. For $\beta \neq 90^\circ$, the value of $\Delta\tilde{\omega}$ increases rapidly with $\tilde{\omega}_s$ for $\tilde{\omega}_s < 1$ and then approaches the value, $\sin\beta$, asymptotically for large $\tilde{\omega}_s$.

The normal behavior can now be explained in greater detail. For a fixed value of β, an increase in ω_s causes $\bar{\omega}_m$ to move away from $\bar{H}$ and towards $\bar{\omega}_s$. With allowance for the change in scale, due to the increased length of $\bar{\omega}_s$, the tip of $\bar{\omega}_m$ lies on a new semi-circle of larger radius which intersects the tips of $\bar{\omega}_s$ and the projection of $\bar{\omega}_s$ on $\bar{H}$. Thus both α and $\Delta\omega$ are increased, although $\Delta\omega$ is not proportional to ω_s. It is clear from either Figure 1 or 2 that as $\tilde{\omega}_s \to \infty$, $\alpha \to \beta$ ($\beta<90^\circ$) or $\alpha \to 180^\circ-\beta$ ($90^\circ<\beta<180^\circ$).

Figure 1 shows that the magnetic dipole is fixed relative to the magnetic field of the earth and to the absolute rotation vector of the shell. Since the absolute rotation vector of the magnet coincides with the dipole axis, the arms of the cruciform rotate about the dipole axis at a rate ω_m corresponding to the projection of $\bar{\omega}_s$ on $\bar{m}$. The axis of relative rotation between damper parts is stationary relative to $\bar{\omega}_s$ and $\bar{H}$, but appears to rotate relative to the axes of the magnet in a plane normal to the dipole axis. With respect to axes fixed in the shell, the axis of relative rotation appears to precess around $\bar{\omega}_s$.

The motion just described is obtained if the damping torque is given by (1). Unless $\theta=0°$, $90°$, or $180°$, the motion is complicated by the fact that the axes of absolute rotation of the magnet assembly and the shell do not coincide, so that the axis of relative rotation precesses in the damper. If the rate of precession is large, it is not clear that a viscous law accurately describes the true nature of the damper. Also, it is questionable to use the value of K_Ω corresponding to rotation about a fixed axis, particularly since K_Ω is, in general, a function of the direction cosines of the axis.

From consideration of Figure 1, it is apparent that precession of the axis of relative rotation is most rapid for θ near 0° or 180°, but on the other hand, $\Delta\omega \to 0$ as $\beta \to 0$ or 180°, and in the limit, the magnet swivels about the dipole axis, which coincides with the earth's magnetic field vector, at the same

rate as the shell. Thus, no steady-state damping is obtained when $\beta = 0^{\circ}$ or 180°.

The value of the shape factor S, which determines K_{Ω} according to (3.16-24), has been investigated as a function of the axis location in the plane normal to $\bar{m}$. It was first necessary to obtain a sequence of direction cosines, u_x and u_y, which rotated the axis through sampling intervals of 15° in the plane. It was found that the value of S is apparently constant in the plane for a fixed geometry. This result is remarkable, because sample calculations show that, for points outside of the particular plane, the value of S varies considerably.

Based on these considerations, it seems reasonable to assume a constant value for K_{Ω} in the plane normal to $\bar{m}$ and to assume that a viscous law holds true provided that the absolute rotation vector of the shell does not approach the direction of the earth's magnetic field.

Some useful design criteria can be derived from consideration of Figure 2. First, capture of the magnetic dipole is ensured for all β $(0<\beta<\pi)$ provided that

$$\tilde{\omega}_s = \frac{\omega_s}{\tau} = \left(\frac{K_{\Omega}}{m\bar{H}}\right) \omega_s < 1 \tag{25}$$

or

$$\frac{K_{\Omega}}{m} < \frac{H}{\omega_s} \tag{26}$$

This criterion sets a lower limit on m, for specified K_Ω.

Since a large deflection angle of the dipole tends to reduce the component of shell rotation that is damped, it is desirable to restrict the deflection to small angles; e.g., $\alpha<45^\circ$. From Figure 2, $\alpha = 45^\circ$ corresponds to $\tilde{\omega}_s = 1/\sqrt{2}$. The appropriate criterion is, therefore,

$$\frac{K_\Omega}{m} < \frac{H}{\sqrt{2}\omega_s} \qquad (\alpha<45^\circ) \tag{27}$$

3.18. EFFECTIVE DAMPING TORQUE FOR SATELLITE LIBRATIONS

According to Figure (3.17-1), the torque, $\bar{N} = K_\Omega \Delta\bar{\omega}$, exerted by the damper on the satellite (shell) is not directed along the axis of absolute rotation ($\bar{\omega}_s$ axis) of the satellite unless $\beta = 90°$. The object of this section is to obtain the effective damping torque $\bar{N}_e$, which is the component of $\bar{N}$ along $\bar{\omega}_s$.

The effective damping torque is

$$\bar{N}_e = (\bar{N}\cdot\bar{e}_s)\bar{e}_s = (K_\Omega \Delta\bar{\omega}\cdot\bar{e}_s)\bar{e}_s = (K_\Omega \Delta\omega \sin\gamma)\bar{e}_s \tag{1}$$

where $\bar{e}_s$ is a unit vector along $\bar{\omega}_s$ and γ is defined in Figure (3.17-1). But

$$\sin\gamma = \Delta\omega/\omega_s \tag{2}$$

$$\therefore \quad N_e = K_\Omega \frac{(\Delta\omega)^2}{\omega_s} = K_\Omega \tau \frac{(\Delta\tilde{\omega})^2}{\tilde{\omega}_s} = mH \frac{(\Delta\tilde{\omega})^2}{\tilde{\omega}_s} \tag{3}$$

where $\Delta\tilde{\omega}$ is given by (3.17-24). In terms of $\tilde{\omega}_s$ and β.

$$N_e = \frac{(mH)^2}{2K_\Omega \omega_s}\left[1 + \tilde{\omega}_s^2 - (1 + 2\tilde{\omega}_s^2 \cos 2\beta + \tilde{\omega}_s^4)^{\frac{1}{2}}\right]$$

$$= \frac{mH}{2\tilde{\omega}_s}\left[1 + \tilde{\omega}_s^2 - (1 + 2\tilde{\omega}_s^2 \cos 2\beta + \tilde{\omega}_s^4)^{\frac{1}{2}}\right] \tag{4}$$

In general, N_e is a non-linear function of ω_s, unless $\beta = 90°$. For $\beta = 90^\circ$ and $\tilde{\omega}_s < 1$,

$$N_e = mH\tilde{\omega}_s = K_\Omega \omega_s \tag{5}$$

Ideal viscous (rate) damping is obtained only when the absolute rotation vector of the satellite is normal to the earth's magnetic field vector. The effective damping coefficient then equals the damping coefficient for relative rotation.

For $\beta \neq 90^\circ$ and $\tilde{\omega}_s << 1$:

$$N_e \approx \frac{mH}{2} \tilde{\omega}_s (1-\cos 2\beta) = \frac{K_\Omega}{2} (1-\cos 2\beta)\omega_s \tag{6}$$

$$\approx K_e \omega_s \tag{7}$$

where

$$K_e = \frac{K_\Omega}{2} (1-\cos 2\beta) \tag{8}$$

For $\tilde{\omega}_s << 1$, the effective damping is approximately proportional to the absolute rotation rate, ω_s, but the damping coefficient depends upon the value of β. The effectiveness ratio, K_e/K_Ω, is plotted versus $|90^\circ-\beta|$ in Figure 1. Note that for $|90^\circ-\beta| \leq 30^\circ$, the effectiveness ratio is 0.75 or better. For $|90^\circ-\beta| = 45^\circ$, the ratio is 0.5.

Figure 2 shows the non-linear relationship between N_e and $\tilde{\omega}_s$ for $0 \leq \tilde{\omega}_s \leq 1$ on a linear scale. The same function is plotted for $0.1 \leq \tilde{\omega}_s \leq 10$ on a log scale in Figure 3. Figure 3 shows that the effective torque increases with $\tilde{\omega}_s$ to a maximum value at $\tilde{\omega}_s = 1$ and then decreases for $\tilde{\omega}_s > 1$ ($\beta \neq 90^\circ$).

The percent non-linearity of the effective torque (4) relative to the linearized torque (6) is plotted versus $\tilde{\omega}_s$ with β as a

parameter in Figure 4. The percent non-linearity is found to be less than 5%, if $|90^\circ-\beta|\leq 45^\circ$ and $\tilde{\omega}_s<0.3$.

Since the damper torque $\bar{N}$ is not directed along $\bar{\omega}_s$, there exists a component torque normal to $\bar{\omega}_s$, unless $\beta = 90^\circ$. This torque tends to perturb the attitude of the satellite and must be considered when assessing the steady-state pointing accuracy.

3.19 DAMPING OF TRANSIENT LIBRATIONS

The object of this section is to investigate damping of transient librations of a gravity-gradient stabilized satellite which uses a magnetically anchored eddy current damper. Several restrictions and assumptions will be needed to facilitate the analysis:

1. Librations occur only about pitch axis,

2. Circular orbit,

3. Small libration angles,

4. Neglect perturbing torques including damper induced perturbation,

5. Effective damping torque is proportional to instantaneous rate of pitch motion,

6. Earth's magnetic field is described by dipole model.

The equation for pitch motion of a gravity-gradient stabilized satellite is the following:

$$I_Y \ddot{\theta} + K_e \dot{\theta} + 3\omega_0^2 (I_X - I_Z) \theta = 0 \qquad (1)$$

where

θ = pitch angle from local vertical

I_Y = moment of inertia about pitch axis

I_X = moment of inertia about roll axis

I_Z = moment of inertia about yaw axis

K_e = effective damping coefficient

ω_0 = orbital angular rate

According to (3.18-8), the effective damping coefficient depends upon the angle β between the axis of absolute rotation (pitch axis) and the earth's magnetic field intensity vector.

$$K_e = \frac{K_\Omega}{2} (1-\cos 2\beta) \tag{2}$$

where K_Ω is the damping coefficient for relative motion between damper parts. Although (1) is linear by virtue of the small angle assumption, K_e depends upon β which, in general, varies during an orbit. Thus, the effective damping coefficient is a time-varying quantity. For the present analysis, an average damping coefficient will be assumed, which depends on the orbital inclination.

Assuming a dipole model for the earth's magnetic field, the vertical and horizontal components of the field intensity vector are given by

$$H_v = -\frac{2m_e}{r_o^3} \sin\varphi_m \tag{3}$$

$$H_h = \frac{m_e}{r_o^3} \cos\varphi_m \tag{4}$$

where m_e is the dipole moment of the earth's field, r_o is the orbital radius, and φ_m is the magnetic latitude. With respect to orbital reference axes, x^o, y^o, z^o, in the direction of the orbital motion, the normal to the orbital plane, and the local vertical, the field components are

$$H_{xo} = H_h \cos\alpha \tag{5}$$

$$H_{yo} = +H_h \sin\alpha \tag{6}$$

$$H_{zo} = H_v \tag{7}$$

where α is the angle between the orbital plane and the magnetic meridian passing through the satellite position. For the present analysis, the effect of a pitch angle on the field components along the roll and yaw axes can be neglected, so that the components are

$$H_X \approx H_h \cos\alpha \tag{8}$$

$$H_Y = +H_h \sin\alpha \tag{9}$$

$$H_Z \approx H_v \tag{10}$$

The components can be expressed in terms of the orbital inclination angle i_m with respect to the magnetic equator and the angle θ_m of the satellite from the ascending node as follows:

$$H_X \approx \frac{m_e}{r_0^3} \sin i_m \cos \theta_m \tag{11}$$

$$H_Y = +\frac{m_e}{r_0^3} \cos i_m \tag{12}$$

$$H_Z \approx \frac{2m_e}{r_0^3} \sin i_m \sin \theta_m . \tag{13}$$

Denoting a set of unit vectors along the roll, pitch, and yaw axes by $\bar{i}$, $\bar{j}$, and $\bar{k}$ respectively,

$$\bar{H} \cdot \bar{j} = H_Y = H \cos \beta \tag{14}$$

where

$$\bar{H} = \bar{i}\, H_X + \bar{j}\, H_Y + \bar{k}\, H_Z$$

$$\therefore \quad \cos \beta = \frac{H_Y}{H} = + \frac{m_e}{r_0^3} \frac{\cos i_m}{H} \tag{15}$$

From (11), (12), and (13)

$$H = (H_x^2 + H_y^2 + H_z^2)^{\frac{1}{2}}$$

$$\approx \frac{m_e}{r_o^3} (\sin^2 i_m \cos^2 \theta_m + \cos^2 i_m + 4\sin^2 i_m \sin^2 \theta_m)^{\frac{1}{2}}$$

$$\approx \frac{m_e}{r_o^3} (1 + 3\sin^2 i_m \sin^2 \theta_m)^{\frac{1}{2}} \approx \frac{m_e}{r_o^3} \left[1 + \frac{3}{2} \sin^2 i_m (1-\cos 2\theta_m)\right]^{\frac{1}{2}}$$

$$\approx \frac{m_e}{r_o^3} \left(1 + \frac{3}{2} \sin^2 i_m\right)^{\frac{1}{2}} (1 - \delta \cos 2\theta_m)^{\frac{1}{2}} \qquad (16)$$

where $\delta = \dfrac{3\sin^2 i_m}{2+3\sin^2 i_m}$ (17)

Note that δ ranges from zero to 3/5 as i_m varies from 0° to 90°,

$$\therefore \cos \beta \approx - \cos i_m \left(1 + \frac{3}{2} \sin^2 i_m\right)^{-\frac{1}{2}} (1 - \delta \cos 2\theta_m)^{-\frac{1}{2}} \qquad (18)$$

But

$$K_e = \frac{K_\Omega}{2} (1-\cos 2\beta) = K_\Omega \sin^2 \beta \qquad (19)$$

From (18),

$$\sin^2 \beta = 1 - \cos^2 \beta$$

$$= 1 - \cos^2 i_m \left(1 + \frac{3}{2} \sin^2 i_m\right)^{-1} (1 - \delta \cos 2\theta_m)^{-1} \qquad (20)$$

$$\therefore \quad K_e = K_\Omega \left[1 - \cos^2 i_m \left(1 + \frac{3}{2} \sin^2 i_m\right)^{-1} (1 - \delta \cos 2\theta_m)^{-1}\right] \qquad (21)$$

The average damping coefficient will be computed over half an orbit, assuming that i_m is fixed. Actually i_m varies from orbit to orbit, because the magnetic dipole does not coincide with the earth's rotation axis; however, for low and medium altitude orbits, the period of variation is long compared with the orbital period.

$$\left\langle K_e \right\rangle_o = \frac{1}{\pi} \int_0^{\pi} K_e \, d\theta_m \tag{22}$$

$$= \frac{K_\Omega}{\pi} \int_0^{\pi} \left[1 - k(1-\delta\cos 2\theta_m)^{-1} \right] d\theta_m \tag{23}$$

where

$$k = \cos^2 i_m \left(1 + \frac{3}{2} \sin^2 i_m \right)^{-1} \tag{24}$$

Let

$$I = \int \frac{d\theta_m}{1-\delta\cos 2\theta_m} \tag{25}$$

According to formula 213, page 74, of [6],

$$I = \frac{1}{2\sqrt{1-\delta^2}} \tan^{-1}\left(\frac{\sqrt{1-\delta^2}\,\sin 2\theta_m}{\cos 2\theta_m - \delta} \right); \quad (\delta^2 < 1) \tag{26}$$

To evaluate the definite integral, it is necessary to account for the multi-valued nature of the inverse tangent function. Let $v = \tan^{-1} u$, where

$$u = \frac{\sqrt{1-\delta^2}\sin 2\theta_m}{\cos 2\theta_m - \delta} \tag{27}$$

Table 1 shows a sequence of points as θ_m ranges from 0 to π.

θ_m	u	v
0	0	0
$(\frac{1}{2})\cos^{-1}\delta$	∞	$\pi/2$
$\pi/4$	$-\sqrt{1-\delta^2}/\delta$	$\pi/2<v<\pi$
$\pi/2$	0	π
$3\pi/4$	$+\sqrt{1-\delta^2}/\delta$	$\pi<v<3\pi/2$
$(\frac{1}{2})\cos^{-1}\delta$	∞	$3\pi/2$
π	0	2π

Table 1

The total change in v is, therefore, 2π.

$$\therefore \quad \langle K_e \rangle_0 = K_\Omega \left(1 - \frac{k}{\sqrt{1-\delta^2}}\right) \tag{28}$$

But

$$1-\delta^2 = 1 - \frac{3\sin^2 i_m}{2+3\sin^2 i_m} = \frac{2}{2+3\sin^2 i_m} = \frac{1}{1+(3/2)\sin^2 i_m} \tag{29}$$

$$\therefore \quad k = (1-\delta^2)\cos^2 i_m \tag{30}$$

$$1 - \frac{k}{\sqrt{1-\delta^2}} = \frac{\sqrt{1-\delta^2} - k}{\sqrt{1-\delta^2}} = 1 - \sqrt{1-\delta^2}\cos^2 i_m \tag{31}$$

$$\therefore \quad \langle K_e \rangle_0 = K_\Omega \left[1 - \left(1 + \frac{3}{2}\sin^2 i_m\right)^{-1} \cos^2 i_m\right] \tag{32}$$

A graph of $\langle K_e \rangle_0 / K_\Omega$ versus i_m is plotted in Figure 1. The ratio varies from zero for $i_m = 0^\circ$ to unity at $i_m = 90^\circ$.

Assuming that the instantaneous damping coefficient in (1) can be replaced by the averaged value given by (31), then in terms of the dimensionless quantities,

$$\omega_p^2 = 3\bar{\omega}_0 \left(\frac{I_x - I_y}{I_y}\right) \tag{33}$$

$$\text{and } \zeta = \frac{1}{2} \frac{\langle K_e \rangle_0}{I_y \ \omega_p} \tag{34}$$

(1) becomes

$$\ddot{\theta} + 2\zeta\omega_p\dot{\theta} + \omega_p^2\theta = 0 \tag{35}$$

The transient solution for $\zeta \ll 1$ is

$$\theta \approx \theta_0 e^{-\zeta\omega_p t} \cos \omega_p t \tag{36}$$

where θ_o is the initial pitch angle. The time constant for decay of pitch oscillations to θ_o/e ($e \approx 2.718$) is

$$t_p = 1/\zeta\omega_p = \frac{2I_y}{\langle K_e \rangle_o} \tag{37}$$

$$\therefore \langle K_e \rangle_o = \frac{2I_y}{t_p} \tag{38}$$

Formula (38) gives the effective damping coefficient corresponding to a specified pitch axis moment of inertia and time constant.

Although the effective damping coefficient is independent of orbital radius, for a specified value of K_Ω, according to (32), the formula is valid only when the linearity criterion, $\tilde{\omega}_s << 1$, is satisfied. To see how the damper design depends upon orbital radius, recall that $\tilde{\omega}_s = K_\Omega/mH$, where m is the dipole moment of the damper magnet and H is the intensity of the earth's magnetic field. For $(\tilde{\omega}_s)_{max} = k$ $(k<<1)$,

$$\frac{m}{K_\Omega} \geq \frac{k^{-1}}{(H)_{min}} \tag{39}$$

For pitch motion and light damping ($\zeta << 1$).

$$(\omega_s)_{max} = (\dot{\theta})_{max} \approx \omega_p \theta_o$$

$$\leq \sqrt{3}\,\omega_o \theta_o \leq \pi \frac{\sqrt{3}}{2} \omega_o \tag{40}$$

since $\theta_o \leq \pi/2$ radians for a captured satellite. But.

$$\omega_o = \mu_g^{\frac{1}{2}} r_o^{-3/2} = \mu_g^{\frac{1}{2}} r_e^{-3/2} \left(\frac{r_o}{r_e}\right)^{-3/2} \tag{41}$$

where $\mu_g = 3.986 \times 10^{20}$ cm^3/sec^2 and $r_e = 6.378 \times 10^8$ cm. Also,

$$H^2 = H_v^2 + H_k^2 = \left(\frac{m_e}{r_o^3}\right)(4 - 3\cos^2\varphi_m) \qquad (42)$$

$$\therefore H_{min} = \frac{m_e}{r_o^3}\left(\frac{r_e}{r_o}\right)^3 \quad \text{at } \varphi_m = 0^\circ \qquad (43)$$

where $m_e = 8.1 \times 10^{25}$ pole-cm.

$$\therefore \frac{m}{K_\Omega} \geq \frac{10.72}{k} \times 10^{-3}\left(\frac{r_o}{r_e}\right)^{3/2} \qquad (44)$$

Figure 2 is a curve showing the ratio, m/K_Ω, versus orbital altitude for 1% maximum non-linearity when $|i_m| > 15^\circ$, corresponding to $k = 0.1$ and dipole deflection angle, $\alpha < 6^\circ$. Thus, the minimum dipole moment needed for a specified orbital altitude and damping coefficient can be determined.

As an example, the GEOS-A design parameters are as follows:

$m = 25{,}000$ pole-cm

$K_\Omega = 70{,}000$ dyne-cm-sec

$h = 600$ n. mi. (orbital altitude)

$\therefore m/K_\Omega = 0.358$

According to Figure 2, linear (rate) damping is assured for an orbital altitude up to about 4250 n. mi. for orbital inclinations in excess of 15° from the magnetic equator.

3.20 SELECTION OF DAMPER PARAMETERS

Since the size and weight of the damper are governed by the choice of the dimensional ratios, a/c, c/r_1, r_1/r_2, the magnetization M, and the desired value of K_Ω, it is of interest to consider how these parameters might be selected.

The a/c ratio and the magnetization M are mainly determined from magnet design considerations. Once a particular alloy (typically Alnico 5) has been selected, the operating flux density, in the case of a bar magnet, depends upon the length-to-diameter ratio, ℓ/d.* For an efficient magnet, in terms of strength per unit volume, the ℓ/d ratio is chosen to obtain an operating point on the demagnetization curve (that part of the B-H hysteresis loop lying in the second quadrant) near the peak energy point (maximum B-H product). It is not easy to predict the optimum shape and the operating point by analytical means, since the air gap of a cylindrical magnet is not well defined. Therefore, the GEOS-A magnet design parameters will be used as a basis for calculations in this section. Since detailed design information is of a proprietary nature, only the results of calculations using design data will be included in this report.

For efficient use of the damper volume and to obtain the maximum centering force from the diamagnetic shell, the c/r_1 ratio should be near unity with the constraint, $a^2 + c^2 < r_1^2$, or

$$c/r_1 < [1 + (a/c)^2]^{-\frac{1}{2}} \qquad (1)$$

The exact choice of c/r_1 would depend upon dimensional tolerances

* $\ell/d \approx 2a/c$

and the amount of deflection of the magnet assembly from center that would be expected in practice.

With r_2 fixed and a/c and c/r_1 specified, there is an optimum shell thickness ratio r_1/r_2, for which K_Ω is a maximum, since in (3.16-24), $S \to 0$ as $r_1 \to 0$ or as $r_1 \to r_2$. The optimum ratio, $(r_1/r_2)_o$, is independent of r_2. The value of S has been plotted versus $\Delta r/r_2$ ($\Delta r = r_2 - r_1$) in Figure 1 based on values of a/c and c/r_1 used in the design of the GEOS-A damper. The optimum value of $\Delta r/r_2$ is about 0.12, corresponding to $(r_1/r_2)_o = 0.88$. The value of $\Delta r/r_2$ used in the GEOS-A damper is less than the theoretical optimum, corresponding to a reduction in damping coefficient of about 25%.

For specified values of a/c, c/r_1, and K_Ω, choosing $r_1/r_2 = (r_1/r_2)_o$ yields a minimum volume damper. A small damper is desirable, because the effect of solar radiation pressure on the satellite attitude is minimized. Figure 2 is a graph showing diameter (copper shell) of a minimum volume damper versus K_Ω. A graph for a damper having the same dimensional ratios as the GEOS-A damper is shown for comparison. At the nominal damping coefficient of 60,600 dyne-cm-sec.*, the minimum volume damper diameter is only 0.2 inch less than the actual design value for the GEOS-A damper.

Assuming fixed dimensional ratios, the damper weight is proportional to overall volume. For reference the weight of the GEOS-A damper is 7 pounds and the overall diameter, including

* This figure does not include the effect of the aluminum shell, which is about 12% of the total damping coefficient of 70,000 dyne-cm-sec.

the aluminum shell is 5". Figure 3 is a curve showing total weight versus d_2, based on dimensional ratios of the GEOS-A damper. The damper weight is given as a function of K_Ω, assuming GEOS-A damper dimensional ratios, in Figure 4.

4. ANALYSIS OF EDDY CURRENT ROD DAMPING CONCEPT

4.1 LIBRATION DAMPING BY MEANS OF EDDY CURRENT RODS

Several passive techniques which require no moving parts for libration damping have been described by R.E. Fischell of APL [7]. These techniques use ferromagnetic rods which are magnetized by the earth's magnetic field. The rods are rigidly attached to the main body of the satellite so that attitude motions move the rods with respect to the earth's magnetic field. The changes in magnetization generate power losses by hysteresis and eddy currents, and the result is a damping torque applied to the satellite.

The specific technique which is considered for use on the GEOS B satellite uses equal volumes of rods mounted parallel to the three principal axes of the satellite. The rods are made of a moderate hysteresis loss material which has a high permeability at the earth's magnetic field intensity. Eddy current damping is obtained by means of power losses in a copper sheath around each rod. Since the remanence of the magnetic material is low, the magnetic induction along each axis is approximately proportional to the component of the applied magnetic field. The induced dipole is, therefore, nearly parallel with the applied field, and the perturbing effect of the induced dipole is much less than for other types of magnetic rod dampers.

4.2 DERIVATION OF THE BASIC TORQUE FORMULA

The torque required to rotate a ferromagnetic rod clad with a conducting sheath in a magnetic field can be derived in a manner similar to the analysis for shorted coil damping by Fischell. Consider a long, cylindrical rod rotating about an axis normal to the longitudinal axis in a magnetic field of intensity $\overline{H}$.

With long rods, the effect of induced poles is to prevent the rod from being magnetized except along the longitudinal axis; hence, only the longitudinal component of the applied field need be considered. The intensity of the internal field differs from the applied field intensity, due to the demagnetization effect of induced poles, by an amount that depends on the length-to-diameter ratio (ℓ/d) of the rod.

$$H_i = H_a - \frac{N}{4\pi} B_i \quad \text{(oersteds)} \tag{1}$$

where B_i is the internal flux density in gauss, and N is the demagnetizing factor. According to Bozorth and Chapin [8],

$$\frac{N}{4\pi} = \frac{4.02 \log_{10} (\ell/d) - .92}{2(\ell/d)^2} \quad (\mu = \infty) \tag{2}$$

for a long cylindrical rod with $\ell/d > 10$. The demagnetization effect can be accounted for by defining an "apparent" permeability, μ', as the ratio of the internal flux density to the applied field intensity. The apparent permeability can be obtained in terms of the true permeability and the ℓ/d ratio by means of a graph which appears in [8].

If H_m is the magnitude of the applied field intensity, then

for a constant rate of rotation ω, the component of $\overline{H}$ along the longitudinal axis of the rod is

$$H = H_m \sin \omega t \tag{3}$$

To evaluate the effectiveness of eddy current damping with a conducting sheath, core losses will be neglected. By hypothesis, the flux density in the rod is also sinusoidal, and

$$B = B_m \sin \omega t = \mu' H_m \sin \omega t \tag{4}$$

where B is the flux density averaged over the rod and μ' in the apparent permeability. The copper sheath is equivalent to a single turn coil around the bar, and the voltage induced around the sheath is

$$v = - \frac{d\varphi}{dt} \times 10^{-8} \quad \text{(volts)} \tag{5}$$

Neglecting leakage flux and assuming a constant flux density in the rod, then

$$v = -A \frac{dB}{dt} \times 10^{-8} = -A \omega B_m \cos \omega t \times 10^{-8} \quad \text{(volts)} \tag{6}$$

where $A = \pi r_1^2$ is the cross-sectional area of the rod, which has radius r_1 cm. The power dissipated in a strip of copper of thickness dr at a radius of r and length ℓ cm. is

$$dP = \frac{v^2 \ell \, dr}{2\pi r \rho} \quad \text{(watts)} \tag{7}$$

where ρ is the resistivity of the copper in ohm-cm. The total power dissipated in the sheath is, therefore,

$$P = \frac{v^2 \ell}{2\pi\rho} \int_{r_1}^{r_2} \frac{dr}{r} = \frac{v^2 \ell}{2\pi\rho} \ln \left(\frac{r_2}{r_1}\right) \quad (8)$$

$$= \frac{A^2 \ell \omega^2}{4\pi\rho} \ln (r_2/r_1)\, B_m^2\, (1 + \cos 2\omega t)\, (10^{-16}) \quad (9)$$

$$P = \frac{A^2 \ell \omega^2}{4\pi\rho} \ln (r_2/r_1)\, \mu'^2\, H_m^2\, (1 + \cos 2\omega t)\, (10^{-16}) \text{ (watts)} \quad (10)$$

The average power dissipated over a complete rotation cycle is

$$\langle P \rangle = \frac{A^2 \ell \omega^2}{4\pi\rho} \ln (r_2/r_1)\, \mu'^2\, H_m^2 \times 10^{-16} \text{ (watts)} \quad (11)$$

The power loss given by (9) corresponds to a viscous damping torque, $N_\omega = K_\omega \omega$ dyne-cm, where

$$K_\omega = \frac{A^2 \ell}{4\pi\rho} \ln (r_2/r_1)\, \mu'^2\, H_m^2 \times 10^{-9} \text{ (dyne-cm-sec)} \quad (12)$$

When several rods are mounted parallel to each other, additional damping is obtained, but not in proportion to their number, because of a proximity effect which reduces the flux density in each rod. The effect can be accounted for by means of a separation coefficient, σ_e. For two rods, the separation coefficient varies from about one-half for adjacent rods to unity for an infinite separation. The damping coefficient for n rods has the form, therefore,

$$K_\omega = \frac{n\sigma_e A^2 \ell}{4\pi\rho} \ln (r_2/r_1)\, \mu'^2\, H_m^2 \times 10^{-9} \text{ (dyne-cm-sec)} \quad (13)$$

It should be emphasized that the above formula involves parameters, σ_e and μ', that cannot be accurately predicted by ordinary analysis and which require careful laboratory measure-

ment for a particular material and geometry. For a given material and shape, the data can be obtained by experiment, and the results can then be substituted to obtain K_w. For the purpose of this report, a rough estimate of these parameters will suffice.

4.3 ANALYSIS OF LIBRATION DAMPING

The object of this section is to obtain rough estimates of the effectiveness of the eddy current rod damping device on a gravitationally stabilized satellite. In order to obtain any results analytically, it becomes necessary to make some gross assumptions and approximations which may not be too realistic; however, the results should at least make possible a comparison in the performance of the alternate damping methods under idealized conditions. A more accurate performance evaluation requires a complete simulation of the non-linear equations of motion, but this task is beyond the scope of the present investigation.

The configuration which will be studied has three equal volumes of rods rigidly mounted along the roll, pitch, and yaw axes of the satellite. With gravity-gradient stabilization, the reference positions for the roll, pitch, and yaw axes are the orbital velocity vector, the normal to the orbit plane, and the local vertical. Only circular orbits will be considered.

Two sets of coordinate systems will be needed. Let x_1, x_2, x_3 denote the roll, pitch, and yaw axes, respectively, of the satellite, and let x_1^o, x_2^o, x_3^o denote the corresponding orbital reference axes. For an arbitrary rotation of the satellite, the components of vector in one coordinate system can be obtained in the other by an orthogonal transformation; i.e.,

$$\underline{x} = \underline{A}\,\underline{x}^o \qquad (1)$$

where $\underline{x} = (x_1, x_2, x_3)^T$ and $\underline{x}^o = (x_1^o, x_2^o, x_3^o)^T$ are column vectors and $\underline{A} = [a_{ij}]$ is a 3x3 orthogonal matrix, where

$$a_{11} = \cos\theta \cos\psi \tag{2a}$$

$$a_{12} = \cos\theta \sin\psi \tag{2b}$$

$$a_{13} = -\sin\theta \tag{2c}$$

$$a_{21} = -\cos\varphi\sin\psi + \sin\varphi\sin\theta\cos\psi \tag{2d}$$

$$a_{22} = \cos\varphi\cos\psi + \sin\varphi\sin\theta\sin\psi \tag{2e}$$

$$a_{23} = \sin\varphi \cos\theta \tag{2f}$$

$$a_{31} = \sin\varphi\sin\psi + \cos\varphi\sin\theta\cos\psi \tag{2g}$$

$$a_{32} = -\sin\varphi\cos\psi + \cos\varphi\sin\theta\sin\psi \tag{2h}$$

$$a_{33} = \cos\varphi \cos\theta \tag{2i}$$

The components of the earth's magnetic field along the satellite axes will be needed. Assuming a dipole model, the vertical and horizontal components of the field intensity vector are given by:

$$H_v = -\frac{2m_e}{r_o^3}\sin\varphi_m \tag{3}$$

$$H_h = \frac{m_e}{r_o^3}\cos\varphi_m \tag{4}$$

where m_e is the dipole moment of the earth's field, r_o is the orbital radius, and φ_m is the magnetic latitude. The components of the field along the orbital reference axes are

$$H_{xo} = H_h \cos\alpha \tag{5}$$

$$H_{yo} = +H_h \sin\alpha \tag{6}$$

$$H_{zo} = H_v \tag{7}$$

where α is the angle between the orbital plane and the magnetic meridian plane. In terms of the orbital inclination, i_m, relative to the magnetic equator and the argument, θ_m, of the satellite position measured from the ascending node of the orbit

$$H_{xo} = \frac{m_e}{r_o^3} \sin i_m \cos \theta_m \tag{8}$$

$$H_{yo} = + \frac{m_e}{r_o^3} \cos i_m \tag{9}$$

$$H_{zo} = \frac{2m_e}{r_o^3} \sin i_m \sin \theta_m \tag{10}$$

In terms of H_{xo}, H_{yo}, and H_{zo},

$$H_x = H_{xo} \cos\theta \cos\psi + H_{yo} \cos\theta \sin\psi - H_{zo} \sin\theta \tag{11}$$

$$\begin{aligned} H_y = {} & H_{xo} (-\cos\varphi \sin\psi + \sin\varphi \sin\theta \cos\psi) \\ & + H_{yo} (\cos\varphi \cos\psi + \sin\varphi \sin\theta \sin\psi) \\ & + H_{zo} \sin\varphi \cos\theta \end{aligned} \tag{12}$$

$$\begin{aligned} H_z = {} & H_{xo} (\sin\varphi \sin\psi + \cos\varphi \sin\theta \cos\psi) \\ & + H_{yo} (-\sin\varphi \cos\psi + \cos\varphi \sin\theta \sin\psi) \\ & + H_{zo} \cos\varphi \cos\theta \end{aligned} \tag{13}$$

The damping for roll, pitch, and yaw motions will be obtained separately, assuming small angular displacements. For small angles,

$$H_x \approx H_{xo} + H_{yo}\psi - H_{zo}\theta \tag{14}$$

$$H_y \approx -H_{xo}\psi + H_{yo} + H_{zo}\varphi \tag{15}$$

$$H_z \approx H_{xo}\theta - H_{yo}\varphi + H_{zo} \tag{16}$$

For roll, pitch, or yaw motion the components are given by Table 1.

Field Component	Roll	Pitch	Yaw
H_x	H_{xo}	$H_{xo}-H_{zo}\theta$	$H_{xo}+H_{yo}\psi$
H_y	$H_{yo}+H_{zo}\varphi$	H_{yo}	$-H_{xo}\psi+H_{yo}$
H_z	$-H_{yo}\varphi+H_{zo}$	$H_{xo}\theta+H_{zo}$	H_{zo}

TABLE 1 - Components of Magnetic Intensity Vector Along Roll, Pitch, and Yaw Axes

The instantaneous power loss in each rod is proportional to the square of the rate of change of the component of $\overline{H}$ along the rod. The rate of change consists of two components, one contributed by the attitude motion and another by the orbital motion of the satellite through the magnetic field of the earth. Because the square is taken, the principle of superposition does not apply, and it is not possible to separate the damping of attitude motions from the perturbing effect of orbital motion. For a preliminary estimate of the effectiveness of transient damping, the effect of orbital motion will simply be ignored. This procedure will yield a "best case" estimate of transient damping. The net torque generated about a particular axis is obtained by combining the torques contributed by the rods normal to the axis. The resulting damping coefficients for roll, pitch, and yaw rates of motion are as follows.

Roll: $$K_{\dot{\varphi}} = k\,(H_{Y_0}^2 + H_{Z_0}^2) \tag{17}$$

Pitch: $$K_{\dot{\theta}} = k\,(H_{Z_0}^2 + H_{X_0}^2) \tag{18}$$

Yaw: $$K_{\dot{\psi}} = k\,(H_{X_0}^2 + H_{Y_0}^2) \tag{19}$$

where k is a coefficient depending upon the rod and sheath parameters; viz.

$$k = \frac{n\sigma_e A^2 \ell \mu'^2}{2\pi\rho} \ln (r_2/r_1) \times 10^{-9} \quad \text{(cgs)} \tag{20}$$

Clearly the damping coefficient for a particular axis of rotation is distinct and varies with the location of the satellite in the earth's magnetic field.

The pitch axis damping coefficient will be investigated in further detail. From (8), (10) and (18)

$$K_{\dot{\theta}} = k\left(\frac{m_e}{r_o^3}\right)^2 \sin^2 i_m\,(\cos^2 \theta_m + 4 \sin^2 \theta_m)$$

$$= k\left(\frac{m_e}{r_o^3}\right)^2 \sin^2 i_m\,(4 - 3\cos^2 \theta_m) \tag{21}$$

The average damping coefficient over an orbit is

$$\langle K_{\dot{\theta}} \rangle = \langle H_{X_0}^2 + H_{Z_0}^2 \rangle$$

$$= \frac{5}{2} k\left(\frac{m_e}{r_o^3}\right)^2 \sin^2 i_m \tag{22}$$

The variation of $\langle K_{\dot{\theta}} \rangle_{\%}$ with i_m as shown in Figure 1. The maximum $\langle K_{\dot{\theta}} \rangle_{\%}$ occurs at $i_m = 90^\circ$, and at $i_m = 0$, $\langle K_{\dot{\theta}} \rangle_{\%}$ is zero. At $i_m = 45^\circ$, the ratio of $\langle K_{\dot{\theta}} \rangle_{\%}$ to the maximum value is 0.5.

Figure 2 shows the effect of orbital altitude h on $\langle K_{\dot{\theta}} \rangle_{\%}$

for h/r_e ranging from zero to 0.7, where r_e is the radius of the earth. Note that $\left(K_{\dot{\theta}}\right)_o$ varies inversely as the sixth power of the orbital radius. The graph shows that doubling altitude from 600 n. mi. to 1200 n. mi. reduces the average damping coefficient by 56.5%.

4.4 SELECTION OF DAMPER ROD PARAMETERS

Formula (4.3-18) for the pitch axis damping coefficient has the form

$$\left\langle K_\theta^{\cdot} \right\rangle = \frac{n\sigma_e \pi}{32\rho} \left(\ell/d_1\right)^{-4} \ell^5 \ln(d_2/d_1)\mu'^2 \left\langle H_\theta^2 \right\rangle \times 10^{-9} \quad \text{(dyne-cm-sec)} \tag{1}$$

where $d_i = 2r_i$ $(i = 1,2)$ and

$$\left\langle H_\theta^2 \right\rangle = \left\langle H_{z_o}^2 + H_{x_o}^2 \right\rangle = \frac{5}{2}\left(\frac{m_e^2}{r_o^6}\right) \sin^2 i_m \tag{2}$$

It is interesting to see how the various rod parameters might be selected in order to calculate the size and weight corresponding to a specified torque coefficient. A practical design basis would be to maximize the ratio of $\left\langle K_\theta^{\cdot} \right\rangle$ to volume for a single rod. The volume of each rod including the sheath, is

$$V = (\pi/4)\, d_2^2\, \ell = (\pi/4)(d_2/d_1)^2\, (d_1/\ell)^2\, \ell^3 \tag{3}$$

$$\therefore \left\langle K_\theta^{\cdot} \right\rangle / V \propto \left[(d_2/d_1)^{-2} \ln(d_2/d_1)\right] (\ell/d_1)^{-2}\, \ell^2\, \mu'^2 \tag{4}$$

The independent design parameters are d_2/d_1, ℓ/d_1, and ℓ. The apparent permeability μ' is a function of ℓ/d_1 and the true permeability μ of the rod core material.

For maximum $\left\langle K_\theta^{\cdot} \right\rangle/V$, the rod should be as long as possible for the available space; i.e. $\ell = \ell_{max}$. The shortest dimension of the GEOS satellite is about 30", along the z-axis.

By partial differentiation, it is found that $\langle K_{\dot{\theta}} \rangle / V$ is maximum as a function of d_2/d_1 for $d_2/d_1 = \sqrt{e} \approx 1.65$.

Because the total space is limited in GEOS, it may be beneficial to use fewer rods while increasing the sheath thickness of each rod. Because no quantitative information is available on the separation coefficient for parallel rods, it is necessary to neglect the proximity effect in the present study.

The choice of ℓ/d_1 presents an interesting problem, because of the complicated way in which μ' depends upon ℓ/d_1. There are two effects to consider. First, the demagnetizing effect of induced poles becomes less as the ℓ/d_1 ratio is made larger, so that the internal field intensity approaches the applied field intensity. For large ℓ/d_1 the ratio of apparent permeability to true permeability is, therefore, close to unity. Second, the true permeability varies with the internal field intensity. For a strong, constant external field, the true permeability rises from an initial value to a maximum value as ℓ/d_1 is increased, and then drops off rapidly as the material begins to saturate.

Because of its high permeability and low hysteresis loss, 4-79 Molybdenum Permalloy is the best available material for the present application; however, it should be noted that Permalloy saturates at about 0.2 oersteds, while the earth's magnetic field at low altitude may be much stronger. Thus, some demagnetization appears to be necessary at low altitudes. Moreover, Bozorth's and Chapin's graph shows that demagnetization has a stabilizing

effect on the apparent permeability, if the true permeability is sufficiently large and ℓ/d_1 is not too large.

These relationships are clarified in Figures 1 and 2. The graphs are based upon published magnetization curves for 4-79 Molybdenum Permalloy [9] and Bozorth's and Chapin's graph [8]. Figure 1 shows the apparent permeability as a function of applied field intensity for several values of ℓ/d_1. The stabilizing effect of demagnetization on μ for smaller ℓ/d_1 is apparent; however, stabilization is obtained at considerable reduction in μ' within the range of practical applied field intensities. Figure 2 is a graph of μ' versus ℓ/d_1 with true permeability μ as a parameter. This graph shows clearly the increase in μ' with ℓ/d_1. The curve for $\mu = 10^5$ will be used as a design basis.

The optimization of $\langle \dot{K}_\theta \rangle / V$ can now be completed. Figure 3 is a graph of $(\ell/d_1)^{-2}\ \mu'^2$ versus ℓ/d_1, based upon data presented in Figure 2. The curve reaches a maximum value at about $\ell/d_1 = 300$; however, as previously noted, μ' is more sensitive to applied field strength at $\ell/d_1 = 300$, so that a somewhat lower value may be preferable.

The damping coefficient for a single rod ($n = 1$, $\sigma_e = 1$) with $\ell = 29"$, $d_1 = 1/8"$ and $d_2 = 3/8"$ has been calculated for a hypothetical polar orbit at earth radius ($r_e = 6.378 \times 10^8$ cm, $i_m = 90^\circ$) to be $\langle \dot{K}_\theta \rangle_o = 1338$ dyne-cm-sec. For four rods spaced well apart, $\langle \dot{K}_\theta \rangle = 5352$ dyne-cm-sec. At orbital altitudes and for lower orbital inclinations, the damping coefficient will be reduced according to

Figures 4.3-1 and 4.3-2. For example, if a 600 n. mi. polar orbit is chosen, the correction factor is 0.38, so that for four rods, $\langle K_\theta^{\cdot} \rangle$ = 1980 dyne-cm-sec.

Each rod weighs about 1.5 lb., so that the total weight of the three sets of four rods is about 18 lb. Assuming that enough space were available, and the resulting payload could be orbited, to get a damping coefficient of 70,000 dyne-cm-sec., about 140 rods along each axis would be needed for a total weight of 636 lb.

5. COMPARISON OF THE TWO DAMPING TECHNIQUES

Enough information has been derived on the performance of the magnetically anchored and the eddy current rod dampers to provide a basis for comparative evaluation. The results of the comparison will enable certain conclusions to be reached concerning the relative merits of the two dampers for use on GEOS satellites.

5.1 OPERATING PRINCIPLE

The same basic operating principle applies to each damper: satellite attitude motions vary the magnetic flux linking a conducting element, and the induced eddy currents dissipate rotational kinetic energy in the form of heat. The implementation of the basic concept is quite different for the two dampers, and this fact leads to significant differences in operation and performance.

With the magnetically anchored damper, damping results from relative motion between a strong permanent magnet, which is oriented by the earth's magnetic field, and a conducting shell attached to the satellite. Since the magnet is free to swivel about its dipole axis, only the component of the satellite rotation that is normal to the dipole axis actually produces a torque. Furthermore, since the torque is generated along the axis of relative motion, only the component of torque along the satellite rotation axis is effective for motion damping. The effect of the component normal to the satellite rotation axis has not been explained for lack of sufficient time to pursue the investigation;

however, it would be interesting to examine this point at a later time.

Although the eddy current rod damper has no moving parts, satellite attitude motions with respect to the earth's magnetic field cause flux variations in high permeability magnetic rods mounted along each principal axis of the satellite. For simple yaw, pitch or roll motion, the torque is directed along the axis of motion; however, the degree of effectiveness with which a particular motion is damped depends on the direction of the earth's magnetic field with respect to the axis of the satellite. The level of flux which is produced in the rods depends not only on the intensity of the applied field and the true permeability of the rod material but also on the shape of the rods, which governs the apparent permeability.

5.2 TORQUE COEFFICIENT

Because the same basic operating principle is used, either damper generates a torque that, to a good approximation is proportional to the rate of rotation about the axis of sensitivity. It is interesting to compare the respective formulas for the basic torque coefficients, since they are analogous:

Magnetically anchored damper:

$$K_\Omega = \frac{8\pi}{\rho} (\mu_o M)^2 r_2^5 S(a/c,\ c/r_1,\ r_1/r_2) \qquad (1)^*$$

Eddy current rod damper:

$$K_\omega = \frac{n\sigma_e \pi}{\rho} (\mu' H)^2 \ell^5 S'(d_1/\ell,\ d_1/d_2) \qquad (2)^{**}$$

*Rotation of shell about axis normal to magnet dipole axis.

**Rotation of n parallel rods about transverse axis normal to magnetic field H.

In each case the torque coefficient is proportional to the square of a magnetic flux density ($\mu' H$ or $\mu_o M$) and is inversely proportional to the electrical resistivity ρ of a conducting element. Also, both formulas contain length raised to the fifth power (r_2^5 or ℓ^5) and a dimensionless shape factor (S or S').

The torque coefficient for the magnetically anchored damper is a function of intrinsic parameters only, since the inducing magnetic field is obtained from a strong permanent magnet. On the other hand, the torque coefficient for the eddy current rod damper is dependent upon an extrinsic quantity, the intensity H of the earth's magnetic field.

5.3 EFFECT OF ORBITAL ALTITUDE

Because the intensity of the earth's magnetic field varies inversely as the cube of distance from the geocenter, the damping coefficient of the eddy current rod damper varies inversely as the sixth power of the distance. Figure 4.3-2 shows the sensitivity of the damping coefficient to orbital altitude. For a change in altitude from 600 to 1200 n. mi. the damping coefficient is reduced by 56.5%.

Although the torque coefficient for the magnetically anchored damper is not affected by orbital altitude, the effective damping torque is constant only so long as the magnet dipole axis is aligned with the magnetic field of the earth. At high altitudes a problem develops, because the magnetic field is not strong enough to maintain the dipole axis in proper alignment. When the dipole axis deflection angle becomes too large, two effects take

place. First, the effective damping torque becomes smaller, and second, the relationship between torque and satellite rotation rate becomes increasingly non-linear. Ultimately, the damper becomes ineffective as shown in Figures 3.18-2 and 3.18-3. These problems are easily eliminated by using a stronger magnet. The resulting weight increase usually does not count as a penalty, because the damper is used as a tip weight at the end of a gravity-gradient stabilization boom. Calculations show that the GEOS-A damper functions properly for altitudes up to several thousand miles.

5.4 EFFECT OF ORBITAL INCLINATION

With both dampers, the effective damping of pitch librations varies with the latitude of the satellite, because the direction of the magnetic field changes with respect to the pitch axis. The average damping over a complete orbit was computed for both dampers. In each case, the average damping is maximum for magnetic polar orbits and is zero for a magnetic equatorial orbit. At intermediate orbital inclinations, comparison of Figures 3.18-1 and 4.3-1 shows that a larger fraction of the maximum average torque is obtained with the magnetically anchored damper.

5.5 SIZE AND WEIGHT

The size and weight of both dampers for a specified damping coefficient has been investigated. Since the damping coefficient for each damper is a function of certain intrinsic parameters, which determine size and weight, it was first necessary to provide a rationale for specifying the parameters.

Since the magnetically anchored damper is used as a boom tip weight, a small damper is desirable to keep the torque caused by solar pressure small. The analysis of Section 3.20 shows that there is an optimum ratio of shell thickness to outside radius, which for a specified torque coefficient, yields a minimum volume damper. The GEOS-A damper design is only slightly larger than the minimum volume design. It turns out that wide range of torque coefficients can be obtained with minor changes in damper size. This is shown in Figure 3.20-2.

If all dimensional ratios are fixed, the magnetically anchored damper weight is proportional to the three-halves power of the torque coefficient. Using GEOS-A damper dimensions and weight as a guide, a graph of weight versus torque coefficient was plotted in Figure 3.20-4.

Analysis of the eddy current rod damper rods in Section 4.4 shows that the ratio of damping coefficient to volume per rod is maximized by making the rod as long as possible. The limiting dimension for the GEOS satellite is about 30" along the vertical axis. There is also an optimum ratio of sheath diameter to core diameter for the rod. The theoretical optimum ratio of sheath diameter to core diameter is smaller than the design figure proposed by the satellite manufacturer by a factor of 1.8. A possible reason for this is that the proximity effect caused by spacing parallel rods closely together was neglected in the analysis for lack of specific information. Analysis based on available data for 4-79 Molybdenum Permalloy and experimental curves on the demagnetizing effect of induced poles in magnetic rods indicates

that a large ratio of length to diameter (≈250) should be used for the ferromagnetic cores.

The weight of the proposed rod configuration is about 18 lb. which exceeds the magnetically anchored damper weight by 11 lb. The damping coefficient for a 600 n. mi. polar orbit is only 1980 dyne-cm-sec, compared with 70,000 dyne-cm-sec for the magnetically anchored damper. It is clearly impractical to achieve a damping level of the same order as that easily obtained with the magnetically anchored damper, since over 600 lb. of rods would be needed.

It should be mentioned that the magnetically anchored damper weight is useful, because it also serves as a necessary boom tip weight, while the eddy current rods are essentially dead weight.

5.6 DAMPING OF INITIAL LIBRATIONS

Because the equations of motion for large angle motion are non-linear, and because of certain complexities in the way either damper functions that are difficult to take into account, an accurate prediction of transient damping time is not possible without computer simulation.

The analysis does show, however, that either damper may be characterized in terms of a certain damping coefficient. It was found that the eddy current rod damper coefficient is more than an order of magnitude smaller than that of the magnetically anchored damper. Computer simulations performed by GE indicate a damping time of about six days for the GEOS-A satellite at 600 nautical mile altitude. Consequently, a damping time on the order of 100 days would be expected with the eddy current rod.

It does not appear to be feasible to improve upon the eddy current rod design, and a significantly higher damping level could be obtained only with an unacceptable weight penalty.

REFERENCES

1. Stratton, Julius Adams, Electromagnetic Theory, McGraw-Hill Book Company, Inc., New York, 1941.

2. Panofsky, Wolfgang K. H. and Melba Phillips, Classical Electricity and Magnetism, Second ed. Addison-Wesley Publishing Co., Inc. Reading, Mass., 1962.

3. Smythe, William R., Static and Dynamic Electricity, McGraw-Hill Book Co., Inc., New York, 1950.

4. Abramowitz, Milton and Irene A. Stegun, Editors, Handbook of Mathematical Functions, National Bureau of Standards Applied Mathematics Series · 55, U. S. Government Printing Office, Washington, D.C., 1964.

5. Goldstein, Herbert, Classical Mechanics, Addison-Wesley Publishing Co., Inc., Reading, Mass., 1950.

6. Burington, Richard Stevens, Handbook of Mathematical Tables and Formulas, Handbook Publishers, Inc., Sandusky, Ohio, 1958.

7. Fischell, Robert E., "Magnetic Damping of the Angular Motions of Earth Satellites," ARS Journal, September, 1961, pp. 1210-1217.

8. Bozorth, R. M. and D. M. Chapin, "Demagnetizing Factors of Rods," Journal of Applied Physics, Volume 13, May, 1942.

9. Alleghany Ludlum Moly Permalloy Blue Sheet, EM-30, Edition 1, Alleghany Ludlum Steel Corporation, Pittsburgh 22, Penn.

APPENDIX A

THE VECTOR POTENTIAL OF A CYLINDRICAL BAR MAGNET

Consider a cylindrical bar magnet, of radius a and length 2c, which is uniformly magnetized in the longitudinal direction. If $\bar{M}$ is the constant magnetic moment per unit volume (amp/m) the magnetic vector potential is given by the formula

$$\bar{A}' = \frac{\mu_o}{4\pi} \int_S \frac{\bar{M}x\bar{n}}{R} \, ds \quad (wb/m) \tag{1}$$

where μ_o is the permeability of free space, R is the distance from an elemental surface area ds at point P′ on the cylinder to the field point P, and $\bar{n}$ is the unit outward normal vector at ds. Obviously no contribution to the integral is obtained from the end surfaces, because $\bar{M}$ and $\bar{n}$ are there collinear, and, hence, $\bar{M}x\bar{n} = 0$.

In terms of unit vectors, $\bar{e}_\rho'$, $\bar{e}_\varphi'$, $\bar{k}'$, in the directions of increasing ρ, φ, and z at the point P′

$$\bar{M}x\bar{n} = M(\bar{k}x\bar{e}_\rho') = M\bar{e}_\varphi' \tag{2}$$

where $M = |\bar{M}|$. In rectangular coordinates

$$\bar{e}_\varphi' = -\bar{i}\sin\varphi' + \bar{j}\cos\varphi' \tag{3}$$

where $\bar{i}$ and $\bar{j}$ are unit vectors along the x and y axes, respectively. Since $ds = ad\varphi' dz'$

$$\bar{A} = \frac{\mu_o Ma}{4\pi} \int_{-c}^{c} \int_{-\pi}^{\pi} \frac{(-\bar{i}\sin\varphi' + \bar{j}\cos\varphi')}{R} \, d\varphi' dz' \tag{4}$$

Denote the spherical polar coordinates of P by r, θ, φ and those of P′ by r′, θ', φ'. Then

$$R = \{r^2 + r'^2 - 2rr' [\cos\theta\cos\theta' + \sin\theta\sin\theta'\cos(\varphi-\varphi')]\}^{\frac{1}{2}} \quad (5)$$

or $$R = (r^2 + r'^2 - 2rr'\cos\alpha)^{\frac{1}{2}} \quad (6)$$

where α is the angle between r and r′. By axial symmetry, $|\bar{A}| = A_\varphi$ is independent of φ, so for convenience, set $\varphi = 0$. Now the $\bar{i}$ component of the integrand in (4) is an odd function of φ', while the $\bar{j}$ component is an even function of φ'. The $\bar{i}$ component of $\bar{A}$ is, therefore, zero, and

$$A_\varphi = |\bar{A}_y| = \frac{\mu_o Ma}{4\pi} \int_{-c}^{c} \int_{-\pi}^{\pi} \frac{\cos\varphi'}{R} \, d\varphi' \, dz'; \quad \cos\varphi = 0 \quad (7)$$

The inverse distance can be expanded in a series of Legendre polynomials (zonal harmonics), $P_n(\cos\alpha)$.

$$R^{-1} = \sum_{n=0}^{\infty} f_n(r,r')P_n(\cos\alpha) \quad (8)$$

where

$$f_n(r,r') = \begin{cases} r'^n/r^{n+1} & , \ r'<r \\ r^n/r'^{n+1} & , \ r<r' \end{cases} \quad (9)$$

According to the biaxial theorem for zonal harmonics,

$$P_n(\cos\alpha) = \sum_{m=0}^{n} (2-\delta_m^o) \frac{(n-m)!}{(n+m)!} P_n^m(\cos\theta) \, P_n^m(\cos\theta') \quad (10)$$

Thus,

$$R^{-1} = \sum_{n=0}^{\infty} \sum_{m=0}^{n} (2-\delta_m^o) \frac{(n-m)!}{(n+m)!} f_n(r,r')P_n^m(\cos\theta)P_n^m(\cos\theta') \times \cos m\varphi' \quad (11)$$

After substituting this expression for R^{-1} in (7), interchanging the order of summation and integration, and integrating over φ', only the m=1 term remains.

$$\therefore A_\varphi = \frac{\mu_o M}{2} \sum_{n=0}^{\infty} \frac{(n-1)!}{(n+1)!} P_n^1(\cos\theta) \times \int_{-c}^{c} f_n(r,r') P_n^1(\cos\theta') dz' \qquad (12)$$

To evaluate the integral, substitute $r' = (a^2 + z'^2)^{\frac{1}{2}}$, $\cos\theta' = z'(a^2+z'^2)^{-\frac{1}{2}}$. Since the expansion will actually be needed only in the region, $r>r'$, the integral will be evaluated for that case only. Thus, $f_n(r,r') = r'^n/r^{n+1}$ and

$$\therefore \int_{-c}^{c} f_n(r,r') P_n^1(\cos\theta') dz' = \frac{1}{r^{n+1}} \int_{-c}^{c} (a^2 + z'^2)^{n/2} P_n^1\left(\frac{z'}{\sqrt{a^2+z'^2}}\right) dz' \qquad (13)$$

By definition,

$$P_n^1(u) = (1-u^2)^{\frac{1}{2}} \frac{dP_n(u)}{du} \qquad (14)$$

and $$P_n(u) = \sum_{s=0}^{[n/2]} (-1)^s \frac{(2n-2s)!}{2^n s!(n-s)!(n-2s)!} u^{n-2s} \qquad (15)$$

where [n/2] denotes the integer part of n/2. Thus,

$$\frac{dP_n(u)}{du} = \sum_{s=0}^{[(n-1)/2]} (-1)^s \frac{(2n-2s)!}{2^n s!(n-s)!(n-2s-1)!} u^{n-2s-1} \qquad (16)$$

Substitution of (14) and (16) into (13) with $u = z'(a^2+z'^2)^{-\frac{1}{2}}$, and interchanging the order of summation and integration gives

$$\int_{-c}^{c} f_n(r,r')P_n^1(\cos\theta')dz'$$

$$= \frac{a}{r^{n+1}} \sum_{s=0}^{[(n-1)/2]} (-1)^s \frac{(2n-2s)!}{2^n s!(n-s)!(n-2s-1)!}$$

$$x \int_{-c}^{c} (a^2+z'^2)^s \; z'^{n-2s-1} \; dz' \qquad (17)$$

For n an even integer, the integrand is an odd function of z', and the value of the integral is zero. For n an odd integer:

$$\int_{-c}^{c} (a^2+z'^2)^s \; z'^{n-2s-1} \; dz' = 2 \int_{0}^{c} (a^2+z'^2)^s z^{n-2s-1} dz' \qquad (18)$$

The binomial theorem gives

$$(a^2+z'^2)^s = \sum_{k=0}^{s} \binom{s}{k} a^{2(s-k)} \; z'^{2k} \qquad (19)$$

$$\therefore \int_{0}^{c} (a^2+z'^2)^s \; z^{n-2s-1} \; dz' = \sum_{k=0}^{s} \binom{s}{k} a^{2(s-k)} \int_{0}^{c} z'^{n-2s+2k-1} \; dz'$$

$$= \sum_{k=0}^{s} \binom{s}{k} \frac{a^{2(s-k)}}{(n-2s+2k)} \; c^{n-2s+2k} \qquad (20)$$

$$\therefore \int_{-c}^{c} f_n(r,r') \; P_n^1(\cos\theta')dz'$$

$$= \frac{a}{r^{n+1}} \sum_{s=0}^{(n-1)/2} \frac{(-1)^s(2n-2s)!}{2^{n-1}s!(n-s)!(n-2s-1)!} \sum_{k=0}^{s} \binom{s}{k} \frac{a^{2(s-k)}}{(n-2s+2k)} \; c^{n-2s+2k} \qquad (21)$$

Finally,

$$A_{\varphi} = \sum_{n=1}^{\infty} a_n(r) P_n^1(\cos\theta) \tag{22}$$

where, for n even, $a_n(r) = 0$, and for n odd,

$$a_n(r) = \frac{\mu_0 Ma}{2^n n(n+1)} \left(\frac{c}{r}\right)^{n+1}$$

$$x \sum_{s=0}^{(n-1)/2} \frac{(-1)^s (2n-2s)!}{s!(n-s)!(n-2s-1)!} \sum_{k=0}^{s} \binom{s}{k} \frac{1}{(n-2s+2k)} \left(\frac{a}{c}\right)^{2(s-k)+1} \tag{23}$$

At $r=r_1$,

$$a_n = a_n(r_1) = \frac{\mu_0 Ma}{2^n} \left(\frac{c}{r_1}\right)^{n+1} \frac{1}{n(n+1)}$$

$$x \sum_{s=0}^{(n-1)/2} \frac{(-1)^s (2n-2s)!}{s!(n-s)!(n-2s-1)!} \sum_{k=0}^{s} \binom{s}{k} \frac{1}{(n-2s+2k)} \left(\frac{a}{c}\right)^{2(s-k)+1} \tag{24}$$

The expansion of A_{φ} in a series of associated Legendre functions $P_m^1(\cos\theta)$ has now been accomplished in a manner that does not require the use of formula (3.9-5) for the coefficients of the expansion.

APPENDIX B

EVALUATION OF $\sigma^2_{nm} + \tau^2_{nm}$

Intuitively, it may be expected that the magnitude of the potential, W', and of the net torque, N_z, is independent of the azimuth angles, Φ_x, Φ_y, Φ_z, since the choice of the azimuth reference axis (ξ) is arbitrary. In fact an expression for the quantity, $\sigma^2_{nm} + \tau^2_{nm}$, can be derived which depends only on the polar angles, Θ_x, Θ_y, Θ_z, of the rotation axis, ζ, relative to the positive magnet axes, x', y', z', respectively. From (3.10-5):

$$\sigma^2_{nm} = \alpha^2_{nm}\cos^2 m\Phi_x + \beta^2_{nm}\cos^2 m\Phi_y + \gamma^2_{nm}\cos^2 m\Phi_z + 2\alpha_{nm}\beta_{nm}\,\mathrm{cosm}\Phi_x\,\mathrm{cosm}\Phi_y + 2\alpha_{nm}\gamma_{nm}\,\mathrm{cosm}\Phi_x\,\mathrm{cosm}\Phi_z + 2\beta_{nm}\gamma_{nm}\,\mathrm{cosm}\Phi_y\,\mathrm{cosm}\Phi_z \quad (1)$$

$$\tau^2_{nm} = \alpha^2_{nm}\sin^2 m\Phi_x + \beta^2_{nm}\sin^2 m\Phi_y + \gamma^2_{nm}\sin^2 m\Phi_z + 2\alpha_{nm}\beta_{nm}\,\mathrm{sinm}\Phi_x\,\mathrm{sinm}\Phi_y + 2\alpha_{nm}\gamma_{nm}\,\mathrm{sinm}\Phi_x\,\mathrm{sinm}\Phi_z + 2\beta_{nm}\gamma_{nm}\,\mathrm{sinm}\Phi_y\,\mathrm{sinm}\Phi_z \quad (2)$$

$$\therefore\quad \sigma^2_{nm} + \tau^2_{nm} = \alpha^2_{nm} + \beta^2_{nm} + \gamma^2_{nm} + 2\alpha_{nm}\beta_{nm}\,\mathrm{cosm}(\Phi_y - \Phi_x) + 2\alpha_{nm}\gamma_{nm}\,\mathrm{cosm}(\Phi_z - \Phi_x) + 2\beta_{nm}\gamma_{nm}\,\mathrm{cosm}(\Phi_z - \Phi_y) \quad (3)$$

The angles, $\Phi_y - \Phi_x$, $\Phi_z - \Phi_x$, and $\Phi_z - \Phi_y$ can be expressed in terms of Θ_x, Θ_y, Θ_z with the aid of spherical trigonometry. With reference to Figure 1, consider the right spherical triangles ABC and ADE formed by great circles in the x', y' and ξ,η planes and the meridian lines through the x' and y' axes from the ζ axis. Note that the ξ axis has been placed arbitrarily

along the line of intersection of the ξ,η and the x',y' planes, so that $\Theta_z>0$, $0<\Theta_x<\pi/2$ and $0<\Theta_y<\pi/2 \Rightarrow \Phi_z=-\pi/2$ radians. From spherical trigonometry,

$$\sin\Phi_x = \cot\Theta_x \cot\Theta_z \tag{4}$$

$$\sin\Phi_y = \cot\Theta_y \cot\Theta_z \tag{5}$$

$$\therefore \quad \cos\Phi_x = (1-\cot^2\Theta_x \cot^2\Theta_z)^{\frac{1}{2}}$$

$$= \frac{1}{\sin\Theta_x \sin\Theta_z} (\sin^2\Theta_x \sin^2\Theta_z - \cos^2\Theta_x \cos^2\Theta_z)^{\frac{1}{2}}$$

$$= \frac{1}{\sin\Theta_x \sin\Theta_z} \left[(1-\cos^2\Theta_x)(1-\cos^2\Theta_z) - \cos^2\Theta_x \cos^2\Theta_z\right]^{\frac{1}{2}}$$

$$= \frac{\cos\Theta_y}{\sin\Theta_x \sin\Theta_z} \qquad (0<\Phi_x<\pi/2) \tag{6}$$

since $\cos^2\Theta_x + \cos^2\Theta_y + \cos^2\Theta_z = 1$. Likewise,

$$\cos\Phi_y = -(1-\cot^2\Theta_y \cot^2\Theta_z)^{\frac{1}{2}} = \frac{-\cos\Theta_x}{\sin\Theta_y \sin\Theta_z} \quad (\pi/2<\Phi_y<\pi) \tag{7}$$

Hence,

$$\cos(\Phi_y-\Phi_x) = \cos\Phi_y \cos\Phi_x + \sin\Phi_y \sin\Phi_x$$

$$= -\frac{\cot\Theta_x \cot\Theta_y}{\sin^2\Theta_z} + \cot\Theta_x \cot\Theta_y \cot^2\Theta_z$$

$$= -\cot\Theta_x \cot\Theta_y \tag{8}$$

$$\sin(\Phi_y-\Phi_x) = \left[1-\cos^2(\Phi_y-\Phi_x)\right]^{\frac{1}{2}} = (1-\cot^2\Theta_x \cot^2\Theta_y)^{\frac{1}{2}}$$

$$= \frac{\cos\Theta_z}{\sin\Theta_x \sin\Theta_y} \tag{9}$$

$$\therefore \quad \tan(\Phi_y-\Phi_x) = \frac{+\cos\Theta_z}{-\cos\Theta_x \cos\Theta_y} \tag{10}$$

$$\text{or} \quad \Phi_y-\Phi_x = \tan^{-1}\left(\frac{+\cos\Theta_z}{-\cos\Theta_x \cos\Theta_y}\right), \quad \left(\frac{\pi}{2}\leq\Phi_y-\Phi_x\leq\pi\right) \tag{11}$$

Next,

$$\cos(\Phi_Z - \Phi_X) = \cos\Phi_Z \cos\Phi_X + \sin\Phi_Z \sin\Phi_X = -\sin\Phi_X \tag{12}$$

since $\Phi_Z = -\pi/2$.

$$\sin(\Phi_Z - \Phi_X) = \sin\Phi_Z \cos\Phi_X - \sin\Phi_X \cos\Phi_Z = -\cos\Phi_X \tag{13}$$

$$\therefore \quad \tan(\Phi_Z - \Phi_X) = \cot\Phi_X = \frac{-\cos\Theta_Y}{-\cos\Theta_X \cos\Theta_Z} \tag{14}$$

$$\text{or} \quad \Phi_Z - \Phi_X = \tan^{-1}\left(\frac{-\cos\Theta_Y}{-\cos\Theta_X \cos\Theta_Z}\right), \qquad (\pi \le \Phi_z - \Phi_x \le 3\pi/2) \tag{15}$$

Finally,

$$\cos(\Phi_Z - \Phi_Y) = -\sin\Phi_Y \ , \quad \sin(\Phi_Z - \Phi_Y) = -\cos\Phi_Y, (\pi/2 < \Phi_Y < \pi) \tag{16}$$

$$\therefore \quad \Phi_Z - \Phi_Y = \tan^{-1}\left(\frac{+\cos\Theta_Y}{-\cos\Theta_Y \cos\Theta_Z}\right), \qquad (\pi/2 \le \Phi_z - \Phi_y \le \pi) \tag{17}$$

Formulas (11), (15), and (17) give $\Phi_Y - \Phi_Z$, $\Phi_Z - \Phi_X$, and $\Phi_Z - \Phi_Y$ in terms of the polar angles Θ_X, Θ_Y, and Θ_Z. The quantity, $\sigma_{n_m}^2 + \tau_{n_m}^2$, can then be computed from (3). The three direction cosines appearing in (10), (15), and (17) are, of course, not independent but must satisfy the relation, $\cos^2\Theta_X + \cos^2\Theta_Y + \cos^2\Theta_Z = 1$.

The results of this appendix apply without restriction on the angles, Θ_X, Θ_Y, Θ_Z, provided that in formulas (11), (15), and the quadrant is defined by the signs of the numerator and denominator in each fraction.

APPENDIX C

EVALUATION OF A CERTAIN INTEGRAL

Denote the modified spherical Bessel functions of the first and second kinds by $\xi_n(\lambda r)$ and $\eta_n(\lambda r)$, respectively, where arg $\lambda = \pi/4$, and let

$$u_n(\lambda r,\lambda) = \alpha(\lambda)\xi_n(\lambda r) + \beta(\lambda)\eta_n(\lambda r) \tag{1}$$

$$v_n(\lambda r,\lambda) = \gamma(\lambda)\xi_n(\lambda r) + \delta(\lambda)\eta_n(\lambda r) \tag{2}$$

where $\alpha^*(\lambda) = \alpha(\lambda^*)$, $\beta^*(\lambda) = \beta(\lambda^*)$, $\gamma^*(\lambda) = \gamma(\lambda^*)$, and $\delta^*(\lambda) = \delta(\lambda^*)$. It is required to evaluate the integral

$$\int_{r_1}^{r_2} r^2 u_n(\lambda r,\lambda)v_n^*(\lambda r,\lambda)dr; \qquad 0<r_1<r_2 \tag{3}$$

By definition, $\xi_n(\lambda r)$ and $\eta_n(\lambda r)$ are solutions of the modified spherical Bessel equation

$$\frac{1}{r}\frac{d^2}{dr^2}(rR) - \left[\lambda^2 + \frac{n(n+1)}{r^2}\right]R = 0 \tag{4}$$

In terms of the modified (cylindrical) Bessel function $I_\nu(z)$,

$$\xi_n(z) = \sqrt{\frac{\pi}{2z}}\ I_{n+\frac{1}{2}}(z) \tag{5}$$

and

$$\eta_n(z) = \sqrt{\frac{\pi}{2z}}\ I_{-n-\frac{1}{2}}(z) \tag{6}$$

Since $I_\nu^*(z) = I_\nu(z^*)$, $\xi_n^*(z) = \xi_n(z^*)$ and $\eta_n^*(z) = \eta_n(z^*)$. Consequently, $v_n^*(\lambda r,\lambda) = v_n(\lambda^* r,\lambda^*)$, and u_n and v_n^* satisfy, respectively, the following two equations:

$$\frac{1}{r}\frac{d^2}{dr^2}(ru_n) - \left[\lambda^2 + \frac{n(n+1)}{r^2}\right]u_n = 0 \tag{7}$$

$$\frac{1}{r}\frac{d^2}{dr^2}(rv_n^*) - \left[\lambda^{*2} + \frac{n(n+1)}{r^2}\right] v_n^* = 0 \tag{8}$$

since $\lambda^2 * = \lambda^{*2}$. Now multiply (7) by $r^2 v_n^*$ and (8) by $r^2 u_n$ and subtract to get

$$rv_n^* \frac{d^2}{dr^2}(ru_n) - ru_n \frac{d^2(rv_n^*)}{dr^2} = (\lambda^2 - \lambda^{*2}) r^2 u_n v_n^* \tag{9}$$

since the terms in n(n+1) cancel. Integrate (9) once with respect to r, using integration by parts on the left-hand-side.

$$\left[rv_n^* \frac{d}{dr}(ru_n) - ru_n \frac{d}{dr}(rv_n^*)\right] = (\lambda^2 - \lambda^{*2}) \int_{r_1}^{r_2} r^2 u_n v_n^* dr \tag{10}$$

or
$$\left[rv_n^*\left(r\frac{du_n}{dr} + u_n\right) - ru_n\left(r\frac{dv_n^*}{dr} + v_n^*\right)\right] = (\lambda^2 - \lambda^{*2}) \int_{r_1}^{r_2} r^2 u_n v_n^* dr \tag{11}$$

$$\therefore \quad \left[r^2\left(v_n^* \frac{du_n}{dr} - u_n \frac{dv_n^*}{dr}\right)\right]_{r_1}^{r_2} = (\lambda^2 - \lambda^{*2}) \int_{r_1}^{r_2} r^2 u_n v_n^* dr \tag{12}$$

Let $z = \lambda r$ and denote differentiation with respect to z by a prime.

$$\frac{du_n}{dr} = \frac{du_n(\lambda r, \lambda)}{dr} = \lambda u_n'(z, \lambda) = \lambda u_n' \tag{13}$$

$$\frac{dv_n^*}{dr} = \frac{dv_n^*(\lambda r, \lambda)}{dr} = \lambda v_n^{*\prime}(z, \lambda) = \lambda v_n^{*\prime} \tag{14}$$

Thus (12) becomes

$$\left[r(v_n^* z u_n' - u_n z v_n^{*\prime})\right]_{r_1}^{r_2} = (\lambda^2 - \lambda^{*2}) \int_{r_1}^{r_2} r^2 u_n v_n^* dr \tag{15}$$

Both $u_n(z)$ and $v_n(z)$ satisfy the elementary recursion formula,

$$z \frac{df_n(z)}{dz} = z f_{n-1}(z) - (n+1) f_n(z) \tag{16}$$

or
$$r \frac{df_n(\lambda r)}{dr} = \lambda r f_{n-1}(\lambda r) - (n+1) f_n(\lambda r) \tag{17}$$

$$\therefore \quad r \frac{df_n^*(\lambda r)}{dr} = \lambda^* r f_{n-1}^*(\lambda r) - (n+1) f_n^*(\lambda r) \tag{18}$$

$$\text{or} \quad z\frac{df^*(z)}{dz} = z^* f^*_{n-1}(z) - (n+1) f^*_n(z) \tag{19}$$

Using (16) and (19) in (15) gives

$$\left(r^2 v_n^*[z u_{n-1} - (n+1)u_n] - u_n[z^* v^*_{n-1} - (n+1)v_n^*]\right)_{r_1}^{r_2} = (\lambda^2 - \lambda^{*2}) \int_{r_1}^{r_2} r^2 u_n v_n^* dr \tag{20}$$

$$\text{or} \quad \left[r^2(\lambda v_n^* u_{n-1} - \lambda^* u_n v^*_{n-1})\right]_{r_1}^{r_2} = (\lambda^2 - \lambda^{*2}) \int_{r_1}^{r_2} r^2 u_n v_n^* dr \tag{21}$$

$$\therefore \quad \int_{r_1}^{r_2} r^2 u_n v_n^* dr = \frac{1}{|\lambda| \operatorname{Im}(\lambda^2)} \left[|z| \operatorname{Im}(z v^* u_{n-1})\right]_{z_1}^{z_2} \tag{22}$$

$$= \frac{1}{|\lambda|^3} \left[|z| \operatorname{Im}(z v_n^* u_{n-1})\right]_{z_1}^{z_2}$$

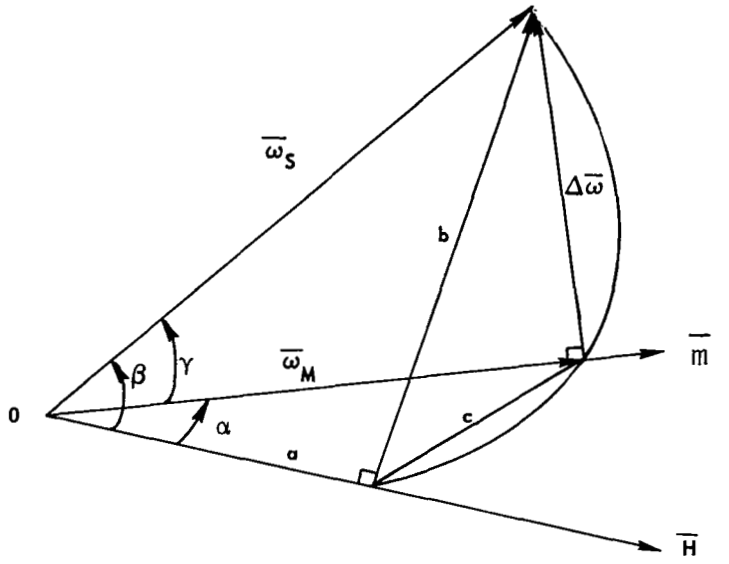

(a) $\beta < 90°$

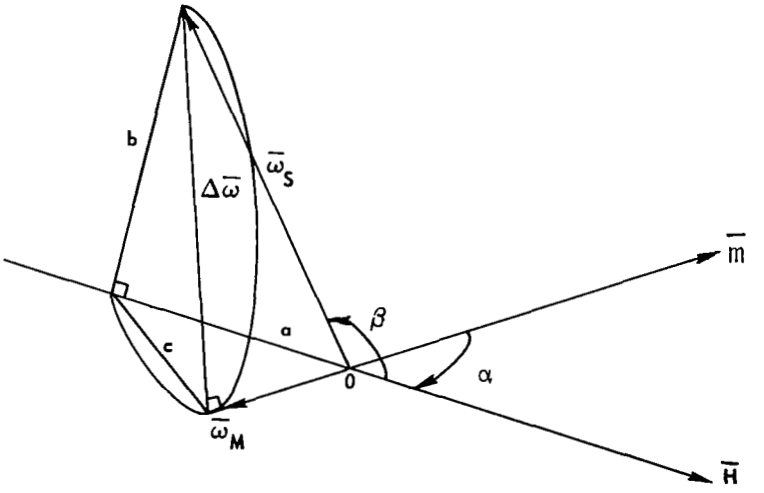

(b) $90° < \beta < 180°$

Figure 3.17-1. Diagram Showing Vector Relationships for Magnetically Anchored Damper Kinematics

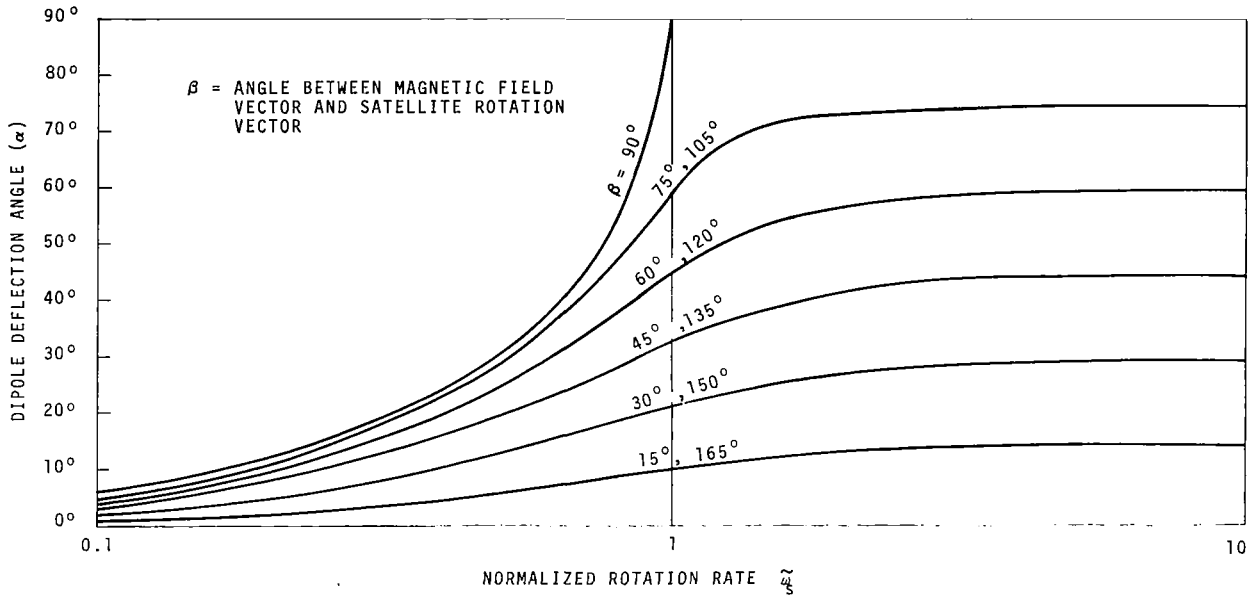

Figure 3.17.2. Dipole Deflection Angle as a Function of Satellite Rotation Rate and Magnetic Field Direction

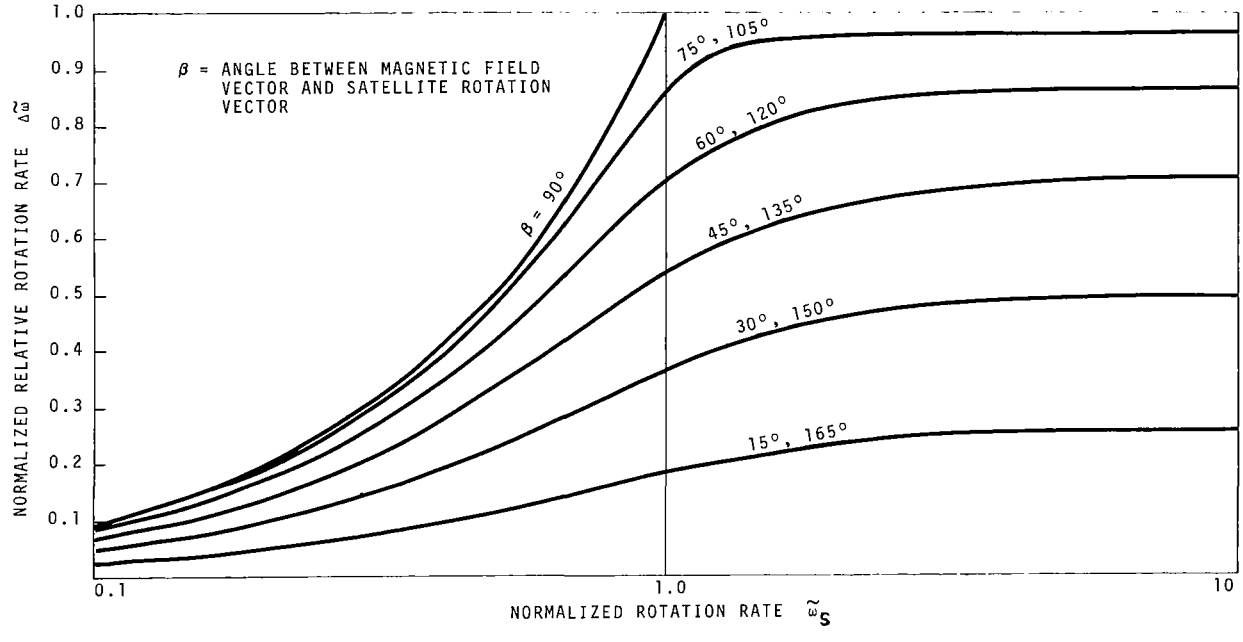

Figure 3.17-3. Damper Rotation as a Function of Satellite Rotation Rate and Magnetic Field Direction

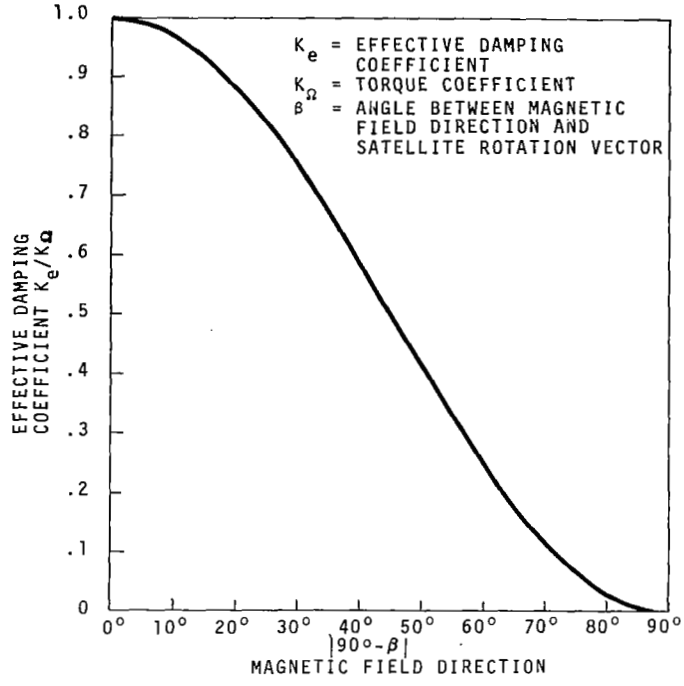

Figure 3.18-1. Effective Damping Coefficient as a Function of Magnetic Field Direction

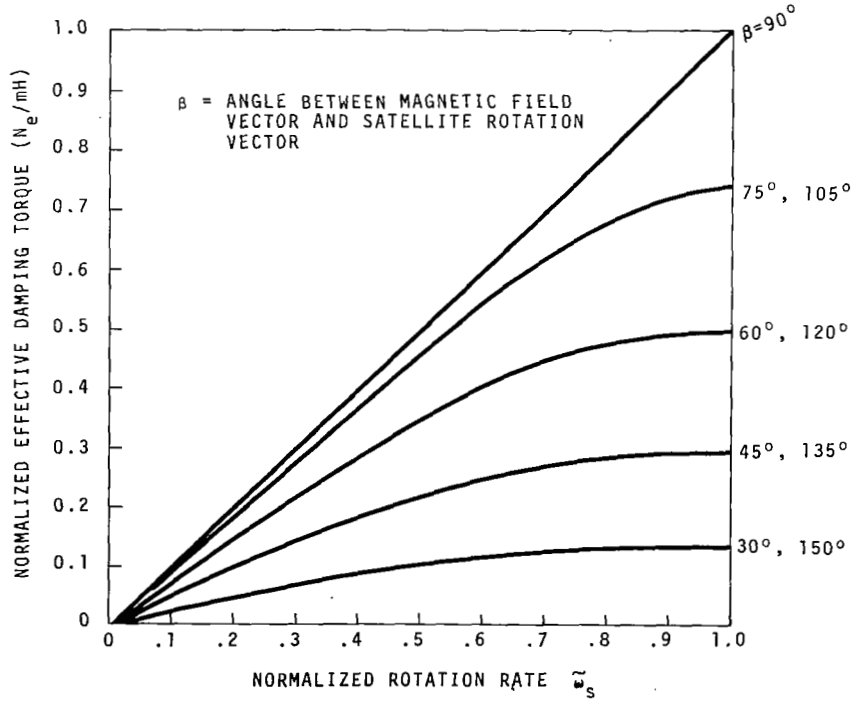

Figure 3.18-2. Effective Damping Torque as a Function of Satellite Rotation Rate

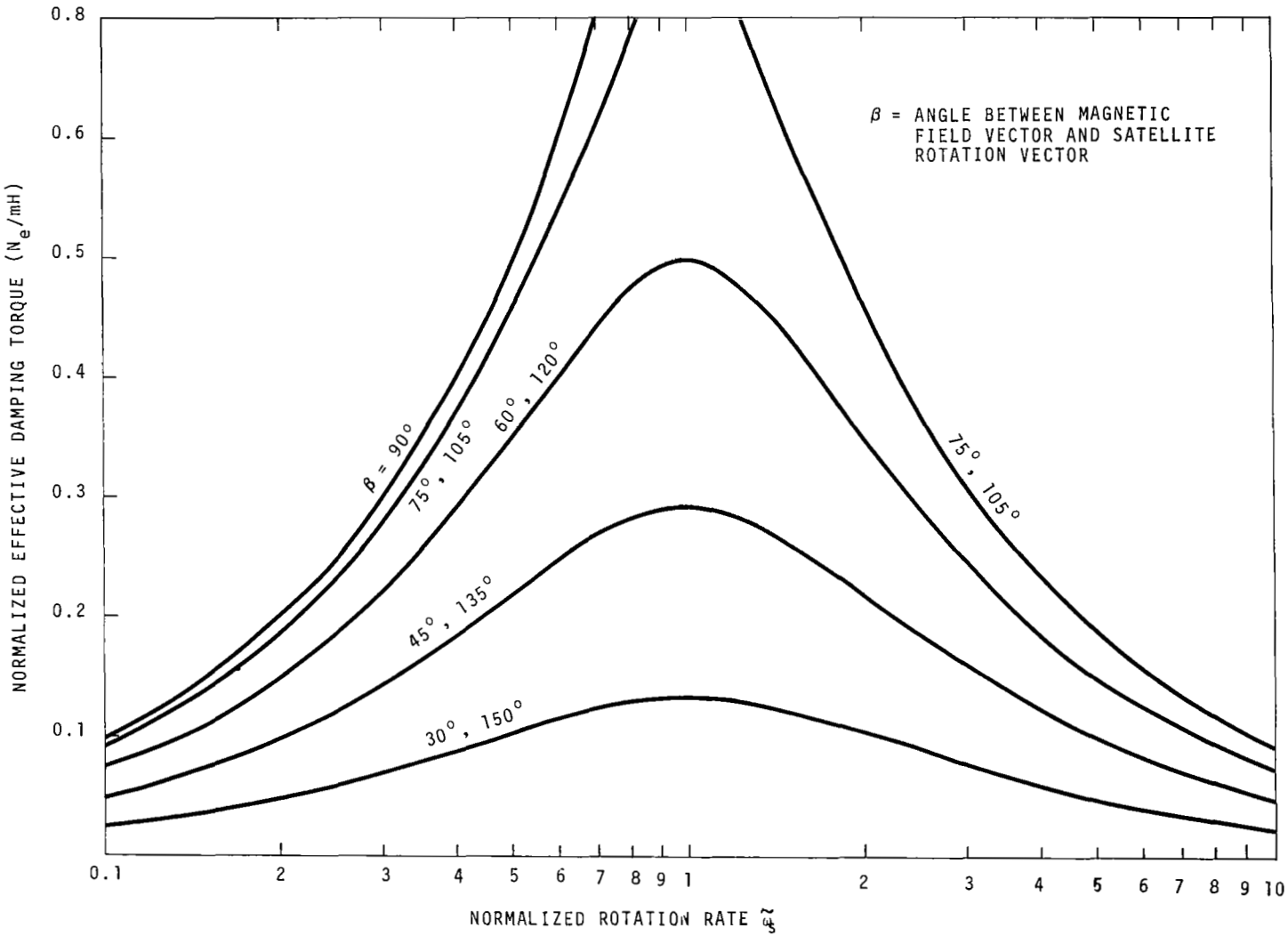

Figure 3.18-3. Effective Damping Torque as a Function of Satellite Rotation Rate

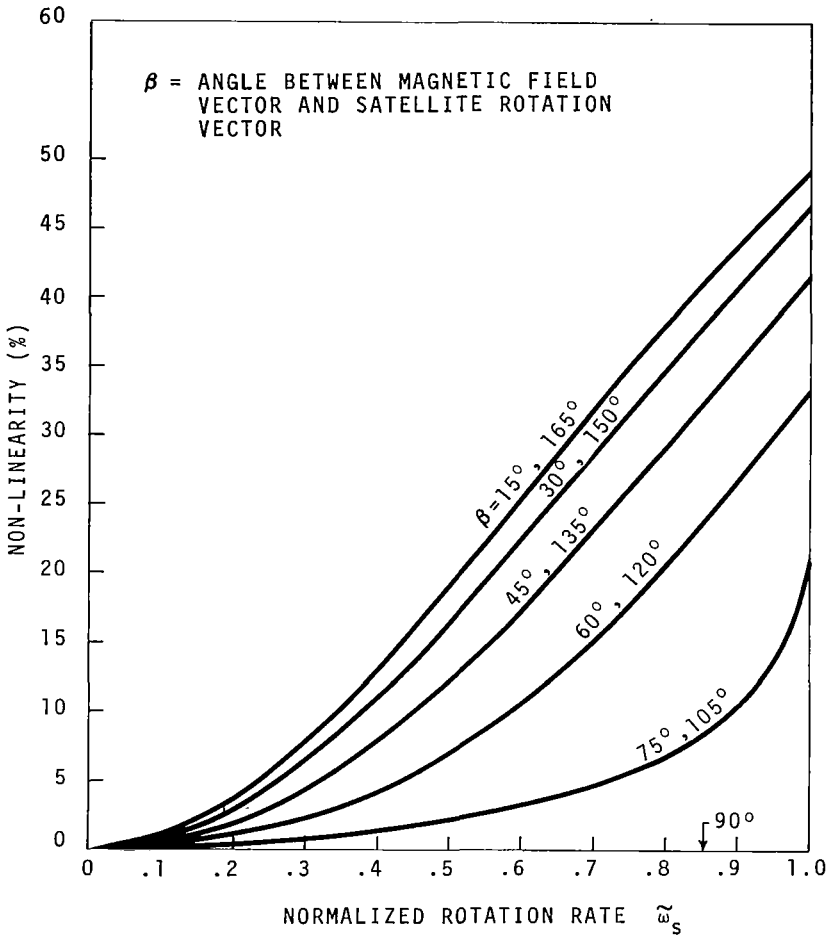

Figure 3.18-4. Non-linearity of Effective Damping Torque as a Function of Satellite Rotation Rate

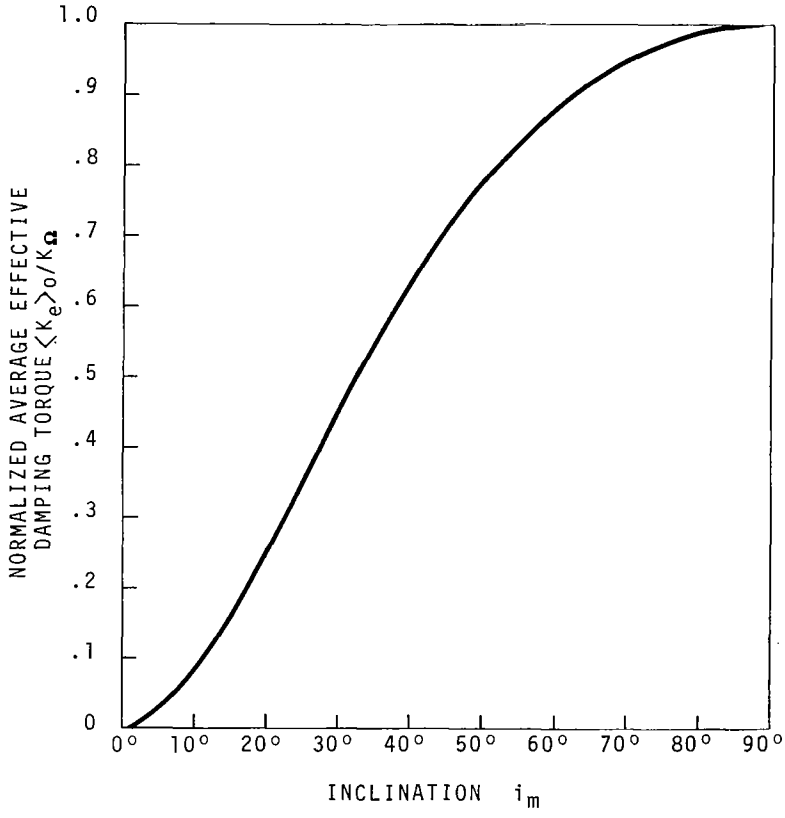

Figure 3.19-1. Average Effective Damping Torque as a Function of Orbital Inclination from Magnetic Equator

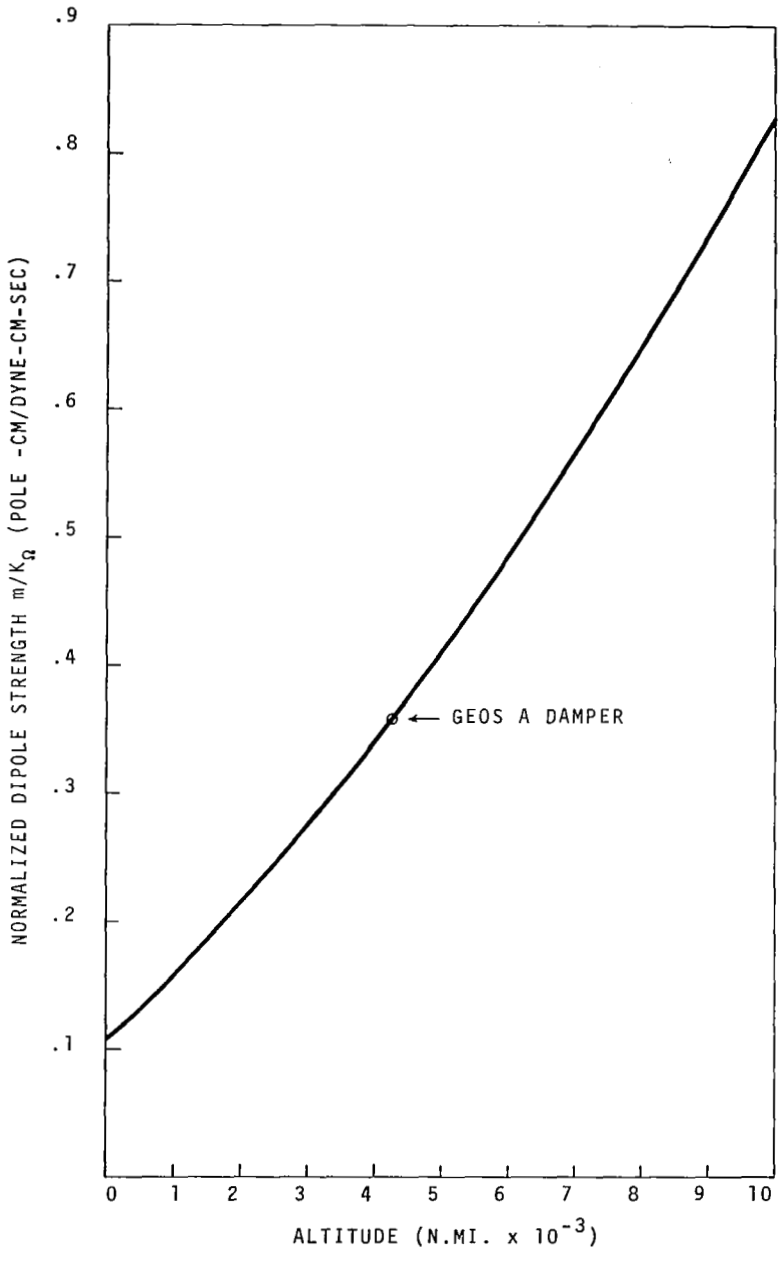

Figure 3.19-2. Minimum Allowable Dipole Strength as a Function of Altitude

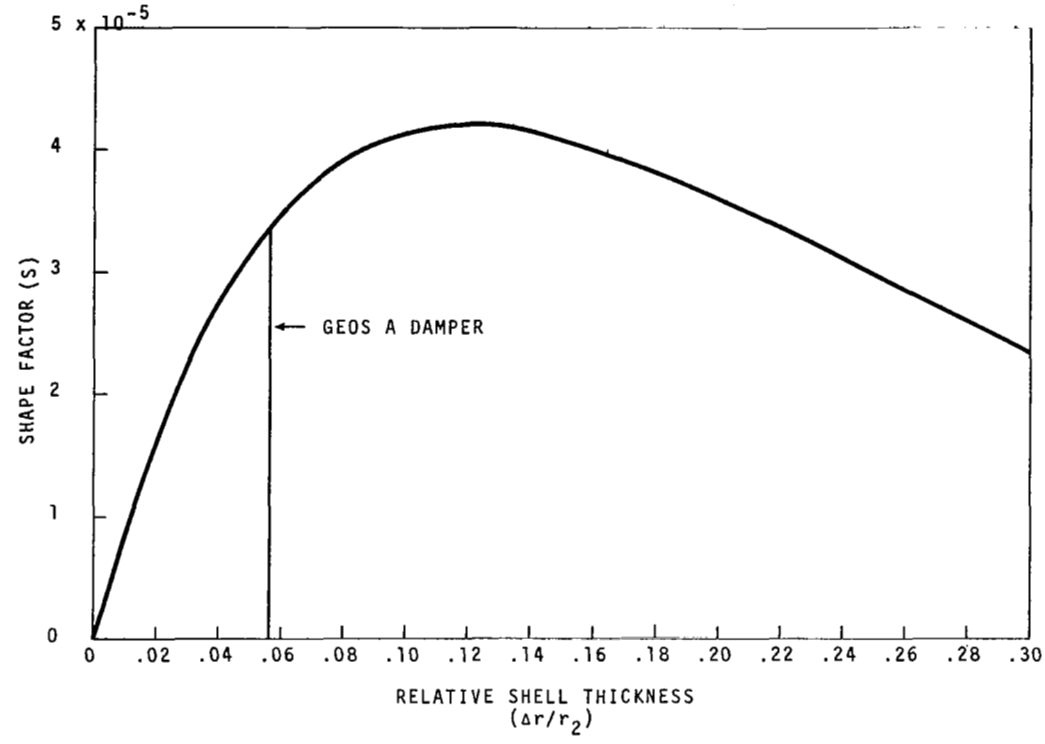

Figure 3.20-1. Shape Factor as a Function of Relative Shell Thickness

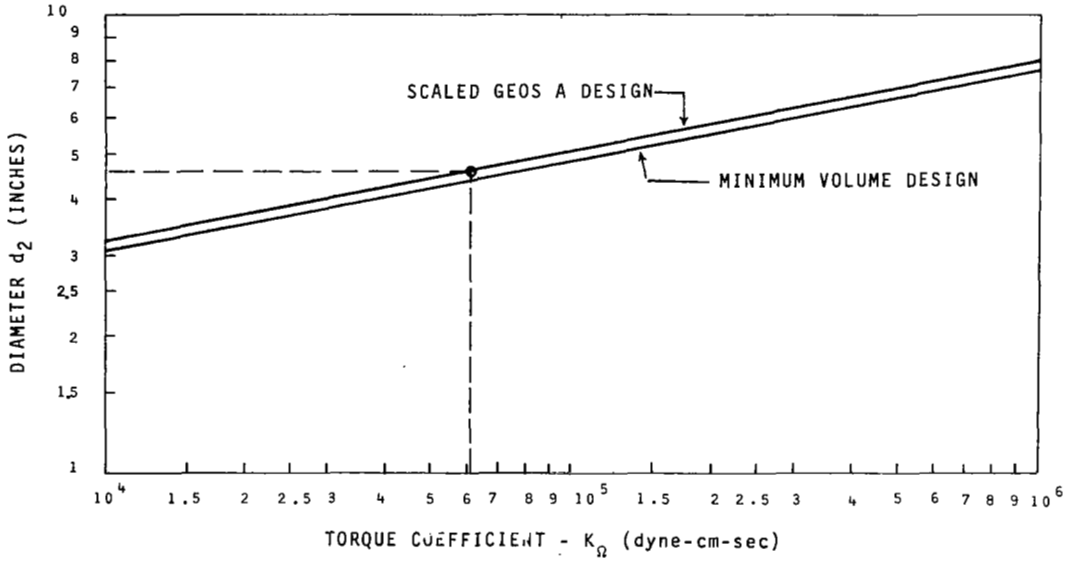

Figure 3.20-2. Diameter of Copper Shell as a Function of Torque Coefficient

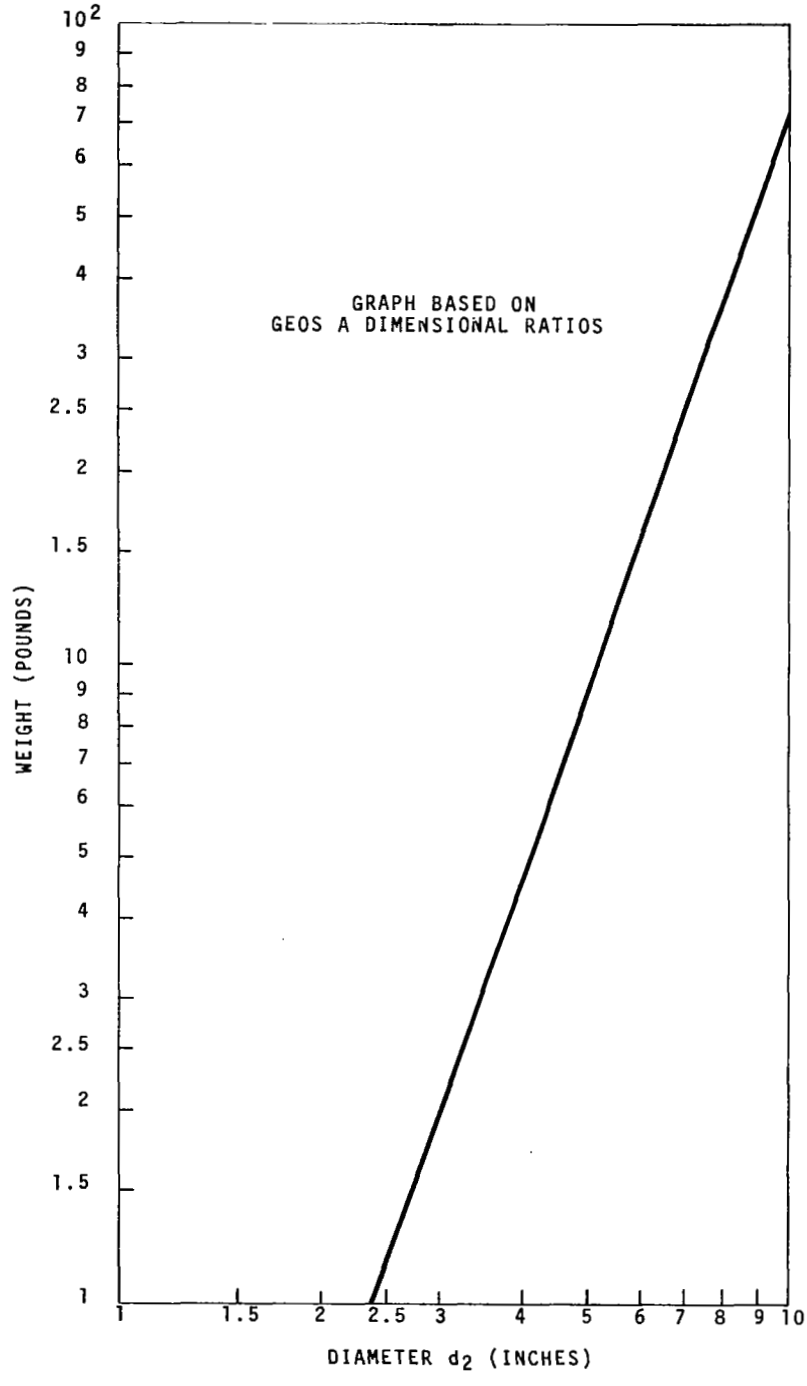

Figure 3.20-3. Damper Weight as a Function of Copper Shell Diameter

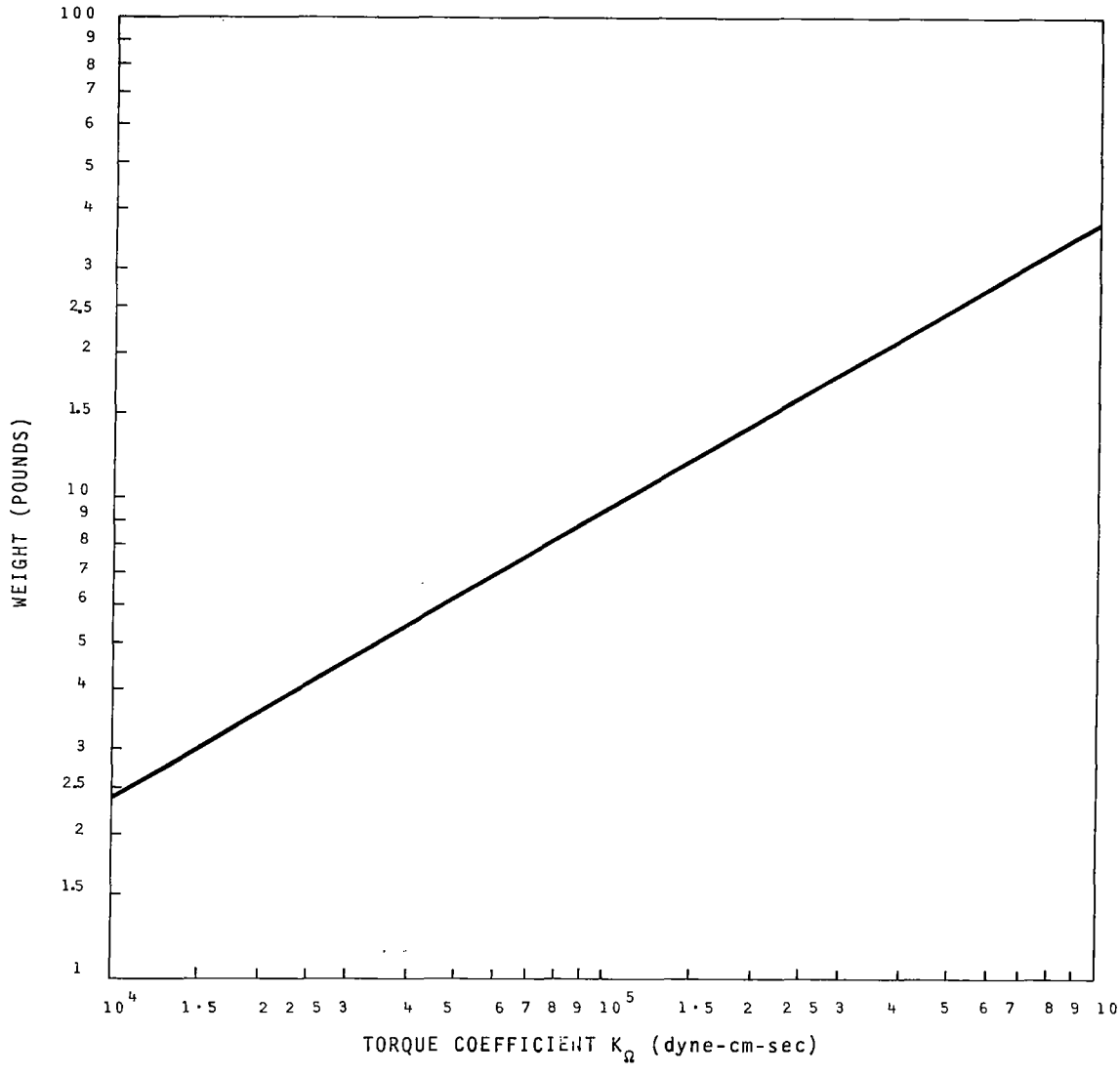

Figure 3.20-4. Damper Weight as a Function Torque Coefficient

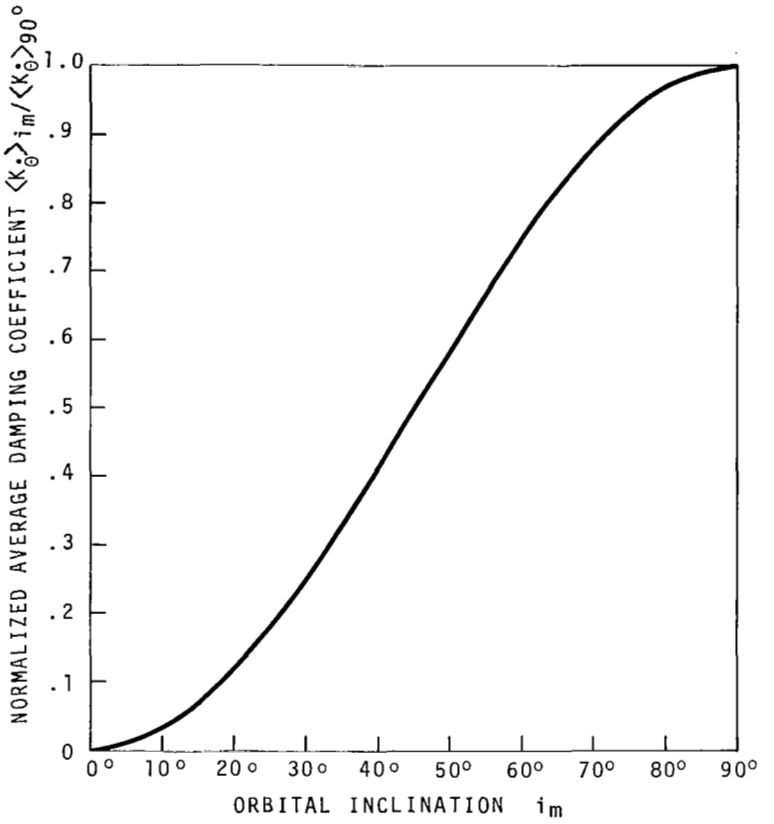

Figure 4.3-1. Average Damping Coefficient as a Function of Orbital Inclination from Magnetic Equator

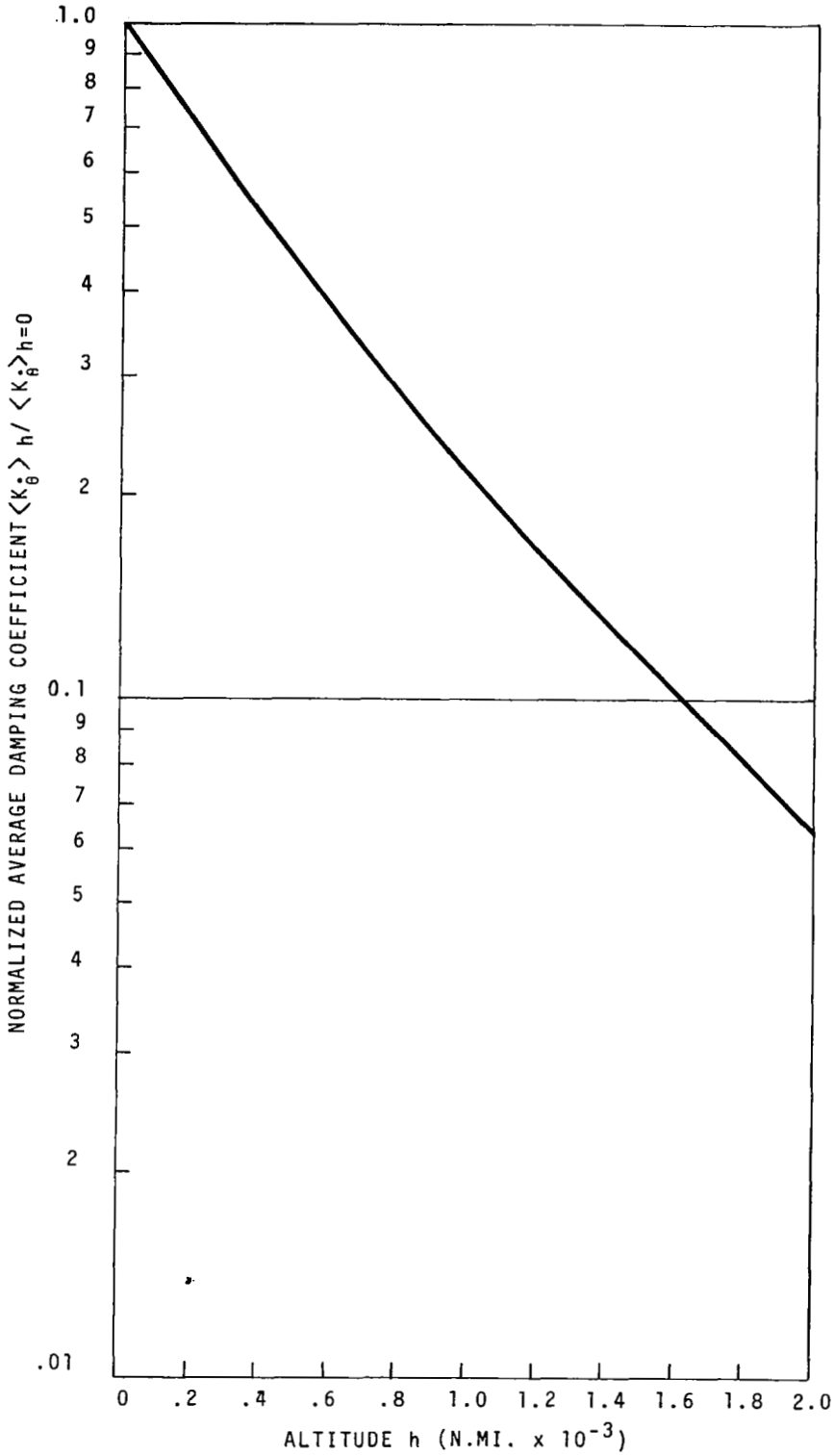

Figure 4.3-2. Average Damping Coefficient as a Function of Altitude

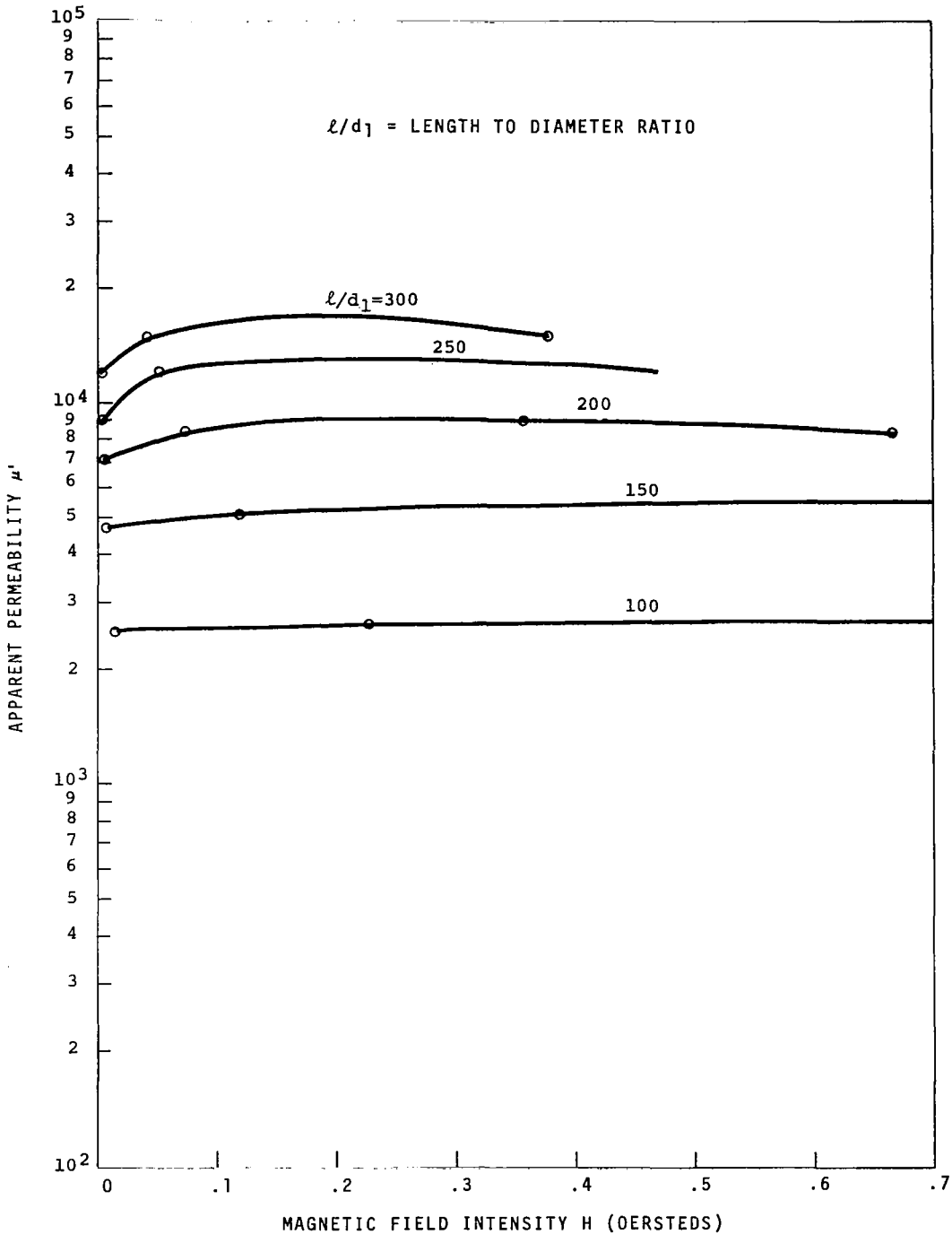

Figure 4.4-1. Apparent Permeability as a Function of Applied Magnetic Field Intensity and ℓ/d_1

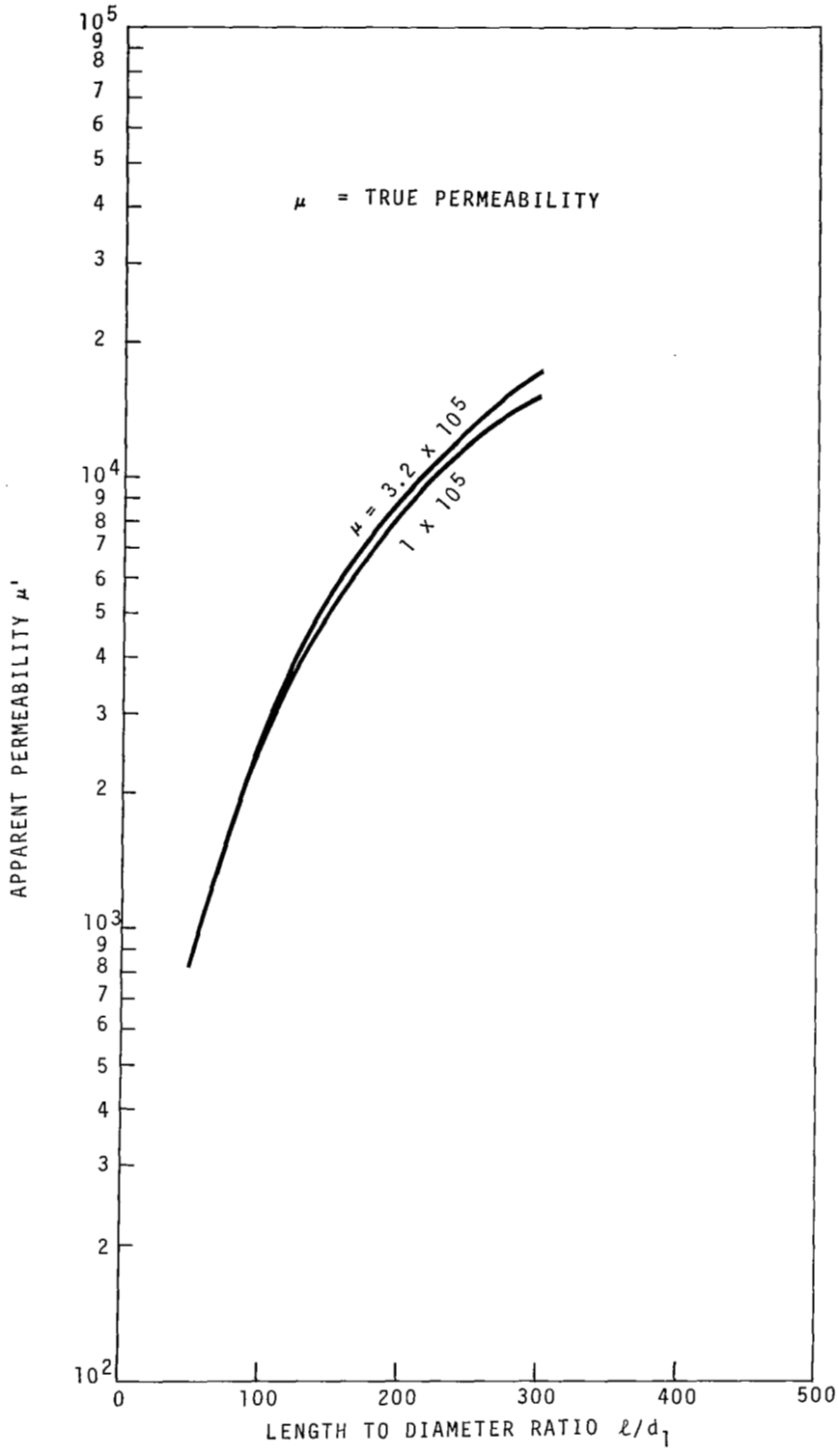

Figure 4.4-2. Apparent Permeability as a Function of ℓ/d_1 and True Permeability

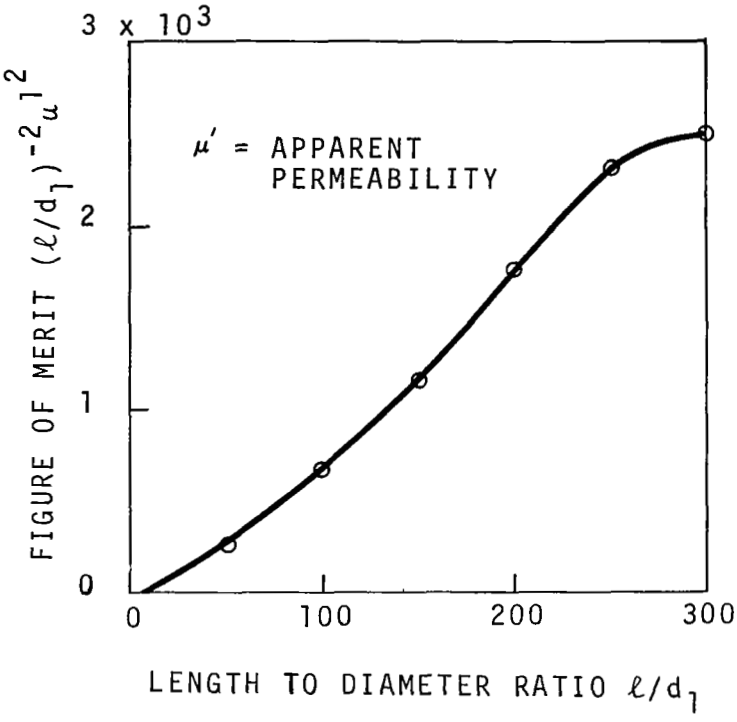

Figure 4.4-3. Figure of Merit $(\ell/d_1)^{-2}\ \mu'^2$ as a Function of ℓ/d_1

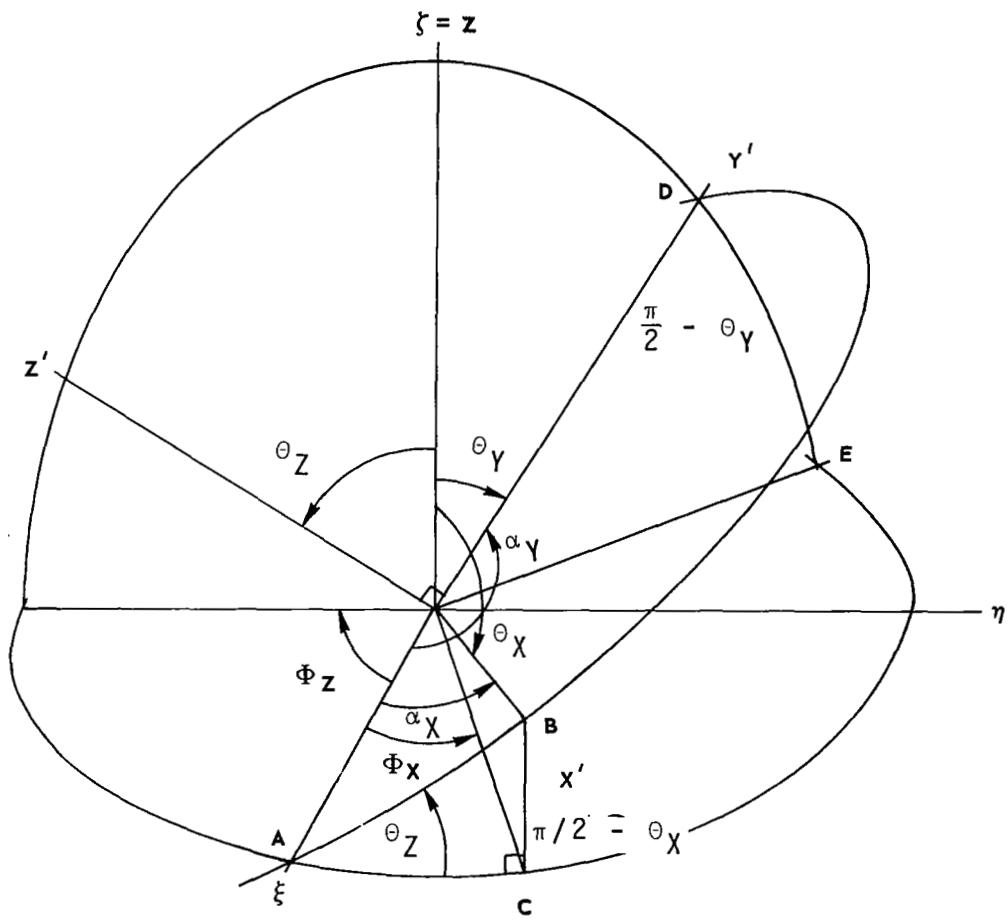

Figure B-1. Geometry for Coordinate Transformations

NASA-Langley, 1969 —— 3 CR-128

NATIONAL AERONAUTICS AND SPACE ADMINISTRATION
WASHINGTON, D. C. 20546

OFFICIAL BUSINESS

FIRST CLASS MAIL

POSTAGE AND FEES PAID
NATIONAL AERONAUTICS A
SPACE ADMINISTRATION

C7L 001 26 51 30S 69033 00903
AIR FORCE WEAPONS LABORATORY/AFWL/
KIRTLAND AIR FORCE BASE, NEW MEXICO 87117

ATT E. LOU BOWMAN, ACTING CHIEF TECH. LIB

POSTMASTER: If Undeliverable (Section Postal Manual) Do Not R

"The aeronautical and space activities of the United States shall be conducted so as to contribute . . . to the expansion of human knowledge of phenomena in the atmosphere and space. The Administration shall provide for the widest practicable and appropriate dissemination of information concerning its activities and the results thereof."

— NATIONAL AERONAUTICS AND SPACE ACT OF 1958

NASA SCIENTIFIC AND TECHNICAL PUBLICATIONS

TECHNICAL REPORTS: Scientific and technical information considered important, complete, and a lasting contribution to existing knowledge.

TECHNICAL NOTES: Information less broad in scope but nevertheless of importance as a contribution to existing knowledge.

TECHNICAL MEMORANDUMS: Information receiving limited distribution because of preliminary data, security classification, or other reasons.

CONTRACTOR REPORTS: Scientific and technical information generated under a NASA contract or grant and considered an important contribution to existing knowledge.

TECHNICAL TRANSLATIONS: Information published in a foreign language considered to merit NASA distribution in English.

SPECIAL PUBLICATIONS: Information derived from or of value to NASA activities. Publications include conference proceedings, monographs, data compilations, handbooks, sourcebooks, and special bibliographies.

TECHNOLOGY UTILIZATION PUBLICATIONS: Information on technology used by NASA that may be of particular interest in commercial and other non-aerospace applications. Publications include Tech Briefs, Technology Utilization Reports and Notes, and Technology Surveys.

Details on the availability of these publications may be obtained from:

SCIENTIFIC AND TECHNICAL INFORMATION DIVISION

NATIONAL AERONAUTICS AND SPACE ADMINISTRATION

Washington, D.C. 20546